Universidad del País Vasco
Euskal Herriko Unibertsitatea
Farmacia y Tecnología Farmaceútica
Facultad de Farmacia

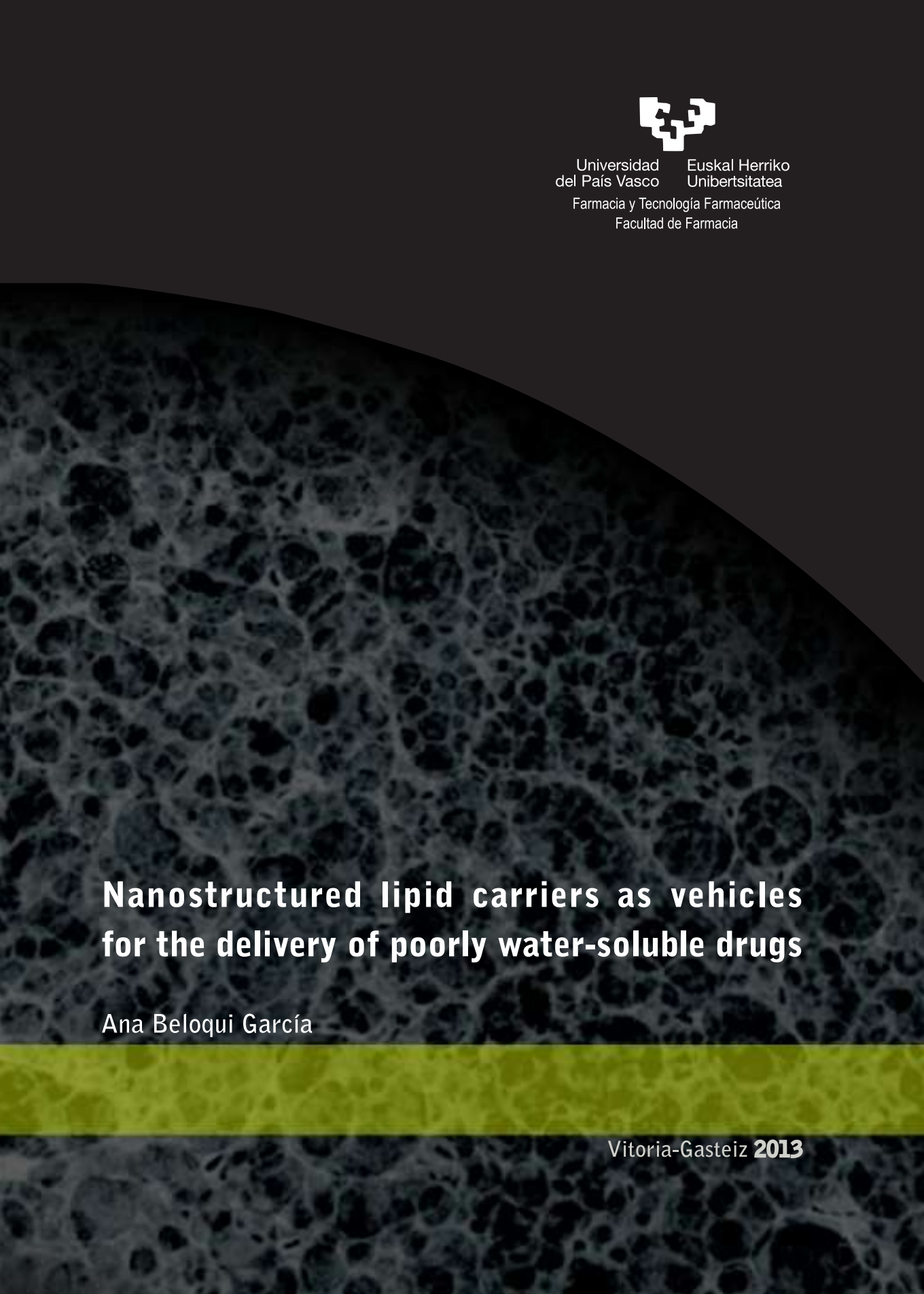

Nanostructured lipid carriers as vehicles for the delivery of poorly water-soluble drugs

Ana Beloqui García

Vitoria-Gasteiz 2013

Nanostructured Lipid Carries as vehicles for the delivery of poorly water-soluble drugs

Lípidos nanoparticulados como vehículo para la administración de fármacos poco solubles

ANA BELOQUI GARCÍA

Laboratorio de Farmacia y Tecnología Farmacéutica
Grupo Farmacocinética, Nanotecnología y Terapia Génica
Universidad del País Vasco/Euskal Herriko Unibertsitatea (UPV/EHU)

Facultad de Farmacia, Vitoria-Gasteiz, 2013

AGRADECIMIENTOS

La tesis ha sido para mí, sin lugar a dudas, uno de los momentos más bonitos de mi vida. Se pasa por momentos muy duros y es un continuo “caerse y levantarse”, fallar y seguir intentándolo, pero para mí el laboratorio se ha convertido en algo más que un trabajo. Si alguien me preguntara cuál es para mí el secreto para acabar una tesis, diría que es un mezcla de motivación, ilusión, paciencia y amor propio. Ha sido un camino largo y tengo que agradecer a mucha gente el que haya seguido adelante con las mismas ganas e ilusión del primer día.

A mis padres, que me han apoyado y ayudado en todo, que nunca me han dicho que algo es imposible o que estoy loca, que siempre han confiado en mi criterio y me han dejado equivocarme. A mi madre, la bondad personificada, por tu apoyo incondicional a diario, tu interés continuo en todo lo que hago y tu continuo sacrificio por mí y por mis hermanas, porque siempre nos has antepuesto a cualquier cosa. A mi padre, por enseñarme que en las cosas que uno quiere hay que poner el corazón y dejarse la piel, por ser el ejemplo personificado del amor propio. Ojalá mis hijos puedan decir alguna vez de mí la mitad de lo que yo puedo decir de vosotros. Os quiero.

A mis hermanas, mis segundos padres, mis mejores amigas. Por estar siempre cuidando de "vuestra pequeña hermana", por vuestro apoyo. Por esos sobrinos que tengo, Paula, Iñigo y Alba, que me dan la vida, la alegría. Gracias.

A Alicia y Marian, porque me distéis una oportunidad cuando lo único que tenía para ofrecer eran ganas. Al resto de mi grupo de investigación (Arantxa, Ana, Edu, Paola, Aritz, Diego) por vuestra ayuda y apoyo. Gracias.

A José Luis Pedraz, por permitirme formar parte de su grupo de investigación y empezar esta aventura.

A Araceli Delgado y Carmen Évora, por abrirme las puertas de vuestro laboratorio y hacerme sentir como en casa. Por vuestro tiempo. A Fanny, María y Bea por la increíble compañía, y al resto del personal del Departamento de Ingeniería Química y Tecnología Farmacéutica (Esther, Ana, Ricardo…). Gracias.

To the LDRI lab in Brussels, especially to Anne des Rieux and Véronique Préat, for giving me the opportunity to take part of your team and work with you, for all the time you dedicated to me. To all my lab mates (Régis, Salomé, Martin, Eduardo, Bernard, Patrick, Julian….) for your continuos efforts on speaking in English and your continuos interest on me. Thank you very much. I really appreciated it.

He tenido la suerte de formar parte de un grupo con una calidad de personas única, de sentir el compañerismo y la amistad sobre todas las cosas: mis compañeros son dueños de buena parte del éxito de esta tesis porque sin ellos nada hubiera sido lo mismo. Tengo mucho que agradecer:

A Ainhoa, mi gran descubrimiento y mi gran pérdida en este laboratorio, mi apoyo diario, mi confidente, mi compañera, mi gran amiga. Por empujarme a diario a mejorar, por creer en mí más que yo misma. No hay un día en que no te eche de menos…

A Aiala y Marta, "mis chinas", mis compañeras de viaje. Por hacerme sonreír y escucharme llorar cuando lo he necesitado. Por nuestras mil y una historias, nuestras mil y una anécdotas. Por estar ahí siempre. Estos años no hubieran sido lo mismo sin vosotras. Gracias.

A Dorleta, que viniste para irte pronto pero para mí te has quedado para siempre. Muchísimas gracias por estar ahí ayer, hoy y siempre, por tu ayuda constante, por tu amistad. Gracias.

A Edorta, porque tu ilusión y ganas son contagiosas. Porque pones el corazón en cada cosa que haces y haces que el que te rodea quiera ser mejor y quiera superarse. Gracias por todas esas horas de comedor, por los cafés, por ese saber escuchar. Gracias.

A Silvia, doy gracias porque tú y yo tuviéramos una segunda oportunidad para conocernos. Gracias a tí hemos sido "el gran grupo amigo" que hoy somos. Por tu sinceridad aunque duela, por decir siempre la verdad. Gracias Sil.

A Aritz, a Ane, a Garazi, a Enara, a Argia…Muchas gracias por esa alegría que nos trajisteis al laboratorio, por las risas, por los lloros, por los desahogos. Nada hubiera sido lo mismo sin vosotros. Gracias.

Al resto de profesores del laboratorio de tecnología farmacéutica (Rosa, Amaia, Manoli, Gorka, Jon…) por hacerme sentir una más. Por interesaros por mí. Gracias.

A mis compañeros de Tecnalia (Arantza, Fer, Esti B, Esti V, Leire P, Leire B, Ana Castilla, Amanda, Zuri, Noe…) por vuestra paciencia. Por siempre poner una buena cara a veinte preguntas, por ayudarme en todo lo que podíais, por enseñarme. Gracias.

A Beatriz de la Riva, por abrirme la puerta de tu casa, tratarme como a tu hermana, por presentarme a tus amigos, por tratarme como si me conocieras de toda la vida, por hacer que Tenerife fuera mi casa y tus padres los míos. Nunca tendré suficientes palabras de agradecimiento, ni entonces ni ahora. A Jose y a Conchi, sobre todo, por vuestra hija.

A mis grandes amigas, Carolina, Caroline y Leyre, por todos estos años de amistad. Por darme un abrazo cuando lo necesitaba y una colleja cuando me la merecía. Por seguir preguntándome qué hago cuando no me entendéis. Gracias.

A Alexander, que aunque te nombro el último, sabes que eres el primero en paciencia conmigo. Eres mi gran apoyo diario, mi gran amigo, mi gran amor…Espero que sigamos siendo como somos el resto de nuestras vidas. Te quiero.

MUCHAS GRACIAS A TODOS, THANK YOU VERY MUCH!

Ana

ACKNOWLEDGEMENTS FOR FINANTIAL SUPPORT

This thesis has been partially supported by the the Basque Government´s Department of Education, Universities and Investigation (IT-341-10) and the University of the Basque Country (UPV/EHU).

A Ainhoa,
mi gran amiga y mi gran ejemplo a seguir

“The important thing is not to stop questioning”
Albert Einstein

GLOSSARY

2-MG: 2-monoglyceride
7α-TMS: 7α-thiomethylspironolactone
AC: fatty acid
ADME: absorption, distribution, metabolism and excretion
AUC: area under the curve
AUMC: area under the first moment curve
BCS: biopharmaceutic classification system
CLSM: confocal laser scanning microscopy
CTAB: cetyl trimethyl ammonium bromide
CM: chylomicron
DMEM: Dulbecco´s modified eagle medium
EE: encapsulation efficiency
EPR: enhanced permeability and retention
EtOH: ethanol
G3P: glicerol-3-phosphate
GRAS: generally recognized as safe
FAE: follicle-associated epithelium
FDA: food and drug administration
HBSS: Hank´s balance solution buffer
HLB: hydrophilic-lipophilic balance
HPLC: high performance liquid chromatography
iTLC: instant thin layer chromatography
i.v: intravenous
LCT: long chain triglycerides
LDC: lipid drug conjugate
LDH: lactate dehydrogenase
LDV: laser doppler velocimetry
LOD: limit of detection
LOQ: limit of quantification
LFCS: lipid formulation classification system
LP: lipoprotein

MßCD: methyl-ß-cyclodextrin
MCT: médium chain triglycerides
MRM: multiple-reaction monitoring
MRT: mean residence time
MTT: 3-(4,5-dimethylthiazol-2-yl)-2,5 diphenylte-trazolium bromide
MWCO: molecular weight cut off
NLC: nanostructured lipid carrier
PBS: phosphate buffer solution
PCS: photon correlation spectroscopy
PEG: polyethilenglycol
PEST: penicillin-streptomicin
P-gp: P-glycoprotein
PI: polydispersity index
PLA: poly lactic acid
PLGA: poly lactic-co- glycolic acid
REL: smooth endoplasmic reticulum
RER: rough endoplasmic reticulum
RES: rethiculo-endothelial system
SEDDS: self-emulsifying drug delivery systems
SG: silica gel
SGF: simulated gastric fluid
SIF: simulated intestinal fluid
SLN: solid lipid nanoparticle
SMEDDS: self-microemulsifying drug delivery systems
SNEDDS: self-nanoemulsifying drug delivery systems
SPN: spironolactone
SQV: saquinavir
TEER: trans-epithelial electrical resistance
TEM: trasmission electron microscopy
TG: triglyceride
VLDL: very low density lipoproteins

INDEX

INTRODUCTION

Formulaciones lipídicas para la administración oral
de fármacos poco solubles

Se estima que el 40% de las nuevas moléculas farmacológicamente activas descubiertas mediante las técnicas actuales (técnicas de *screening in vitro*, química combinatoria) son insolubles o poco solubles en agua[1-3]. Es bien conocido que tanto la solubilidad como la permeabilidad son factores limitantes de la biodisponibilidad de un fármaco[4, 5].

De acuerdo con el sistema de Clasificación Biofarmacéutica[6, 7], los fármacos de la clase II y de la clase IV son los que presentan una baja solubilidad. Los fármacos clase IV presentan, además, una baja permeabilidad. Los principales problemas asociados a los fármacos que presentan baja solubilidad son[2, 5]:

- Precipitación del fármaco tras la administración
- Baja biodisponibilidad
- Variabilidad en la biodisponibilidad
- Ausencia de proporcionalidad dosis-respuesta
- Con frecuencia se requiere utilizar excipientes poco seguros, por ejemplo cosolventes
- Necesidad de condiciones ácidas o básicas extremas para aumentar la solubilidad

Estos factores han hecho que moléculas potencialmente activas no hayan pasado a clínica debido a las dificultades para diseñar formulaciones adecuadas para su administración por vía oral. El reto es formular dichas moléculas en sistemas de administración oral que les confieran una biodisponibilidad adecuada.

Los sistemas de administración de fármacos basados en lípidos están adquiriendo en la última década un gran interés para la vehiculización de fármacos poco solubles[3, 5, 7-15]. Las formulaciones lipídicas pueden favorecer la absorción del fármaco mediante diferentes mecanismos, entre los que destacan el aumento de la solubilidad del fármaco, el aumento de la permeabilidad de la membrana intestinal, la inhibición de los transportadores de salida del fármaco hacia el lumen intestinal,

la reducción de la actividad metabólica, el aumento de la producción de quilomicrones o la estimulación del transporte linfático[3, 7, 9]. El éxito clínico y comercial de varias formulaciones lipídicas que contienen fármacos lipófilos, como es el caso de la ciclosporina (Sandimmun Neoral®) y el ritonavir (Norvir®), ha despertado el interés por el desarrollo de nuevas formulaciones de tipo lipídico.

Durante la pasada década, ha habido un gran avance en el desarrollo de nuevos sistemas de liberación de fármacos. El desarrollo de la nanotecnología y la microtecnología, junto con la proteómica, la genómica y la química combinatoria, ha permitido un gran avance en el diseño de nuevos sistemas de administración de fármacos. Los nuevos sistemas de liberación de fármacos deben proporcionar una biodisponibilidad adecuada, una cinética de liberación controlada, mínima respuesta inmune, fácil administración a los pacientes, y la posibilidad de liberar fármacos tradicionalmente difíciles como son los lipófilos, anfifílicos y las biomoléculas.

La cinética de disolución es la principal responsable de la mejora de las propiedades biofarmacéuticas de compuestos con baja solubilidad acuosa incorporados en formulaciones micro y nanoparticulares. El perfil de disolución de un fármaco incorporado en estos sistemas está condicionado, entre otros, por el tipo de partícula y por características como la forma, tamaño de partícula, carga superficial y eficiencia de encapsulación, de tal manera que podemos modular el proceso de disolución controlando estas variables.

1.-EFECTO DE LOS LÍPIDOS EN LA ABSORCIÓN DE FÁRMACOS

El interés por la administración de fármacos mediante el uso de formulaciones lipídicas es relativamente reciente y está relacionado con el desarrollo de las mismas en los últimos 10-15 años, en respuesta a la necesidad de vehiculizar nuevos compuestos químicos de baja solubilidad y/o baja permeabilidad[11, 12].

Los lípidos y los excipientes lipídicos mejoran la absorción y disposición del fármaco[9, 15] mediante tres mecanismos:

a) El aumento de la disolución del fármaco en el tracto gastrointestinal
b) La modificación del transporte y disposición del fármaco en el enterocito

c) La estimulación del transporte linfático y, por tanto, reducción del metabolismo de primer paso hepático

La figura 1 recoge el efecto de los lípidos y excipientes lipídicos en la absorción de fármacos.

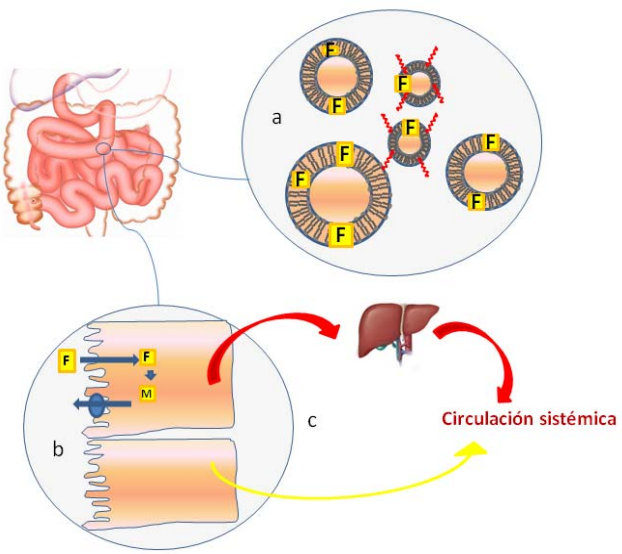

Figura 1. Efecto de los lípidos y excipientes lipídicos en la absorción de fármacos. Procesos mediante los cuales afectan a la absorción: (a) incremento de la disolución del fármaco (F) en el lumen intestinal mediante la alteración de la composición y características coloidales del entorno del fármaco- por ejemplo, mediante la formación micelas, micelas mixtas o vesículas; (b) interacción en los procesos metabólicos y de transporte que tienen lugar en el enterocito; (c) también pueden alterar el mecanismo de transporte hacia la circulación sistémica mediante la estimulación del transporte linfático, que puede conllevar una reducción en el efecto de primer paso que sufren algunos fármacos, evitando el paso del mismo a través del hígado.

Los lípidos provenientes de la dieta o de la formulación incrementan la capacidad de solubilización del fluido gastrointestinal. La acción combinada de

componentes exógenos y endógenos (secreción de sales biliares, fosfolípidos y colesterol) favorecen el proceso de solubilización del fármaco[9]. El conocimiento del efecto que los lípidos producen en el tracto gastrointestinal es imprescindible para entender el papel que juegan como excipientes en una formulación.

I. Efecto de los lípidos en el tracto gastrointestinal

Los lípidos en el tracto gastrointestinal estimulan la contracción de la vesícula biliar y las secreciones biliares y pancreáticas, incluyendo las sales biliares, los fosfolípidos y el colesterol[9, 14, 16, 17]. La secreción biliar promueve la formación de diferentes especies coloidales, incluyendo micelas mixtas y vesículas (ver figura 1). El papel de estas especies coloidales es el de favorecer la disolución de los compuestos poco solubles resultantes de la digestión de lípidos, como por ejemplo, los ácidos grasos o los monoglicéridos[17].

En condiciones de ayuno, las "especies solubilizantes" presentes en el contenido intestinal son las sales biliares, fosfolípidos y colesterol. En ausencia de lípidos exógenos, la capacidad de disolución del intestino delgado es baja y depende de la concentración de sales biliares más que de la estructura de la especie coloidal.

La adición de lípidos exógenos (provenientes de la ingesta de comida o de la formulación) aumenta de forma significativa la capacidad de solubilizar el fármaco y es dependiente de la naturaleza de los productos de la digestión, por ejemplo la longitud de cadena de los ácidos grasos, y de las características de las especies coloidales que se forman[9]. Depende, además, de la concentración de lípido, aumentando la capacidad de solubilización al aumentar la concentración de éste[8]. En un estudio llevado a cabo por *Kossena y cols.* en humanos, se demostró que incluso la presencia de una pequeña cantidad de triglicéridos de cadena larga (LCT) en el tracto gastrointestinal, estimula la secreción biliar[17]. Se observaron también cambios en el vaciado gástrico, pero estos cambios en el vaciado y en la secreción no se observaron cuando se administró la misma cantidad de lípidos de cadena media (MCT). Los mecanismos mediante los cuales los lípidos reducen el vaciado gástrico se desconocen aunque parece que están involucrados factores como la osmolaridad o el pH[9].

Estudios llevados a cabo con fármacos poco solubles como la cinarizina o la halofantrina[18-20] ponen de manifiesto los beneficios del uso de ácidos grasos de cadena larga debido al aumento de la disolución y la biodisponibilidad con respecto a ácidos grasos de cadena media. Sin embargo, otros estudios demuestran un mayor aumento de la biodisponibilidad con la administración de lípidos de cadena media que con la administración de lípidos de cadena larga, como es el caso de fármacos como la griseofulvina[21] o la progesterona[22]. Un estudio llevado a cabo por *Dahan y cols* con dexametasona incorporada en formulaciones lipídicas[21] con LCT y MCT, puso de manifiesto que el uso de uno u otro tipo de lípido no modificaba la absorción del fármaco. Estos resultados vuelven a sugerir que el aumento de la biodisponibilidad o de la disolución de un fármaco en el tracto gastrointestinal es dependiente del fármaco utilizado y de las propiedades fisicoquímicas del mismo.

Tras la ingesta, la digestión de triglicéridos provenientes de la dieta y los lípidos de la formulación tiene lugar en el estómago gracias a la secreción de lipasa gástrica. El peristaltismo del estómago contribuye también a esta digestión. Este movimiento mecánico, sumado a la presencia de productos anfifílicos resultantes de la digestión inicial de los lípidos (diglicéridos y ácidos grasos), facilita la formación de una emulsión. En el intestino delgado, la lipasa pancreática, junto con la co-lipasa, completan la ruptura de los triglicéridos a diglicéridos, monoglicéridos y ácidos grasos, produciendo posteriormente 2-monoglicéridos y ácidos grasos libres. La presencia de lípidos exógenos en el intestino delgado también estimula la secreción de lípidos biliares endógenos como las sales biliares, fosfolípidos o colesterol desde la vesícula biliar. En presencia de sales biliares, los productos resultantes de la digestión de los lípidos (monoglicéridos, ácidos grasos y lisofosfolípidos) son incorporados a una serie de estructuras coloidales, incluidas vesículas multilamilares o unilamilares, micelas o micelas mixtas. Esta unión aumenta significativamente la capacidad de solubilización en el intestino delgado de productos de digestión lipídica y fármacos.

II. Disposición y transporte del fármaco en el enterocito

Tras el paso a través de la membrana apical del enterocito, los productos de la digestión lipídica –monoglicéridos y ácidos grasos- pueden difundir a través del

enterocito y entrar en el sistema portal o pueden ser transformados nuevamente a triglicéridos por la vía del 2-monoglicérido (2-MG) asociada al retículo endoplasmático liso (REL) o por la vía del ∝-glicerol-3-fosfato (G3P) asociada al retículo endoplasmático rugoso (RER). Los triglicéridos formados por estas vías entran al retículo endoplasmático y se asocian a lipoproteínas (LPs). Estas lipoproteínas son transportadas al aparato de Golgi, exocitadas desde el enterocito y captadas por el sistema linfático intestinal. Como las lipoproteínas están formadas principalmente por lípidos y el aparato de Golgi participa en el transporte a circulación sistémica a través del sistema linfático intestinal, a este pool de lípidos se le llama "pool lipídico precursor linfático" (*lymph lipid precursor pool*) (figura 2). Existe otro pool lipídico citosólico dentro del enterocito. Este pool está formado por excedentes de triglicéridos provenientes de la vía G3P y de lípidos endógenos captados del suministro sanguíneo intestinal en forma de ácidos grasos o remanentes de quilomicrones (CM). Los lípidos citosólicos pueden ser hidrolizados por la lipasa citosólica y los productos de digestión resultantes pueden ser incorporados a las vías de resíntesis de triglicéridos. Sin embargo, la mayor parte de estos lípidos son captados en forma de TG o ácidos grasos libres y llevados hasta el sistema portal; estos lípidos se conocen como "pool lipídico precursor portal" (*portal lipid precursor pool*)[9] (línea punteada, figura 3). El transporte y salida de estos lípidos dentro del enterocito parecen influir en la disposición intracelular de los fármacos lipofílicos[23]. En la figura 3 se presenta un esquema con las diferentes vías de absorción y vehiculización de lípidos dentro del enterocito.

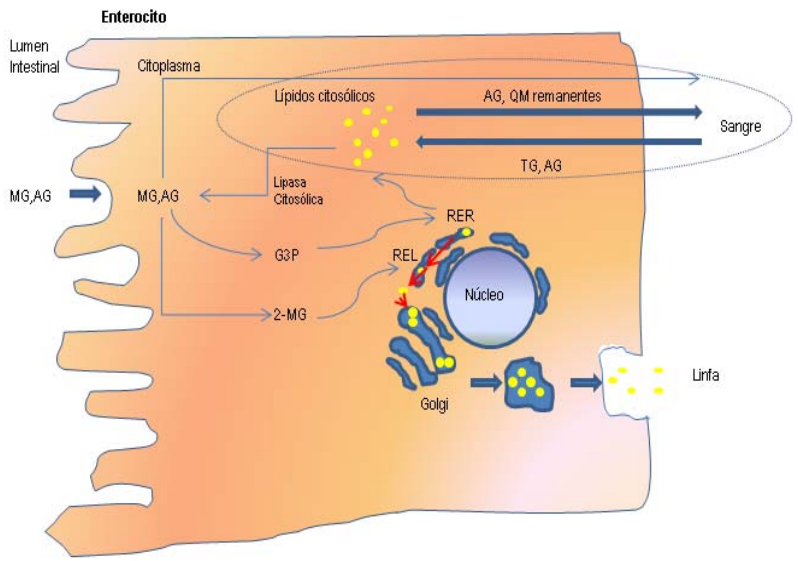

Figura 2. Absorción y disposición de lípidos en el interior del enterocito. GI: tracto gastrointestinal; MG: monoglicérido; AG: ácidos grasos; 2-MG: 2-monoglicérido; G-3P: glicerol-3-fosfato; REL: retículo endoplasmático liso; RER: retículo endoplasmático rugoso; TG: triglicéridos

Los mecanismos mediante los cuales los fármacos se unen a los quilomicrones no se conocen y poco se conoce acerca de los centros de unión intracelulares, la contribución de los lípidos o el fármaco al modelo de distribución dentro del enterocito o el papel de diferentes proteínas de unión y transporte[24, 25]. Lo que sí se conoce es que fármacos como la halofantrina, anfotericina B o la ciclosporina A se asocian a lipoproteínas[26]. Una de las hipótesis es que los fármacos son transportados en linfa asociados al núcleo triglicérido de los quilomicrones (junto con las VLDL, las lipoproteínas mayoritarias secretadas desde el enterocito)[24, 27].

III. El transporte intestinal linfático

Como se ha comentado anteriormente, los lípidos estimulan el transporte linfático. *Charman y cols*[9, 23, 25] sugieren que el transporte linfático de fármacos lipófilos tiene lugar de manera mayoritaria cuando estos tienen un coeficiente de reparto octanol/agua mayor de 5 y una solubilidad en triglicéridos de cadena larga de más de 50 mg por gramo.

El sistema linfático es una red de vasos, nódulos y tejidos linfoides distribuidos por el organismo siguiendo el recorrido del sistema vascular. La principal función del sistema linfático es mantener el balance de fluidos corporales devolviendo el exceso de líquidos, proteínas y productos de desecho desde el tejido intersticial a la circulación sanguínea. Asimismo, el tejido linfoide es un componente primordial del sistema de defensa inmunitario[9].

El sistema linfático intestinal (mesentérico) es el responsable del transporte de los lípidos provenientes de la dieta y de ciertos componentes altamente lipófilos (como son las vitaminas o fármacos liposolubles) desde las células epiteliales del intestino delgado hasta la circulación sistémica. Lo interesante de esta vía, en cuanto a biodisponibilidad y absorción de fármacos se refiere, es que la linfa proveniente del conducto torácico y mesentérico no pasa a través del hígado antes de acceder a circulación sistémica, con lo que proporciona una vía de transporte de fármacos que evita los problemas asociados al metabolismo de primer paso hepático[9].

2.- FORMULACIONES LIPÍDICAS

El creciente número de nuevos fármacos de baja solubilidad junto con el conocimiento de efecto de los lípidos como promotores de la absorción de fármacos poco solubles, ha propiciado que el interés por el desarrollo de formulaciones lipídicas se haya incrementado significativamente durante los últimos años. Tanto es así que la “American Association of Pharmaceutical Scientists” ha formado un grupo de trabajo denominado “Lipid-based Drug Delivery Systems Focus Group” (www.aaps.org/inside/focus_group/Lipid/index.asp).

Teniendo en cuenta la gran variedad de excipientes y sistemas de administración de naturaleza lipídica que se pueden utilizar, es necesario un exhaustivo conocimiento de las propiedades físico-químicas tanto del fármaco como de los excipientes lipídicos, así como del proceso de digestión en el tracto gastrointestinal de estos últimos. Además, es necesaria una adecuada caracterización de los sistemas de administración basados en lípidos, su estabilidad, clasificación y aspectos regulatorios. De esto dependerá el número de formulaciones que potencialmente pueden alcanzar el mercado[28].

Clasificación de los lípidos y tensioactivos utilizados en las formulaciones lipídicas

Los lípidos utilizados para preparar formulaciones lipídicas, incluidos los tensioactivos, fueron ya clasificados por *Small*[29] en lípidos polares y no polares, según su interacción con el agua y su comportamiento en la interfase agua-aire. Los lípidos no polares no se extienden para formar una monocapa sobre la superficie del agua, y son insolubles en ella. Ejemplos de lípidos no polares son los alcanos, aceite de parafina, ésteres de colesterol y ésteres de ácidos grasos, incluidas las ceras. Los lípidos polares se dividen en 1) lípidos insolubles que no se hinchan (clase I), que son los más hidrofóbicos, 2) lípidos insolubles que se hinchan (clase II) y 3) lípidos polares, que a su vez, se dividen en dos subclases (IIIA y IIIB) dependiendo de si forman o no líquidos cristalinos a altas concentraciones. En la tabla 1 se recoge la clasificación de los lípidos de acuerdo con este sistema.

Tabla 1. Clasificación de lípidos según su carácter polar o no polar[29].

Clase	Ejemplos	Comportamiento
No polares	Alcanos, aceite de parafina, ésteres de colesterol y ésteres de ácidos grasos, incluidas las ceras	No se extienden para formar monocapas sobre la superficie del agua. Insolubles en agua
Polares		
Insolubles que no se hinchan (Clase I)	Triacilglicéridos, diacilglicéridos, colesterol, ácidos grasos de cadena larga	Insolubles en agua que no se hinchan por captación de agua. Forman monocapas estables sobre la superficie del agua
Iinsolubles que se hinchan (Clase II)	Fosfolípidos y 2-monoacilglicéridos	Forman monocapas estables sobre la superficie del agua. Insolubles en agua Por encima de la temperatura de transición de fases, pueden incorporar agua entre el grupo polar, formando una estructura lipídica hinchada (estado cristalino líquido)
Polares solubles (Clase IIIA)	Liso-fosfolípidos, sales sódicas o potásicas de ácidos grasos de cadena larga, tensioactivos aniónicos, catiónicos y no iónicos	Forman monocapas estables in la interfase y forman micelas cuando su concentración está por encima de la concentración crítica micelar
Polares solubles (Clase IIIB)	Sales biliares, saponinas y compuestos solubles en agua con anillos aromáticos	Son capaces de formar micelas, así como monocapas inestables. No forman líquidos cristalinos a altas concentraciones

Además, existe una clasificación empírica de los lípidos polares en función del balance hidrofilia-lipofilia (HLB), que ha sido utilizado para la preparación de emulsiones. El HLB considera la contribución relativa de los fragmentos hidrofílicos e hidrofóbicos de las moléculas. Puede tomar valores del 1 al 20, de tal forma que los tensioactivos hidrofílicos presenta valores altos de HLB, mientras que los tensioactivos hidrófobos tienen valores de HLB bajos[28].

Clasificación de los sistemas de liberación basados en lípidos y tensioactivos

El término "formulación lipídica" incluye una gran variedad de formulaciones. *C.W.Pouton*[5, 30] clasificó las formulaciones lipídicas en función de la capacidad solubilizante de las mismas (LFCS, *"Lipid formulation classification system"*). Divide las formulaciones lipídicas en cuatro clases. La clase I incluye lípidos que requieren ser digeridos. Las formulaciones de la clase II son sistemas de liberación de fármacos auto emulsionables (SEDDS; *Self- emulsifying drug delivery systems*) insolubles en agua. Las formulaciones de la clase III son SEDDS o sistemas de liberación de fármacos auto microemulsionables (SMEDDS; *Self microemulsifying drug delivery systems*) que contienen tensioactivos insolubles en agua y/o cosolventes o una gran cantidad de componentes solubles en agua. Las formulaciones de la clase IV no contienen lípidos y están formadas por tensioactivos hidrófilos y cosolventes[5]. En la tabla 2 aparecen resumidas las características, ventajas y desventajas de las formulaciones lipídicas según el sistema de clasificación de *Pouton*.

Tabla 2. Clasificación de las formulaciones lipídicas de Pouton[7].
GRAS: *Generally Recognized as Safe;* SEDDS:*Self Emulsiying Drug Delivery System;* SMEDDS: *Self Micro Emulsiying Drug Delivery System*

Clase LFCS	Características	Ventajas	Desventajas
Tipo I	No dispersables Requieren digestión	GRAS; simples; compatibilidad con cápsulas	Baja capacidad solvente si el fármaco no es muy lipófilo
Tipo II	SEDDS sin componentes solubles en agua	Pérdida de capacidad solvente improbable	Dispersión o/w turbia (tamaño de partícula 0.25-2 μm)
Tipo III	SEDDS/SMEDDS con componentes solubles en agua	Dispersiones transparentes o casi; absorción de fármaco sin digestión	Posible pérdida de capacidad solvente; peor digeridas
Tipo IV	Formulaciones sin lípidos formadas por tensioactivos hidrófilos y cosolventes	Capacidad solvente para la mayoría de fármacos	Pérdida de capacidad solvente sobre la dispersión; puede no ser digerida

La clasificación de *Pouton* es un sistema muy práctico y útil para ordenar la gran cantidad de lípidos y tensioactivos que pueden ser utilizados para administrar fármacos poco solubles. *Müllertz y cols*[28] han propuesto modificar esta clasificación, teniendo en cuenta el sistema de clasificación de *Small*[29]. Estos autores proponen clasificar los lípidos teniendo en cuenta las diferencias en su interacción con el agua, su comportamiento en la interface agua-aire y el HLB, de tal forma que quedarían divididos en las siguientes categorías:

- Lípidos no polares y lípidos polares clase I
- Lípidos polares clase II
- Lípidos polares clase IIIA con bajo HLB
- Lípidos polares clase IIIA con alto HLB y cosolventes

A continuación se describirán brevemente los sistemas lipídicos más utilizados:

Soluciones oleosas

Son formulaciones a base de excipientes lipídicos que mantienen el fármaco en solución. Entre los lípidos más comúnmente utilizados están los ácidos grasos de cadena media y de cadena larga. Como se ha comentado en los apartados anteriores, existen evidencias de que las soluciones de ácidos grasos de cadena larga son más eficientes que los de cadena media, aunque debido al limitado número de estudios y a que el tipo de fármaco también influye, es difícil sacar conclusiones. Existen numerosos estudios en los que la biodisponibilidad de fármacos poco solubles se incrementa significativamente cuando se utilizan este tipo de formulaciones[31].

Emulsiones

Otra opción para incrementar la absorción de compuestos poco solubles es la preparación de emulsiones. Se han hecho numerosos estudios para demostrar la utilidad de las emulsiones para incrementar la biodisponibilidad de fármacos poco solubles, entre ellos, griseofulvina[32], ubiquinone[33], retinil palmitato[34]. En el caso de 4-hidroxylfenilretinamida (Avanti® Polar Lipids 2006), la formulación en una emulsión lipídica permitió reducir la dosis al 20% de la dosis utilizada en la formulación convencional, obteniéndose concentraciones máximas en sangre equivalentes.

Sistemas autoemulsionables (SEDDS)

Debido a su estabilidad termotrópica, los sistemas autoemulsionables forman una emulsión burda y lechosa cuando se dispersan en agua. También se han denominado sistemas microautoemulsionables (SMEDDS) y nanoautoemulsionables (SNEDDS), dependiendo del tamaño de la emulsión que forman. La microemulsión es termodinámicamente estable, mientras que una nanoemulsión sufre espontáneamente el fenómeno de coalescencia, aunque pueden tener una alta estabilidad cinética. Por ello, es difícil distinguir las micro de las nanoemulsiones. Las microemulsiones presentan un gran potencial para

incrementar la biodisponibilidad de fármacos de las clases II y IV. Sin embargo, el desarrollo de estos sistemas puede ser complicado y se requiere un gran conocimiento a nivel físico-químico, termodinámico y del proceso de digestión gastrointestinal. *Müllertz* ha publicado recientemente un artículo en el que describe una estrategia para el desarrollo de sistemas autoemulsionables[28].

Saquinavir (Invirase®) y ritonavir (Norvir®) son ejemplos de fármacos cuya biodisponibilidad por vía oral se incrementó notablemente cuando se formularon en sistemas autoemulsionables[31]. Las formulaciones lipídicas de ciclosporina A Sandimmun® y Sandimmun® Neoral®, son quizá los sistemas a base de lípidos y tensioactivos más conocidos[35]. Sandimmun® es una formulación autoemulsionable que contiene Labrafil M 1944 CS (ácidos grasos polioxietilados), aceite de oliva y etanol[36] que cuando se diluye en agua se dispersa dando lugar a una macroemulsión. En 1994, apareció una nueva formulación (Sandimmun® Neoral®), también un sistema autoemulsionable, que se emulsiona espontáneamente dando una microemulsión con un tamaño inferior a 100 nm. Esta formulación contiene Cremophor RH40 (aceite de castor polyoxil hidrogenado), glicéridos de aceite de maíz, propilenglicol y etanol[36]. Varios estudios han demostrado la mayor biodisponibilidad de la ciclosporina con Sandimmun® Neoral®[37].

Liposomas

Los liposomas fueron los primeros sistemas compuestos por una bicapa de fosfolípidos y los sistemas lipídicos nanoparticulados pioneros[38]. Desde su descubrimiento en 1965, se han logrado numerosos avances como la obtención de liposomas de circulación porlongada (pegilados), liposomas para la administración de ácidos nucleicos, liposomas dirigidos mediante ligandos, liposomas que contienen combinaciones de fármacos, etc.

Un ejemplo destacado del éxito de estos se encuentra en la comercialización los mismos; es el caso del Ambisome®/Caelyx®, liposomas de anfotericina B/ doxorrubicina clorhidrato.

Sin embargo, a pesar de la comercialización y el éxito de esta formulación, los liposomas siguen teniendo asociados problemas de inestabilidad química y

física que pueden llevar a la agregación de los liposomas y la precipitación del fármaco durante su almacenamiento[39].

Sistemas lipídicos nanoparticulados

Las nanopartículas sólidas lipídicas (SLNs) surgieron en los años 90 como sistemas alternativos a otros sistemas coloidales (nanoemulsiones, liposomas y nanopartículas poliméricas)[40, 41]. Generalmente son de forma esférica, con un diámetro comprendido entre 50 y 1000 nm, y están compuestas mayoritariamente por lípidos biocompatibles y biodegradables, capaces de incorporar tanto fármacos lipófilos como hidrófilos. Al igual que emulsiones y liposomas, son fisiológicamente compatibles y, al igual que las nanopartículas poliméricas, es posible modular la liberación del fármaco desde la matriz lipídica. Además, poseen ciertas ventajas adicionales como es la protección del fármaco en su matriz. Sin embargo, presentan las siguientes desventajas:

- Capacidad de carga de fármaco relativamente baja
- Expulsión del fármaco desde la matriz durante el almacenamiento

En la figura 3 se observan nanopartículas sólidas lipídicas elaboradas en nuestro laboratorio con Precirol ATO®5.

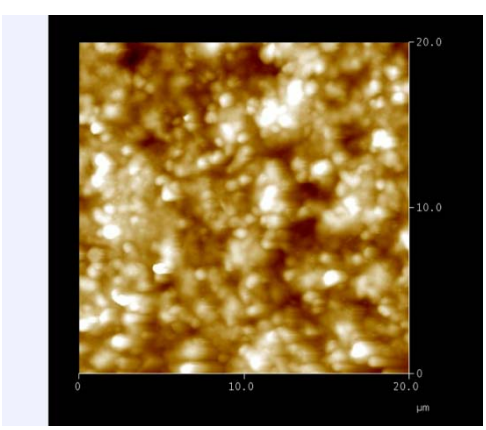

Figura 3. Fotografía obtenida mediante microscopía de fuerza atómica de nanopartículas sólidas lipídicas elaboradas con Precirol ATO®5.

Debido a las desventajas que presentan las SLNs, surgieron los lípidos nanoestructurados (Nanostructured Lipid Carriers, NLCs)[42-45]. Los NLCs están formados por moléculas lipídicas de diferente naturaleza, de tal manera que contienen lípidos sólidos y líquidos a temperatura ambiente. La matriz lipídica resultante presenta un punto de fusión menor que las SLNs, pero sigue siendo sólida a la temperatura corporal. En las NLCs, la matriz lipídica está más desestructurada, pudiendo englobar una mayor cantidad de fármaco. Además, evita o reduce la expulsión del mismo durante el almacenamiento[39, 45].

En la figura 4 se recoge una fotografía obtenida por microscopia electrónica de transmisión (TEM) de nanopartículas lipídicas de saquinavir preparadas en nuestro laboratorio con Precirol ATO®5, Mygliol 812, Tween 80 y Poloxamer 188.

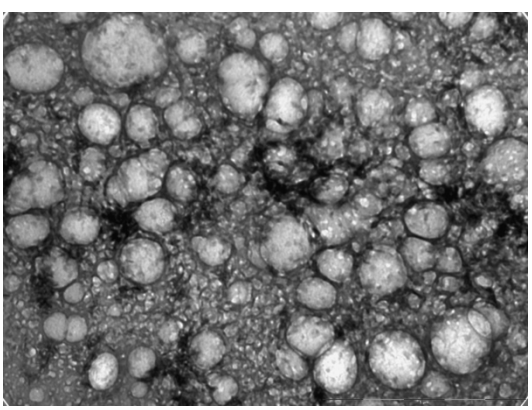

Figura 4. Fotografía de Nanostructured Lipid Carriers (NLCs) con saquinavir obtenida con microscopia electrónica de transmisión.

La diferencia básica entre la estructura de las SLNs y las NLCs, es que en el caso de estas últimas, la matriz lipídica está más desestructurada, pudiendo englobar una mayor cantidad de fármaco. Así, el uso de formulaciones lipídicas en forma de NLCs puede incrementar la biodisponibilidad de fármacos poco solubles combinando los beneficios de las formulaciones lipídicas con el hecho de ser formuladas en forma de nanopartículas[46]. En la figura 5 se recoge un esquema con la estructura de las SLNs y NLCs.

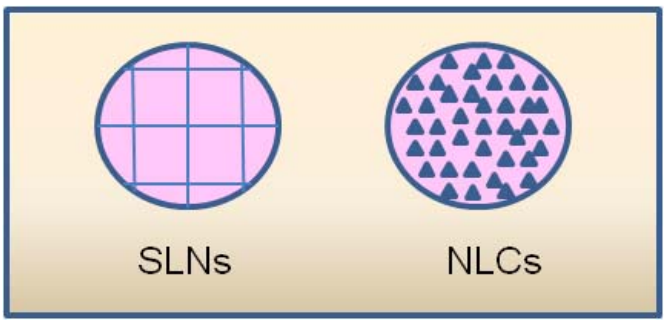

Figura 5. Representación de las estructuras correspondientes a SLNs y NLCs.

Las hipótesis que se barajan para explicar el incremento en la absorción de fármacos a partir de nanopartículas lipídicas se recogen en la figura 6. Una hipótesis es que las nanopartículas se adhieran a la pared de la mucosa intestinal y sean captadas en su totalidad, produciéndose después el metabolismo de los lípidos en el interior del enterocito. Posteriormente, debido al carácter lipófilo del fármaco, éste se anclaría en el interior del núcleo de las lipoproteínas. Otra hipótesis es la degradación en el lumen intestinal de los lípidos que forman parte de las nanopartículas por las lipasas y co-lipasas secretadas en el intestino, lo que supondría la expulsión del fármaco desde las nanopartículas. La unión del fármaco libre a sales biliares da lugar la formación de micelas solubles que atraviesan más fácilmente la pared intestinal.

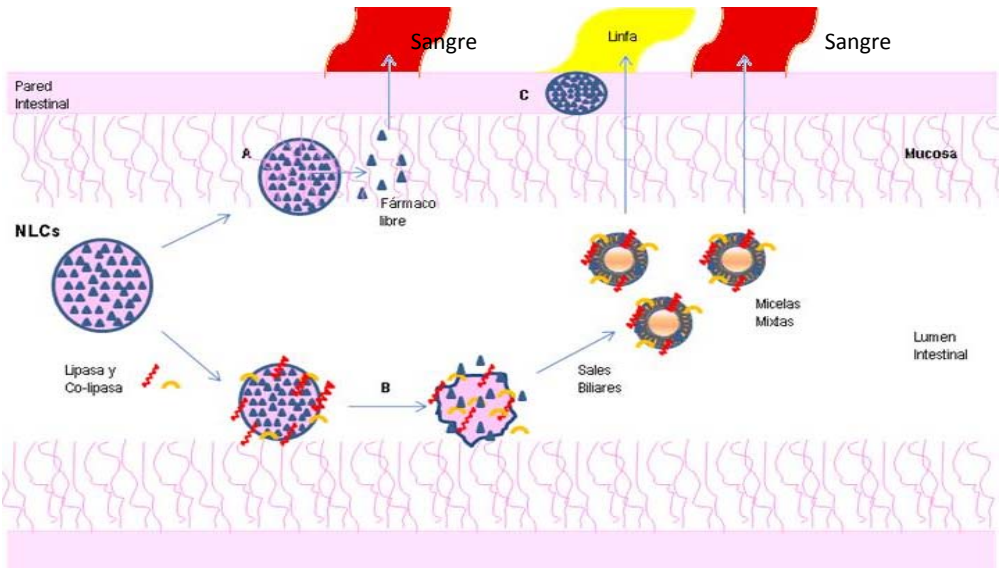

Figura 6. Mecanismos que justifican el aumento de absorción de fármacos a partir de nanopartículas lipídica. A) Mucoadhesión de las nanopartículas que irían liberando el fármaco por la degradación con el paso del tiempo B) Degradación de las nanopartículas lipídicas por parte de las lipasa y co-lipasas pancreáticas y posterior formación de micelas mediante la emulsificación por sales biliares, que accederían a linfa o sangre posteriormente C) Las NLCs atravesarían la barrera mucosa, accediendo al interior de los enterocitos donde serían procesadas; el fármaco se uniría a lipoproteínas y pasarían a linfa o a sangre.

Debido al carácter lipófilo de las SLNs y NLCs, la capacidad de carga de fármacos hidrófilos es limitada. Por ello, surgieron los conjugados lípido-fármaco (LDC). Un fármaco hidrofílico es transformado en una molécula más hidrofóbica, insoluble, al conjugarla con un compuesto lipídico. La conjugación puede llevarse a cabo mediante una unión covalente, o simplemente por formación de una sal con un ácido graso (por ejemplo, si el fármaco tiene grupos funcionales protonables)[42].

En resumen, las formulaciones lipídicas son una prometedora alternativa para administrar fármacos poco solubles. Actualmente existen comercializadas varias formulaciones lipídicas en forma de emulsiones, liposomas, SEDDS, SMEDDS. Algunos ejemplos destacados son el Ambisome®/Caelyx® (liposomas de

anfotericina B/ doxorrubicina clorhidrato), Diprivan®/Stesolid® (emulsión lipídica coloidal de propofol/ diazepam), Sandimmun® (SMEDDS de ciclosporina) o Konakion MM® (dispersión micelar de vitamina K)[47]. Sin embargo, a pesar de los avances, todavía quedan algunos problemas por resolver y son muchos los fármacos poco solubles que siguen sin poder ser formulados. Los esfuerzos que actualmente se están dedicando al estudio de las formulaciones lipídicas contribuirán sin duda al incremento del número de este tipo de formulaciones en los próximos años.

1. Dahan, A. y Hoffman, A. The effect of different lipid based formulations on the oral absorption of lipophilic drugs: the ability of in vitro lipolysis and consecutive ex vivo intestinal permeability data to predict in vivo bioavailability in rats. *Eur J Pharm Biopharm* 67, 96-105 (2007).
2. Merisko-Liversidge, E. y Liversidge, G. Drug nanoparticles: formulating poorly water-soluble compounds. *Toxicol Pathol* 36, 43-8 (2008).
3. O'Driscoll, C.M. y Griffin, B.T. Biopharmaceutical challenges associated with drugs with low aqueous solubility-The potential impact of lipid-based formulations. *Adv Drug Deliv Rev* 60, 617-624 (2008).
4. Lipinski, C., Lombardo, F., Dominy, B. y Feeney, P. Experimental and computational approaches to estimate solubility and permeability in drug discovery and development settings. *Adv Drug Deliv Rev* 46, 3-26 (2001).
5. Pouton, C.W. Formulation of poorly water-soluble drugs for oral administration: Physicochemical and physiological issues and the lipid formulation classification system. *Eur J Pharm Sci* 29, 278-287 (2006).
6. Amidon, G., Lennernäs, H., Shah, V. y Crison, J. A theoretical basis for a biopharmaceutic drug classification: the correlation of in vitro drug product dissolution and in vivo bioavailability. *Pharm Res* 12, 413-20 (1995).
7. Pouton, C.W. y Porter, C.J.H. Formulation of lipid-based delivery systems for oral administration: Materials, methods and strategies. *Adv Drug Deliv Rev* 60, 625-637 (2008).
8. Porter, C.J.H., Pouton, C.W., Cuine, J.F. y Charman, W.N. Enhancing intestinal drug solubilisation using lipid-based delivery systems. *Adv Drug Deliv Rev* 60, 673-691 (2008).
9. Porter, C., Trevaskis, N. y Charman, W. Lipids and lipid-based formulations: optimizing the oral delivery of lipophilic drugs. *Nat Rev Drug Discov* 6, 231-48 (2007).
10. Trevaskis, N.L., Charman, W.N. y Porter, C.J.H. Lipid-based delivery systems and intestinal lymphatic drug transport: A mechanistic update. *Adv Drug Deliv Rev* 60, 702-716 (2008).
11. Jannin, V., Musakhanian, J. y Marchaud, D. Approaches for the development of solid and semi-solid lipid-based formulations. *Adv Drug Deliv Rev* 60, 734-746 (2008).
12. Chen, M. Lipid excipients and delivery systems for pharmaceutical development: a regulatory perspective. *Adv*

Drug Deliv Rev 60, 768-77 (2008).

13. Hauss, D.J. Oral lipid-based formulations. *Adv Drug Deliv Rev* 59, 667-676 (2007).
14. Dahan, A. y Hoffman, A. Rationalizing the selection of oral lipid based drug delivery systems by an in vitro dynamic lipolysis model for improved oral bioavailability of poorly water soluble drugs. *J Control Release* 129, 1-10 (2008).
15. Chakraborty, S., Shukla, D., Mishra, B. y Singh, S. Lipid - An emerging platform for oral delivery of drugs with poor bioavailability. *Eur J Pharm Biopharm* 73, 1-15 (2009).
16. Kossena, G., Charman, W., Boyd, B., Dunstan, D. y Porter, C. Probing drug solubilization patterns in the gastrointestinal tract after administration of lipid-based delivery systems: a phase diagram approach. *J Pharm Sci* 93, 332-48 (2004).
17. Kossena, G. y cols. Low dose lipid formulations: effects on gastric emptying and biliary secretion. *Pharm Res* 24, 2084-96 (2007).
18. Caliph, S., Charman, W. y Porter, C. Effect of short-, medium-, and long-chain fatty acid-based vehicles on the absolute oral bioavailability and intestinal lymphatic transport of halofantrine and assessment of mass balance in lymph-cannulated and non-cannulated rats. *J Pharm Sci* 89, 1073-84 (2000).
19. Kaukonen, A., Boyd, B., Porter, C. y Charman, W. Drug solubilization behavior during in vitro digestion of simple triglyceride lipid solution formulations. *Pharm Res* 21, 245-53 (2004).
20. Kaukonen, A., Boyd, B., Charman, W. y Porter, C. Drug solubilization behavior during in vitro digestion of suspension formulations of poorly water-soluble drugs in triglyceride lipids. *Pharm Res* 21, 254-60 (2004).
21. Dahan, A. y Hoffman, A. The effect of different lipid based formulations on the oral absorption of lipophilic drugs: The ability of in vitro lipolysis and consecutive ex vivo intestinal permeability data to predict in vivo bioavailability in rats. *Eur J Pharm Biopharm* 67, 96-105 (2007).
22. Dahan, A. y Hoffman, A. Use of a dynamic in vitro lipolysis model to rationalize oral formulation development for poor water soluble drugs: correlation with in vivo data and the relationship to intra-enterocyte processes in rats. *Pharm Res* 23, 2165-74 (2006).
23. Trevaskis,N. Porter,C. y Charman,W. The lymph lipid precursor pool is a key determinant of intestinal lymphatic drug transport. *J*

Pharmacol Exp Ther 316, 881-891 (2006).

24. Gershkovich, P. y Hoffman, A. Uptake of lipophilic drugs by plasma derived isolated chylomicrons: Linear correlation with intestinal lymphatic bioavailability. *Eur J Pharm Sci* 26, 394-404 (2005).
25. Porter, C. y Charman, W. Intestinal lymphatic drug transport: an update. *Adv Drug Deliv Rev* 50, 61-80 (2001).
26. Chung, N.S. y Wasan, K.M. Potential role of the low-density lipoprotein receptor family as mediators of cellular drug uptake. *Adv Drug Deliv Rev* 56, 1315-1334 (2004).
27. Sachs-Barrable, K., Lee, S.D., Wasan, E.K., Thornton, S.J. y Wasan, K.M. Enhancing drug absorption using lipids: A case study presenting the development and pharmacological evaluation of a novel lipid-based oral amphotericin B formulation for the treatment of systemic fungal infections. *Adv Drug Deliv Rev* 60, 692-701 (2008).
28. Müllertz, A., Ogbonna, A., Ren, S. y Rades, T. New perspectives on lipid and surfactant based drug delivery systems for oral delivery of poorly soluble drugs. *J Pharm Pharmacol* 62, 1622-36 (2010).
29. Small, D.M. A classification of biologic lipids based upon their interaction in aqeous systems. *J Am Oil Chem Soc* 45, 108-19 (1968).
30. Pouton, C.W. Lipid formulations for oral administration of drugs: non-emulsifying, self-emulsifying and 'self-microemulsifying' drug delivery systems. *Eur J Pharm Sci* 11 Suppl 2, S93-8 (2000).
31. Fatouros, D.G., Karpf, D.M., Nielsen, F.S. y Mullertz, A. Clinical studies with oral lipid based formulations of poorly soluble compounds. *Ther Clin Risk Manag* 3, 591-604 (2007).
32. Bates, T.R. y Sequeria, J.A. Bioavailability of micronized griseofulvin from corn oil-in-water emulsion, aqueous suspension, and commercial tablet dosage forms in humans. *J Pharm Sci* 64, 793-7 (1975).
33. Weis, M. y cols. Bioavailability of four oral coenzyme Q10 formulations in healthy volunteers. *Mol Aspects Med* 15 Suppl, s273-80 (1994).
34. Lepage, G. y cols. Effect of an organized lipid matrix on lipid absorption and clinical outcomes in patients with cystic fibrosis. *J Pediatr* 141, 178-85 (2002).
35. Mueller, E.A. y cols. Improved dose linearity of cyclosporine pharmacokinetics from a microemulsion formulation. *Pharm Res* 11, 301-4 (1994).
36. Klyashchitsky, B.A. y Owen, A.J. Drug Delivery Systems for Cyclosporine: Achievements

and Complications. *J Drug Target* 5, 443-458 (1998).

37. Odeberg, J.M., Kaufmann, P., Kroon, K.-G. y Höglund, P. Lipid drug delivery and rational formulation design for lipophilic drugs with low oral bioavailability, applied to cyclosporine. *Eurn J Pharm Sci* 20, 375-382 (2003).
38. Allen, T.M y Cullis, P.R. Liposomal drug delivery systems: from concept toclinical applications. *Adv Drug Deliv Rev* 66, 36-48 (2013).
39. Mehnert, W. y Mäder, K. Solid lipid nanoparticles: production, characterization and applications. *Adv Drug Deliv Rev* 47, 165-96 (2001).
40. Müller, R.H., Mäder, K. y Gohla, S. Solid lipid nanoparticles (SLN) for controlled drug delivery - a review of the state of the art. *Eur J Pharm Biopharm* 50, 161-77 (2000).
41. Gasco, M.R. Lipid nanoparticles: perspectives and challenges. *Adv Drug Deliv Rev* 59, 377-8 (2007).
42. Muchow, M., Maincent, P. y Muller, R.H. Lipid nanoparticles with a solid matrix (SLN, NLC, LDC) for oral drug delivery. *Drug Dev Ind Pharm* 34, 1394-405 (2008).
43. Teeranachaideekul, V., Müller, R.H. y Junyaprasert, V.B. Encapsulation of ascorbyl palmitate in nanostructured lipid carriers (NLC)--Effects of formulation parameters on physicochemical stability. *Int J Pharm* 340, 198-206 (2007).
44. Fang, J.Y., Fang, C.L., Liu, C.H. y Su, Y.H. Lipid nanoparticles as vehicles for topical psoralen delivery: solid lipid nanoparticles (SLN) versus nanostructured lipid carriers (NLC). *Eur J Pharm Biopharm* 70, 633-40 (2008).
45. Müller, R.H., Radtke, M. y Wissing, S.A. Nanostructured lipid matrices for improved microencapsulation of drugs. *Int J Pharm* 242, 121-128 (2002).
46. Merisko-Liversidge, E.M. y Liversidge, G.G. Drug nanoparticles: formulating poorly water-soluble compounds. *Toxicol Pathol* 36, 43-8 (2008).
47. Bunjes, H. Lipid nanoparticles for the delivery of poorly water-soluble drugs. *J Pharm Pharmacol* 62, 1637-1645 (2010).

Nanopartículas lipídicas para la administración intravenosa
de fármacos poco solubles

La nanotecnología ofrece grandes oportunidades en medicina en el campo de la imagen, el diagnóstico y la terapéutica[48-51]. Actualmente se están llevando a cabo numerosos avances en el campo de la llamada "*nanoteracnóstica*[52,53]. Los sistemas de administración de fármacos nanoparticulados representan una alternativa para la mejora de las terapias actuales por su capacidad de superar múltiples barreras biológicas y liberar el compuesto terapéutico en el lugar de acción a los niveles necesarios; como resultado, se obtiene una mayor eficacia terapéutica, una reducción o mejora de los efectos adversos y un mayor cumplimiento del tratamiento por parte de los pacientes[54].

Muy frecuentemente, los sistemas basados en nanopartículas se administran por vía parenteral. Hay que tener en cuenta que el desarrollo de las nanomedicinas no es diferente del desarrollo de cualquier producto farmacéutico, en este sentido, no solamente hay que demostrar su eficacia sino que también es necesario certificar su seguridad mediante ensayos preclínicos o clínicos, antes de poder ser aprobados por las autoridades regulatorias[55].

A pesar del potencial de las nanopartículas lipídicas para la administración intravenosa de fármacos, son necesarios todavía estudios *in vivo* para confirmar su seguridad[56]. Entre otros, son necesarios estudios de biodistribución de las nanopartículas en modelos animales. La biodistribución de las nanopartículas está determinada, entre otras, por sus propiedades físico-químicas, como el tamaño, la carga o la naturaleza química de la superficie de las mimas. Nyström y Fadeel[55] han publicado recientemente una revisión de los desafíos pendientes en el campo de la nanomedicina para la correcta valoración de la eficacia y seguridad de las nanomedicinas, enumerando seis puntos claves a solventar en un futuro próximo:

1. Diseñar métodos de estudio *in vitro* validados, como tests de *nanoseguridad;*
2. Establecer modelos *ex vivo* relevantes para las diferentes vías de administración;
3. Desarrollar modelos *in silico* para predecir la respuesta biológica y toxicológica de las nanomedicinas;

4. Mejorar el conocimiento de los procesos de absorción, distribución, metabolismo y excreción (ADME) de los nanomateriales *in vivo*;

5. Mejorar el conocimiento de las interacciones entre los nanomateriales y los diferentes componentes del organismo;

6. Aumentar el conocimiento interdisciplinar y la creación de grupos de investigación interdisciplinares para mejorar los procesos de desarrollo de nanomedicinas desde el punto de vista tecnológico, clínico, biológico y toxicológico.

1.-FACTORES DETERMINANTES DE LA BIODISTRIBUCIÓN DE NANOPARTÍCULAS TRAS LA ADMINISTRACIÓN INTRAVENOSA

Conocer el comportamiento y la biodistribución de las nanopartículas *in vivo* se ha convertido en una cuestión de gran interés dentro de la comunidad científica ya que resulta de gran utilidad para predecir la eficacia y la seguridad de las nanopartículas.

Una vez en el torrente circulatorio, una de las principales causas de la desaparición de las nanopartículas es el llamado proceso de *opsonización*. Este fenómeno consiste en el anclaje de proteínas plasmáticas en la superficie de la nanopartícula y su posterior reconocimiento por parte de los macrófagos, conocidos como sistema retículoendotelial (RES) o sistema fagocítico mononuclear (SFM)[57]. Normalmente, la mayoría de las partículas opsonizadas son eliminadas mediante un mecanismo mediado por un receptor en tan sólo unos minutos debido a la alta concentración de células fagocíticas en el hígado o el bazo, o son excretadas[54]. Durante los últimos 20 años, se han estudiado numerosas estrategias para incrementar el tiempo de residencia de las nanopartículas en el torrente sanguíneo y su acumulación en tejidos específicos según el tratamiento para el que han sido desarrolladas. Las propiedades de superficie de la nanopartículas pueden favorecer o impedir el anclaje de proteínas plasmáticas y así minimizar la pérdida de partículas e incrementar el tiempo de circulación de las mismas. La carga

superficial, así como la hidrofobicidad de las nanopartículas, pueden afectar a la interacción de las partículas con proteínas plasmáticas y el aclaramiento debido a la acción de los macrófagos, jugando un papel importante en la biodistribución de las nanopartículas[54,57].

La interacción de las nanopartículas con el sistema biológico depende, entre otros factores, de parámetros como el tamaño de partícula, la carga superficial, la composición, etc…y puede ser modulada mediante diferentes estrategias como la funcionalización de las partículas con diferentes ligandos como el polietilenglicol (PEG).

Tamaño

Teniendo en cuenta determinados procesos fisiológicos como la filtración hepática, la extravasación de tejidos y la excreción renal, parece obvio que el tamaño de partícula es un parámetro determinante en la biodistribución de las nanopartículas. Las nanopartículas con un tamaño de partícula medio próximo a 100 nm presentan un tiempo de residencia en sangre prolongado y una relativa baja captación por parte del RES. *Liu y cols.*[58] investigaron la biodistribución de liposomas con tamaños comprendidos entre 30-400 nm en sangre, hígado, bazo y tumores tras la administración intravenosa de los mismos. A las 4 h post-inyección observaron que el 60% de los liposomas con tamaños comprendidos entre 100-200 nm se detectaban en sangre, mientras que sólo el 20% de la dosis inyectada de liposomas >250 nm ó <50 nm se detectó en sangre. Nanopartículas poliméricas no pegiladas de ácido polilácticoglicólico, de policaprolactona y de co-polímeros de las mismas, de tamaños comprendidos entre 90-105 nm, son secuestras rápidamente del torrente sanguíneo en cuestión de minutos y se acumulan mayoritariamente en el hígado y el bazo[59], aunque la pegilación de las mismas da como resultado una mayor permanencia de las mismas en el torrente sanguíneo[60]. *Gaumet y cols*. en su revisión sobre la influencia del tamaño en la biodistribución de las nanopartículas exponen que nanopartículas poliméricas (poloxamer 407, PEG-PLGA) o compuestas de quitosanos, con tamaños entre 30-150 nm, se localizan principalmente en la médula ósea, corazón, riñón y estómago tras su administración intravenos [61].

La acumulación selectiva de nanopartículas está favorecida en algunos tejidos debido a la presencia de una vasculatura porosa. Entre estos tejidos se encuentran el hígado, el bazo, la médula ósea o los tumores[61], estos últimos debido al denominado *fenómeno de permeabilidad y retención aumentado* (EPR). *Decuzzi y cols.*[62] enfatizan la importancia del tamaño y la forma en la distribución de las partículas, sugiriendo el uso de partículas de pequeño tamaño para garantizar una mayor uniformidad en la biodistribución de las mismas en modelos tumorales. La figura 7 muestra la acumulación en tejidos de partículas de silicona esféricas y no-esféricas tras su administración intravenosa en un modelo tumoral de ratón.

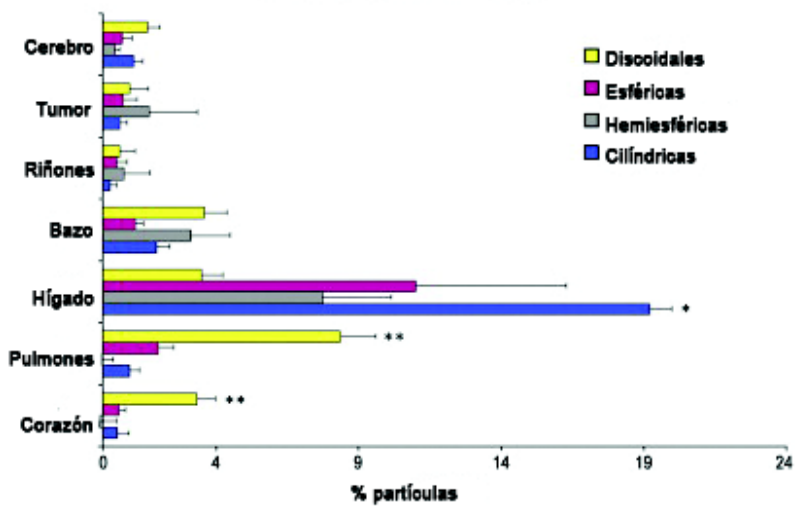

Figura 7. Acumulación en tejidos de partículas de silicona según su forma en un modelo tumoral de ratón. Re-impreso con permiso de [62].

Carga superficial

La carga superficial juega un papel muy importante en la entrada celular no específica y en la adsorción de proteínas en circulación sobre la superficie de las nanopartículas circulantes. En general, las nanopartículas cargadas positivamente se espera que presenten una mayor internalización celular no específica y corta semivida en sangre[63]. Además, la carga superficial de ciertos tipos de

nanopartículas, como las compuestas por óxido de hierro u oro, permite aumentar la estabilidad y prevenir de una posible agregación en solución acuosa por medio de la repulsión electroestática[64,65]. *He y cols.* evaluaron la captación celular y biodistribución de nanopartículas cargadas negativamente (nanopartículas de carboximetil-quitosanos marcadas con rodamina-B) y positivamente (nanopartículas de hidroclorhidro-quitosanos)[62,66]. Las partículas con carga superficial >-15 mV presentaron una captación fagocítica mayor por parte de los macrófagos murinos, y las partículas con cargas superficiales menores de este valor promovían un mayor tiempo de residencia de las nanopartículas en sangre y mayor acumulación en tumores en un modelo de ratón tumoral.

Yamamoto y cols. evaluaron el efecto de la carga superficial en micelas compuestas por co-polímeros de PEG-PLGA mediante ligandos de carga neutra (tirosina) y negativa (tirosina-glutamina). No observaron ninguna diferencia en el aclaramiento sanguíneo; sin embargo, las micelas cargadas negativamente presentaron una acumulación 10 veces menor en el hígado y en el bazo 4 horas después de la administración intravenosa[67]. Sin embargo, *Juliano y cols.* observaron que liposomas neutros y cargados positivamente eran eliminados del torrente sanguíneo más lentamente que los cargados negativamente, lo que podría ser explicado por la tendencia a la coalescencia de los liposomas cargados negativamente en presencia de proteínas e iones calcio en el plasma sanguíneo[68]. La inconsistencia de estos resultados ha sido atribuida a los diferentes tipos de nanopartículas, a la variación en la estabilidad de las nanopartículas en función de la carga superficial, a la naturaleza de los grupos responsable de la carga y a otros factores, como la falta de homogeneidad en los tamaños de partícula[69].

Composición

La composición es un factor determinante de las propiedades fisicoquímicas de las nanopartículas. Así, el tipo de tensoactivo utilizado determina la carga superficial de las nanopartículas, la hidrofobicidad de las mismas determinando la estabilidad de la formulación. La composición de las nanopartículas condiciona factores involucrados en la biodistribución de las nanopartículas mencionados anteriormente como la carga o el tamaño. De ahí que la composición

de las nanopartículas determine la interacción de las nanopartículas sobre los sistemas biólogicos. Son estas interacciones las que determinarán el destino de las nanopartículas una vez administradas dentro del organismo.

Es conocido que la unión a proteínas plasmáticas es la mayor causa que provoca cambios en el tamaño y carga superficial de las nanopartículas. Este hecho condiciona, por tanto, el perfil de biodistribución de las nanopartículas[70,71]. El concepto de corona nanopartícula-proteína está basado en el hecho de que ciertas proteínas plasmáticas se unen a la superficia de las nanopartículas, provocando cambios conformacionales en la superficie y favoreciendo la fagocitosis por parte del RES[72,73]. Es un hecho demostrado el que la inestabilidad de las nanopartículas *in vivo* puede llevar a la agregación de las mismas en el torrente sanguíneo e interferir en su biodistribución. Los tensioactivos previenen de esta agregación de las nanopartículas y, así, también disminuyen la formación de complejos nanomaterial-proteína que pueden influir en la disposición y captación de las nanopartículas, pudiendo tener una variedad de implicaciones biológicas y toxicológicas[74,75]:

i. las proteínas unidas a la superficie de las nanopartículas pueden enmascarar dicha superficie y así reducir la respuesta del sistema inmune sobre las nanopartículas, reduciendo su toxicidad
ii. la unión de proteínas a la superficie de las nanopartículas puede dar como resultado una vehiculización de proteínas activas ancladas a la superficie de las nanoartículas hacia las células
iii. las proteínas ancladas pueden sufrir cambios conformacionales en su estructura, desnaturalizándose y previniendo así de una posible interacción con las células y previniendo de su toxicidad
iv. la presencia de proteínas a nivel superficial puede interferir en la detección de las nanopartículas en los ensayos de toxicidad (por ejemplo, la detección de la producción de citoquinas [76])
v. la adsorción de proteínas a la superficie de las nanopartículas puede mejorar la dispersión de las suspensiones nanopartículadas (por ejemplo, previniendo la aglomeración y agregación entre nanopartículas).

Por tanto, parece esencial identificar las moléculas biológicas que ´cubren´ la superficie de las nanopartículas y cómo la formación de complejos nanopartícula-proteína puede condicionar su eficacia y toxicidad.

La superficie de las nanopartículas es frecuentemente modificada con la intención de controlar las interacciones nanopartícula-proteína. Por ejemplo, la pegilación es una estrategia consolidada para lograr un aumento de la semivida de las nanopartículas en sangre, ya que está demostrado que disminuye el reconocimiento de las mismas por parte del RES mediante la introducción de propiedades de "enmascaramiento" y la reducción de la adsorción de proteínas (opsonización)[77]. *Gref y cols.*[59] fueron los primeros en descubrir las ventajas de la pegilación de las nanopartículas poliméricas. Los autores observaron que una proporción de tan sólo un 0,5% de polietilenglicol (PEG) en nanopartículas de ácido polilácticoglicólico (PLA) era suficiente para disminuir significativamente la cantidad de proteínas plasmáticas adsorbidas a la superficie en comparación con nanopartículas no pegiladas. Este mismo efecto del PEG ha sido también descrito en liposomas[78] y nanopartículas lipídicas[79,80]. En la figura 8 se representa un esquema con la distribución preferencial de nanopartículas condicionadas por una diferente naturaleza fisicoquímica de superficie y una cantidad de proteínas variable unida a su superficie[70].

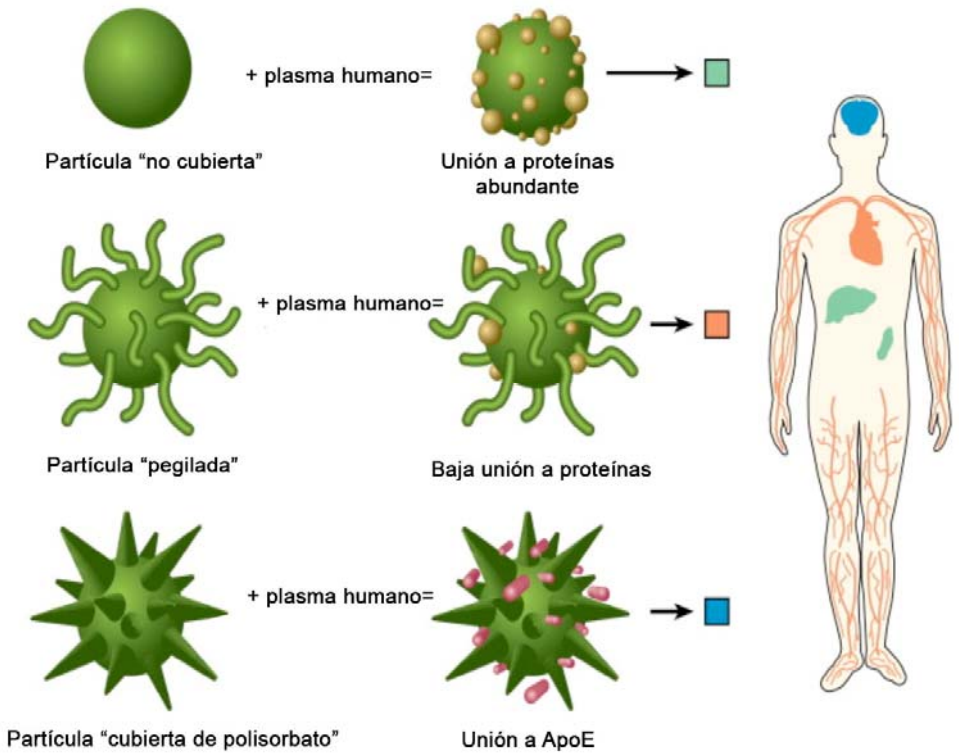

Figura 8. Biodistribución de nanopartículas según las propiedades fisicoquímicas y la cantidad de proteínas plasmáticas unidas a su superficie. Re-impreso con permiso de [70].

Se puede concluir que las propiedades físico-químicas de las nanopartículas (por ejemplo, el tamaño, la carga superficial, la hidrofobicidad, el tipo y cantidad de tensioactivo) determinan el perfil de unión a proteínas plasmáticas de las mismas (por ejemplo, la composición cualitativa y cuantitativa de las proteínas, la conformación de las mismas) y condicionan su biodistribución[81].

2.-NANOPARTÍCULAS LIPÍDICAS PARA LA ADMINISTRACIÓN INTRAVENOSA DE FÁRMACOS POCO SOLUBLES

En el año 1960, *Wretlind* desarrollaba la primera emulsión lipídica de uso parenteral (Intralipid®). Éste era el comienzo de un nuevo sistema de administración de fármacos lipófilos, en los que estos podían ser fácilmente incorporados en gotículas lipídicas. Diazelmus® (1970) y Diprivan® (1980) son ejemplos de productos comercializados con éxito basados en este sistema de administración de fármacos. La mayor ventaja de las emulsiones lipídicas es la reducción de efectos adversos en el lugar de administración. Sin embargo, presentan una gran desventaja: la baja estabilidad física del fármaco contenido en estas emulsiones debido a la disminución de la carga, puede provocar la agregación del fármaco, la expulsión del fármaco o, eventualmente, la ´rotura´ de la emulsión[82].

Al igual que para la administración oral de fármacos lipófilos poco solubles, los liposomas son también utilizados para la administración de fármacos por vía intravenosa. Formulaciones liposomales de uso parenteral comercializadas con éxito son el Ambisome® (1990, Europa; 1997, EE UU), el DaunoXome® (1996, Europa y EE UU) y el Doxil® (1995, EE UU; 1996, Europa). Las mayores desventajas que presentaban estas formulaciones, no totalmente resueltas, era la limitada estabilidad física de las dispersiones, la expulsión del fármaco, la baja actividad debida a la baja especificidad por los órganos tumorales, el aclaramiento por parte del RES y las dificultades en el escalado[83].

Las nanopartículas poliméricas podrían ser consideradas la primera generación de sistemas coloidales cuyo objetivo era el de mejorar la administración parenteral de fármacos. Su tamaño nanoparticulado, su capacidad para controlar la liberación del fármaco y la flexibilidad de su superficie para sufrir modificaciones fueron las principales características que motivaron el estudio de éstas para su administración intravenosa. Sin embargo, debido a ciertas desventajas como los problemas en el escalado a la hora de prepararlos a nivel industrial, el elevado precio de los polímeros biodegradables, la potencial toxicidad y efecto alérgeno de los polímeros biodegradables, no existe aún un producto comercializado basado en ´nano´ partículas poliméricas 35 años después de ser descritas por primera vez por

Speiser y Birenbach[84]. Sin embargo, sí que existen en el mercado sistemas basados en ´micro´ partículas poliméricas como formulaciones depot, como es el caso del Lupron® para la administración de leuprolide o Parlodel® para la administración de bromocriptina.

Desde los años 90, un gran número de investigadores ha centrado también su interés en la formulación de fármacos poco solubles basados en SLNs para su administración intravenosa. Como se ha mencionado anteriormente, las SLNs combinan las ventajas de los liposomas, nanopartículas poliméricas y las emulsions, pero, al mismo tiempo, minimizan o carecen de las desventajas asociadas con los mencionados anteriormente. Entre sus ventajas se encuentran el que, sea posible la encapsulación tanto de fármacos hidrófilos como lipófilos, su habilidad para la liberación sostenida del fármaco incorporado, su capacidad de prevenir la degradación química, fotoquímica y oxidativa del fármaco, la inmovilización del fármaco en su matriz sólida, el fácil escalado para la producción y elaboración de las SLNs y el uso de lípidos sólidos de bajo coste en comparación con fosfolípidos y polímeros biodegradables[83].

La encapsulación o la asociación de fármacos a nanopartículas altera los perfiles farmacocinéticos intrínsecos de los fármacos. Factores como la carga de fármaco, la concentración del fármaco o la agregación del fármaco en el núcleo lipídico, afectan a la cinética de liberación del fármaco, pudiendo mejorar el perfil de eficacia y seguridad, la frecuencia de administración y las fluctuaciones en las concentraciones plasmáticas del fármaco. En el caso concreto de las SLNs, el estado sólido de su matriz lipídica a temperatura ambiente favorece la estabilidad de las mismas, por lo que representan una atractiva estrategia cuando se necesite una liberación del fármaco durante tiempos prolongados[85].

Las nanopartículas lipídicas, además de constituir un vehículo seguro para incrementar la solubilidad y la estabilidad del fármaco encapsulado, pueden también ayudar a reducir drásticamente la toxicidad asociada al fármaco mediante la reducción de la biodistribución no específica mediante su transporte pasivo y activo, previniendo su secuestro por parte del RES mediante modificaciones de superficie

de la partícula (por ejemplo, pegilación) y minimizando la interacción del fármaco con otros componentes del sistema circulatorio actuando como una barrera física.

Las nanopartículas lipídicas inyectables han sido utilizadas para encapsular agentes anticancerígenos (por ejemplo, doxorrubicina, etopósido, idarrubicina), agentes de imagen (óxido de hierro, CdSEe/ZnS)[86], antiparkinsonianos (bromocriptina)[87], antiVIH (azidotimidina), antirreumáticos (actarit)[88], antiparasitarios (diminazene)[89], antihipertensivos (nitrendipino)[90] y antibióticos (tobramicina), entre otros. Entre las ventajas, un aumento del área bajo la curva concentración-tiempo (AUC) y del tiempo medio de residencia (MRT), un aumento en la eficacia anticancerígena, una mayor capacidad de llegada al cerebro y una mayor concentración de nanopartículas en el órgano/célula diana[56]. En la figura 9 aparecen representados los primeros estudios *in vivo* de SLNs encapsulando un agente anticancerígeno (camptotecina) llevados a cabo por *Yang y cols.* en el año 1999[91]. En la gráfica aparecen representados los perfiles de concentración plasmática del fármaco a lo largo del tiempo. El AUC y el MRT de la camptotecina en SLNs resultaron ser 18 veces mayores que las de la camptotecina en solución.

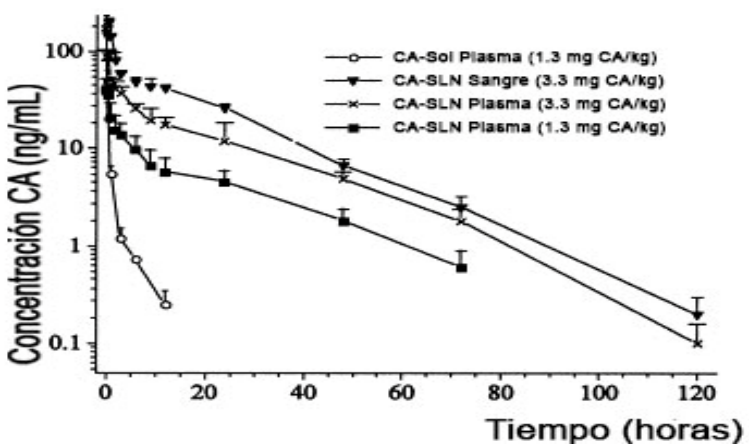

Figura 9. Curvas concentración-tiempo de camptotecina (CA) tras la administración intravenosa de camptotecina en solución (CA-sol) y encapsulada en SLNs (CA-SLNs). Re-impreso con permiso de [86].

Por tanto, las nanopartículas lipídicas constituyen una formulación prometedora para la formulación de fármacos poco solubles para administración parenteral, sin embargo aún son necesarios numerosos estudios *in vivo* que garanticen su uso.

48. Krishnaiah, Y.S.R. Pharmaceutical Technologies for Enhancing Oral Bioavailability of Poorly Soluble Drugs. *J Bioeq Availab* **2**, 28-36 (2010).
49. Merisko-Liversidge, E.M. & Liversidge, G.G. Drug nanoparticles: formulating poorly water-soluble compounds. *Toxicol Pathol* **36**, 43-48 (2008).
50. Zhang, L.*, et al.* Nanoparticles in medicine: therapeutic applications and developments. *Clin Pharmacol Ther* **83**, 761-769 (2008).
51. Hirn, S.*, et al.* Particle size-dependent and surface charge-dependent biodistribution of gold nanoparticles after intravenous administration. *Eur J Pharm Biopharm* **77**, 407-416 (2011).
52. Wang, L.S., Chuang, M.C. & Ho, J.A. Nanotheranostics - a review of recent publications. *Int J Nanomedicine* **7**, 4679-4695 (2012).
53. Mura, S. & Couvreur, P. Nanotheranostics for personalized medicine. *Adv Drug Deliv Rev* **64**, 1394-416 (2012).
54. Alexis, F., Pridgen, E., Molnar, L.K. & Farokhzad, O.C. Factors Affecting the Clearance and Biodistribution of Polymeric Nanoparticles. *Mol Pharm* **5**, 505-515 (2008).
55. Nyström, A.M. & Fadeel, B. Safety assessment of nanomaterials: Implications for nanomedicine. *J Control Release* **161**, 403-408 (2012).
56. Joshi, M.D. & Müller, R.H. Lipid nanoparticles for parenteral delivery of actives. *Eur J Pharm Biopharm* **71**, 161-172 (2009).
57. Li, S.-D. & Huang, L. Pharmacokinetics and Biodistribution of Nanoparticles. *Mol Pharm* **5**, 496-504 (2008).
58. Liu, D., Mori, A. & Huang, L. Role of liposome size and RES blockade in controlling biodistribution and tumor uptake of GM1-containing liposomes. *Biochim Biophys Acta* **1104**, 95-101 (1992).
59. Gref, R.*, et al.* Biodegradable long-circulating polymeric nanospheres. *Science* **263**, 1600-1603 (1994).
60. Gref, R.*, et al.* 'Stealth' corona-core nanoparticles surface modified by polyethylene glycol (PEG): influences of the corona (PEG chain length and surface density) and of the

core composition on phagocytic uptake and plasma protein adsorption. *Colloids Surf B Biointerfaces* **18**, 301-313 (2000).

61. Gaumet, M., Vargas, A., Gurny, R. & Delie, F. Nanoparticles for drug delivery: The need for precision in reporting particle size parameters. *Eur J Pharm Biopharm* **69**, 1-9 (2008).
62. Decuzzi, P.*, et al.* Size and shape effects in the biodistribution of intravascularly injected particles. *J Control Release* **141**, 320-327 (2010).
63. Wang, J., Byrne, J.D., Napier, M.E. & DeSimone, J.M. More effective nanomedicines through particle design. *Small* **7**, 1919-1931 (2011).
64. Thorek, D.L. & Tsourkas, A. Size, charge and concentration dependent uptake of iron oxide particles by non-phagocytic cells. *Biomaterials* **29**, 3583-3590 (2008).
65. Daniel, M.C.*, et al.* Role of surface charge density in nanoparticle-templated assembly of bromovirus protein cages. *ACS Nano* **4**, 3853-3860 (2010).
66. He, C., Hu, Y., Yin, L., Tang, C. & Yin, C. Effects of particle size and surface charge on cellular uptake and biodistribution of polymeric nanoparticles. *Biomaterials* **31**, 3657-3666 (2010).
67. Yamamoto, Y., Nagasaki, Y., Kato, Y., Sugiyama, Y. & Kataoka, K. Long-circulating poly(ethylene glycol)-poly(D,L-lactide) block copolymer micelles with modulated surface charge. *J Control Release* **77**, 27-38 (2001).
68. Juliano, R.L. & Stamp, D. The effect of particle size and charge on the clearance rates of liposomes and liposome encapsulated drugs. *Biochem Biophys Res Commun* **63**, 651-658 (1975).
69. Xiao, K.*, et al.* The effect of surface charge on in vivo biodistribution of PEG-oligocholic acid based micellar nanoparticles. *Biomaterials* **32**, 3435-3446 (2011).
70. Aggarwal, P., Hall, J.B., McLeland, C.B., Dobrovolskaia, M.A. & McNeil, S.E. Nanoparticle interaction with plasma proteins as it relates to particle biodistribution, biocompatibility and therapeutic efficacy. *Adv Drug Deliv Rev* **61**, 428-437 (2009).

71. Dobrovolskaia, M.A.*, et al.* Interaction of colloidal gold nanoparticles with human blood: effects on particle size and analysis of plasma protein binding profiles. *Nanomedicine* **5**, 106-117 (2009).
72. Nel, A.E.*, et al.* Understanding biophysicochemical interactions at the nano-bio interface. *Nat Mater* **8**, 543-557 (2009).
73. Meng, H.*, et al.* Use of Size and a Copolymer Design Feature To Improve the Biodistribution and the Enhanced Permeability and Retention Effect of Doxorubicin-Loaded Mesoporous Silica Nanoparticles in a Murine Xenograft Tumor Model. *ACS Nano* **5**, 4131-4144 (2011).
74. Dutta, D.*, et al.* Adsorbed Proteins Influence the Biological Activity and Molecular Targeting of Nanomaterials. *Toxicol Sci* **100**, 303-315 (2007).
75. Johnston, H., Brown, D., Kermanizadeh, A., Gubbins, E. & Stone, V. Investigating the relationship between nanomaterial hazard and physicochemical properties: Informing the exploitation of nanomaterials within therapeutic and diagnostic applications. *J Control Release* **164**, 307-313 (2012).
76. Brown, D.M., Dickson, C., Duncan, P., Al-Attili, F. & Stone, V. Interaction between nanoparticles and cytokine proteins: impact on protein and particle functionality. *Nanotechnology* **21**, 215104 (2010).
77. Ozcan, I.*, et al.* Pegylation of poly(γ -benzyl-L-glutamate) nanoparticles is efficient for avoiding mononuclear phagocyte system capture in rats. *Int J Nanomedicine* **5**, 1103-1111 (2010).
78. Storm, G., Belliot, S.O., Daemen, T. & Lasic, D.D. Surface modification of nanoparticles to oppose uptake by the mononuclear phagocyte system. *AdvDrug Deliv Rev* **17**, 31-48 (1995).
79. Hoarau, D.*, et al.* Novel Long-Circulating Lipid Nanocapsules. *Pharm Res* **21**, 1783-1789 (2004).
80. Ballot, S.*, et al.* ^{99m}Tc/^{188}Re-labelled lipid nanocapsules as promising radiotracers for imaging and therapy: formulation and biodistribution. *Eur J Nucl Med Mol Imaging* **33**, 602-607 (2006).
81. Muller, R.H. & Keck, C.M. Challenges and solutions for

the delivery of biotech drugs--a review of drug nanocrystal technology and lipid nanoparticles. *J Biotechnol* **113**, 151-170 (2004).

82. Collins-Gold, L., Feichtinger, N. & Wärnheim, T. Are lipid emulsions the drug delivery solution? *Modern Drug Discovery* **3**, 44-48 (2000).
83. Wissing, S.A., Kayser, O. & Müller, R.H. Solid lipid nanoparticles for parenteral drug delivery. *Adv Drug Deliv Rev* **56**, 1257-1272 (2000).
84. Allemann, E., Gurny, R. & Doelker, E. Drug-loaded nanoparticles - preparation methods drug targeting issues. *Eur J Pharm Biopharm* **39**, 173-191 (1993).
85. Constantinides, P.P., Chaubal, M.V. & Shorr, R. Advances in lipid nanodispersions for parenteral drug delivery and targeting. *Adv Drug Deliv Rev* **60**, 757-767 (2008).
86. Liu, W.*, et al.* Preparation and characterization of novel fluorescent nanocomposite particles: CdSe/ZnS core-shell quantum dots loaded solid lipid nanoparticles. *J Biomed Mater Res A* **84**, 1018-1025 (2008).
87. Esposito, E.*, et al.* Solid lipid nanoparticles as delivery systems for bromocriptine. *Pharm Res* **25**, 1521-1530 (2008).
88. Ye, J., Wang, Q., Zhou, X. & Zhang, N. Injectable actarit-loaded solid lipid nanoparticles as passive targeting therapeutic agents for rheumatoid arthritis. *Int J Pharm* **352**, 273-279 (2008).
89. Olbrich, C., Gessner, A., Schröder, W., Kayser, O. & Müller, R.H. Lipid-drug conjugate nanoparticles of the hydrophilic drug diminazene-cytotoxicity testing and mouse serum adsorption. *J Control Release* **96**, 425-435 (2004).
90. Manjunath, K. & Venkateswarlu, V. Pharmacokinetics, tissue distribution and bio-availability of nitrendipine solid lipid nanoparticles after intravenous and intra-duodenal administration. *J Drug Target* **14**, 632-645 (2006).
91. Yang, S.C.*, et al.* Body distribution in mice of intravenously injected camptothecin solid lipid nanoparticles and targeting effect on brain. *J Control Release* **59**, 299-307 (1999).


OBJECTIVES

As mentioned in the introductory section, many efforts are being made for the development of new technologies to overcome the crescent problem related with poorly water-soluble drugs. As an alternative, formulations based on lipid nanoparticles have emerged during the last decade as promising vehicles for poorly water-soluble compounds. It is important to note that nanomedicines are not different from other pharmaceutical products insofar as the safety of any new drug or drug carrier always has to be carefully assessed, through preclinical and clinical trials, prior to its approval by the regulatory agencies.

Taking into account these considerations, the main objective of the present study was to design and evaluate NLCs as a vehicle for the delivery of poorly water-soluble drugs following both the oral and the intravenous routes.

To fulfill this goal, three more specific objectives were considered:

1. To evaluate the tissue distribution of three lipid formulations based on nanostructured lipid carriers (NLCs) after intravenous administration to rats. The formulations varied in terms of particle size, surface charge and surfactant content. The ultimate scope of this work was to gain insight into how the biodistribution is affected by these physicochemical properties in order to better optimize new formulations for specific biomedical applications.

2. To investigate the potential of NLCs as an oral delivery system for poorly water-soluble compounds. For this purpose, we encapsulated spironolactone a drug with low solubility (class II drug according to the Biopharmaceutic Classification System) that undergoes efficient first-pass effect. These characteristics made it a good candidate as for being formulated in lipid nanoparticles.

3. To investigate the mechanism of transport of NLCs across the intestinal barrier. The nanocarriers containing saquinavir (SQV), a class IV drug and a P-glycoprotein (P-gp) substrate, were evaluated in an *in vitro* Caco-2 model, simulating the enterocyte barrier, and a Caco-2/Raji cell M inverted culture model, simulating the intestinal follicle-associated epithelium (FAE model). The influence of particle size, surface charge and surfactant content of the NLCs on SQV transport was studied along with the ability of NLCs to overcome the P-gp efflux.

EXPERIMENTAL DESIGN

European Journal of Pharmaceutics and Biopharmaceutics, 2013, Accepted

Biodistribution of Nanostructured Lipid Carriers (NLCs) after intravenous administration to rats: influence of technological factors

A. Beloqui[1], M. A. Solinís[1], A. Delgado[2], C. Évora[2], A. del Pozo-Rodríguez[1], A. R. Gascón[1,*]

[1]*Pharmacokinetics, Nanotechnology and Gene Therapy Group, Laboratory of Pharmacy and Pharmaceutical Technology, School of Pharmacy, University of the Basque Country UPV/EHU, Vitoria-Gasteiz, Spain*
[2]*Department of Chemical Engineering and Pharmaceutical Technology, University of La Laguna, La Laguna, Tenerife, Spain*

ABSTRACT

Nanoparticles for medical applications are frequently administered via parenteral administration. In this study, the tissue distribution of three lipid formulations based on nanostructured lipid carriers (NLCs) after intravenous administration to rats was evaluated. NLCs were prepared by a high-pressure homogenization method and varied in terms of particle size, surface charge and surfactant content. The ^{99m}Tc radiolabeled NLCs were intravenously administered to rats and radioactivity levels in blood and tissues were measured. C_{max}, AUC_{0-24} and MRT_{0-24} were obtained from the radioactivity level versus time profiles. The radiolabeled nanocarriers exhibited a long circulation time since radioactivity was detected in blood even 24 h post-injection. No differences on the MRT values in blood among the NLCs were observed, inspite of the different particle size and surface charge. The highest radioactivity levels were measured in the kidney, followed by the bone marrow, the liver and the spleen. In the kidney there was a higher accumulation of the positive nanoparticles and, in the liver, negative nanoparticles were more uptaken than positive ones. NLCs with the largest particle size showed a higher uptake in the lung and lower accumulation in liver and bone marrow, in comparison with the smaller ones.

Keywords: size, charge, surfactant, nanostructured lipid carriers, biodistribution, high-pressure homogenization, mean residence time

1.-Introduction

Nanotechnology provides important opportunities in imagining, diagnostics and therapeutics [1-4].

Nanoparticulated drug delivery systems have the potential to improve current disease therapies due to their ability to overcome multiple biological barriers and to release a therapeutic compound in the optimal dosage range. This may result in an increased therapeutic efficacy, reduced side effects and a better patient compliance [5]. After the successful development of the submicron parenteral emulsions, continuous efforts have been made to develop novel colloidal nanocarriers in order to improve the parenteral delivery. Nanocarriers have been employed for the delivery of anticancer agents [6], imaging agents [7], antiparasitics [8] agents for liver [9], the cardiovascular and central nervous system targeting [10, 11] or gene therapy [12], among others .

Polymeric nanoparticles were the first generation of novel colloidal carriers developed to improve the parenteral delivery [13]. However, they present certain disadvantages such as a high cost of biodegradable polymers, difficulties when scaling-up, and potential toxicity [14]. Lipid-based nanoparticles represent an alternative to polymeric nanoparticles as they are generally composed of lipid components that are mostly extracted from natural sources and are biocompatible and biodegradable *in vivo*. Moreover, numerous lipid excipients used to prepare lipid nanoparticles have been employed in FDA approved pharmaceutical products and have well-established safety profiles and toxicological data [15]. Although the potential of lipid nanoparticles for the intravenous delivery of drugs has been stated, there is still a necessity of *in vivo* studies establishing their parenteral acceptability for their further commercialization [14].

It is important to note that nanomedicines are not different from other pharmaceutical products insofar as the safety of any new drug or drug carrier always has to be carefully assessed, through pre-clinical and clinical trials, prior to its approval by the regulatory agencies [16]. Nyström and Fadeel [16] have recently postulated six challenges to

overcome in the foreseeable future for the safety assessment of nanomaterials, and among these, the understanding of the absorption, distribution, metabolism and excretion (ADME) of the nanomaterials *in vivo* is a mainstay. The biodistribution of nanoparticles is mainly determined by their chemical and physical properties, such as size, charge, and surface chemistry [17]. Decuzzi *et al.* [18] emphasized on the importance of size and shape in the determination of particle biodistribution.

Nanoparticles for medical applications are frequently administered via parenteral administration. In this study, the tissue distribution of three lipid formulations based on nanostructured lipid carriers (NLCs) after intravenous administration to rats was evaluated. The formulations varied in terms of particle size, surface charge and surfactant content. The ultimate scope of this work was to gain insight into how the biodistribution is affected by these physicochemical properties in order to better optimize new formulations for specific biomedical applications.

2. Materials and methods

2.1. Materials

Precirol ATO®5 was kindly provided by Gattefossé (Madrid, Spain). Tween 80 and cetyl trimethyl ammonium bromide (CTAB) were provided by Vencaser (Bilbao, Spain). Poloxamer 188 was a gift of BASF (Madrid, Spain). Miglyol 812 N/F was purchased from Sasol (Germany). $Na^{99m}TcO_4$ was obtained from a $^{99}Mo/^{99m}Tc$ generator (Drytec™) purchased from GE Healthcare Bio-Sciences. Ultrapure water was obtained from a Milli-Q® Plus apparatus (Millipore). Other chemicals were all analytical grade.

2.2. Preparation of NLCs

NLCs were prepared by the high pressure homogenization technique [19]. Precirol ATO®5 (5 g) (10% w/v) (solid lipid) and Miglyol 812 (0.5 mL) (1% w/v) (liquid lipid) were chosen as lipid matrix. The lipid phase was melted at 75 ºC until a uniform and clear oil phase was obtained. The surfactant solution was composed by Tween 80 (2 or 1% w/v) and Poloxamer 188 (1 or 0.5% w/v) which provided negative surface charge (N3 or N1.5, respectively), or Tween 80

(1% w/v) and CTAB (0.5% w/v) (P1.5), which provided positive surface charge. The hot aqueous phase was then added to the oil phase and the mixture was sonicated for 15 seconds to form a hot pre-emulsion, which was subsequently homogenized at 80°C and 500 Bar using a Stansted nG12500 homogenizer (SFP, Essex, UK) for ten homogenization cycles. In order to obtain particles with a larger particle size (N1.5 formulation), the pre-emulsion undergoing no homogenization process was assayed. The composition of the evaluated formulations is summarized on Table 1.

2.3. NLC characterization: size and zeta potential measurements

The size of NLCs was determined by photon correlation spectroscopy (PCS) and the zeta potential was measured by Laser Doppler Velocimetry (LDV) using a Malvern Zetasizer Nano ZS (Malvern Instruments Ltd., Worcestershire, U.K). Samples were diluted in MilliQ™ water before measurement.

2.4 Radiolabeling of NLCs

NLCs were labeled with ^{99m}Tc by direct labeling method using $SnCl_2 \cdot H_2O$ as reducing agent under nitrogen atmosphere [20]. Ascorbic acid was incorporated as antioxidant and due to the weak acid pH, to prevent the hydrolysis of Sn^{2+} and formation of radiocolloids (reduced and hydrolysed ^{99m}Tc). Briefly, 100 μL of an aqueous solution containing $SnCl_2 \cdot H_2O$ (1%) and ascorbic acid (5%) were added to 3 mL of NLC suspension (83±9 mg/mL) in a vial under nitrogen atmosphere and mixed. Then, 1 mL of ^{99m}Tc-eluate (1-1.5 mC_i), derived from a commercial ^{99}Mo/^{99m}Tc generator (Drytec™), was added to the vial maintaining the nitrogen atmosphere. The reaction mixture was gently stirred and incubated at room temperature for 10 min under slow orbital shaking at 150 rpm (Grant-bio, Grant Instruments). Afterwards, 100 μL of $NaHCO_3$ 0.5M were added to the labeled NLC suspension in order to achieve a pH of 5 (the pH of the original NLC suspension).

2.5 Labeling efficiency

Labeling efficiency and stability of the radiolabeled formulations was performed by two methods, instant thin layer chromatography (iTLC) and ultrafiltration. The radiolabellig stability was checked for a period of 24h after initial NLCs radiolabeling

The iTLC was carried using silica gel (SG)-coated strips (Varian Iberica, S.L.) with acetone as the mobile phase. Briefly, 5 μL of the labeled formulation was applied at 1 cm from the end of the strip and was allowed to migrate 8 cm from the point of application. The radioactivity was quantified by cutting the strip in two equal halves and then measuring the radioactivity in a gamma counter (Packard, Cobra II). Free $^{99m}TcO_4^-$ migrates with acetone to the front of the strip while the radiolabeled formulation remains at the application point.

By the ultrafiltration method, the radiolabeled NLC suspension was centrifuged (3000 rpm, 20 min) using Millipore (Madrid, Spain) Amicon® ultra centrifugal filters (molecular weight cutoff, MWCO, 100,000 Da). Free $^{99m}TcO_4^-$ was quantified by measuring the radioactivity in the filtrate using the gamma counter (Packard, Cobra II).

In vivo labeling efficiency was corroborated by comparing the radiolabeled NLC biodistribution with the biodistribution of a mixture composed by free $^{99m}TcO_4^-$ and unlabeled NLCs.

2.6 Biodistribution studies of ^{99m}Tc-NLCs in rats

Biodistribution studies were carried out in triplicate in Sprague-Dawley male rats (250-300 g). Animals were obtained from the University of La Laguna (Spain). Animals were handled in accordance with the Principles of Laboratory Animal Care [20]. Each rat received 250 μL (60-65 μC_i) of ^{99m}Tc-NLCs suspension intravenously or 1 mL (150-160 μC_i) orally administered under fasted conditions. At prefixed times (0.25, 0.5, 1, 2, 4, 8 and 24 h) rats were sacrified. Blood samples were collected (by cardiac puncture) and the heart, liver, lungs, kidneys, spleen, small intestine, brain and one femur were removed. Bone marrow was estimated as a 16% (w/w) of the femur [21]. Organ and blood

associated activity was counted using a gamma counter (Packard, Cobra II). Thyroid was also removed as a target organ for free $^{99m}TcO_4^-$ detection [22]. Results are expressed as a percentage of the total administered dose per gram of tissue and are a mean of the three rats ± S.D.

In order to check the *in vivo* radiolabeling stability, a mixture of free $^{99m}TcO_4^-$ (1-1.5 mC_i) and the NLC suspension was injected to establish the thyroid uptake in rats. At different time intervals (0.25, 1 and 2h) rats were sacrificed and radioactivity measured in blood and organs as detailed above.

2.7 Pharmacokinetic analysis

Plasma radioactivity levels were obtained from mice and were pooled to provide mean concentration data. Tissue concentrations were equally obtained.

Pharmacokinetic parameters were calculated by a non-compartment method using WinNonlin 4.1 (WinNonlin Professional version 4.1; Pharsight Corp.; Mountain View, California). The maximum radioactivity levels (C_{max}), the mean residence time (MRT_{0-24}) and the area under the curve (AUC_{0-t}) of radioactivity concentration versus time up to the last quantifiable time point parameters were used to compare the different formulations. The tissue to blood radioactivity ratio was calculated as the $AUC_{0-t,tissue}/AUC_{0-t,blood}$ ratio.

2.8 Statistical analysis

Statistical analysis was performed using SPSS 17.0 (SPSS®, Chicago, IL, USA). Normal distribution was assessed with the Shapiro-Wilk normality test. One-way ANOVA in multiple comparisons followed by Tukey´s post-hoc test were applied according to the result of the Bartlett's test of homogeneity of variances for the tissue distribution results. All other analyses were performed using a *S*tudent´s t-test. Differences were considered statistically significant at $*p<0.05$. Results are expressed as mean ± SD.

3. Results

3.1 NLCs characterization

In this study, different NLCs were prepared by the high-pressure homogenization technique. Previous studies carried out in our laboratory

allowed us to set the premises for the nanocarriers preparation employing this technique. NLCs composed by Tween 80 (2%) and Poloxamer 188 (1%) (N3) showed a zeta potential of -20±2 mV, particle size of 150±6 nm and polidispersity index (P.I.) of 0.2 (Table 1). When Poloxamer 188 was replaced by CTAB (1% Tween 80 and 0.5% CTAB) (P1.5) cationic NLCs (+44±5 mV) were obtained with a particle size of 180±7 nm and P.I. of 0.26. When the pre-emulsion was not subjected to high pressure homogenization, the NLCs, composed by the surfactants Tween 80 (1%) and Poloxamer 188 (0.5%) (N1.5), showed a zeta potential of -19±3 mV, particle size of 424±16 nm and P.I. of 0.4.

Regarding to radiolabeled particles, a good radiolabeling efficiency was obtained with all the formulations. Particularly, efficiency was 94±3 % and 93±4 % when it was measured by ultrafiltration and by iTLC, respectively. The percentage of free ^{99m}Tc in the labeling NLC suspension did not increase throughout 24 hours at room temperature, being lower than 9% for the three formulations.

Table 1. Characterization of the nanoparticles evaluated in the study. The amounts of Mygliol (1% w/v) and Precirol ATO®5 (10% w/v) were the same in the preparation of all the formulations. Data are expressed as mean ± S.D. (n=3; S.D: standard deviation). § Higher than N3 and N1.5 ($p<0.05$). * Higher than N3 and P1.5 ($p<0.001$). ¥ Higher than N3 ($P<0.05$).

	N3	**N1.5**	**P1.5**
Tween 80 (% w/v)	2	1	1
Poloxamer 188 (% w/v)	1	0.5	-
CTAB (% w/v)		-	0.5
Zeta (mV)	-20±2	-19±3	+44±5§
Size (nm)	150±6	424±16*	180±7
PI	0.2±0.03	0.4±0.04¥	0.3±0.01

3.2 Pharmacokinetics of NLCs in blood

The pharmacokinetic profile of ^{99m}Tc radiolabeled formulations in blood after intravenous administration to rats is shown in Figure 1. The highest radioactivity levels (0.25 h post-administration) ranged from 2.26 to 0.69 %ID/g depending on the administered formulation. Radio-activity was detected 24 h after the administration of the formulations, although the levels at this time were low (approximately 0.1% ID/g). These results show that the nanocarriers last in circulation for at least 24 h. Radioactivity levels measured after the administration of the P1.5 formulation were higher for the first 2 hours than levels measured after the administration of the negative nanocarriers. No significant difference was found between the two NLC formulations with negative charge, N3 and N1.5, in spite of the significant differences in particle size.

C_{max}, AUC_{0-24} and MRT_{0-24} obtained from the radioactivity levels in blood after the administration of the formulations are presented in Table 2. Higher C_{max} and AUC_{0-24} were obtained with the formulation P1.5 than those obtained with the negative nanocarriers; however, no difference in MRT_{0-24} was detected among them. In all cases, MRT_{0-24} was around 7 h.

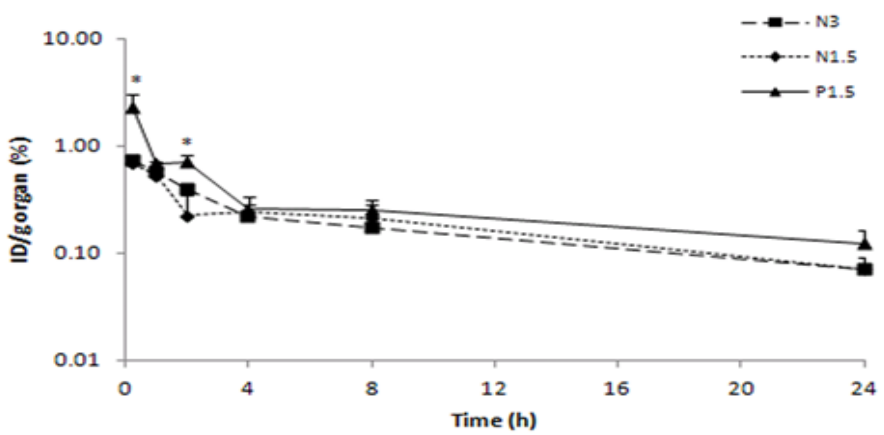

Figure 1. Biodistribution profile of ^{99m}Tc-NLCs in blood after intravenous administration to rats.

Table 2. Pharmacokinetic parameters (C_{max}, AUC_{0-24}, MRT_{0-24}) estimated for the ^{99m}Tc-NLCs (N3, N1.5 and P1.5) after intravenous administration to rats.

		C_{max}	AUC_{0-24}	MRT_{0-24}
		%ID/g	h %ID/g	h
N3	Blood	0.73	4.48	7.02
	Spleen	1.40	10.05	8.92
	Pancreas	0.19	1.16	7.54
	Small intestine	0.32	1.84	7.19
	Liver	2.33	22.05	9.32
	Kidney	3.90	72.29	9.87
	Heart	0.30	1.68	6.56
	Lung	0.45	2.51	7.13
	Bone marrow	3.38	37.46	9.21
N1.5	Blood	0.69	4.61	7.44
	Spleen	1.18	6.94	6.81
	Pancreas	0.37	1.40	6.57
	Small intestine	0.41	1.98	6.22
	Liver	1.15	7.38	6.57
	Kidney	4.59	77.97	9.38
	Heart	0.31	1.63	6.74
	Lung	2.70	9.02	4.94
	Bone marrow	1.49	20.47	9.41
P1.5	Blood	2.26	7.41	6.61
	Spleen	2.10	2.87	9.90
	Pancreas	0.74	3.04	6.75
	Small intestine	0.93	4.17	6.65
	Liver	2.57	11.25	8.69
	Kidney	7.41	112.93	10.76
	Heart	0.85	2.85	6.71
	Lung	1.78	5.69	7.37
	Bone marrow	6.75	56.80	10.20

3.3 Biodistribution of NLCs

The biodistribution of ^{99m}Tc labeled formulations over time after intravenous injection is shown in Figure 2. After 24 h, radioactivity was detected in all organs after the administration of the three formulations, although nnegligible radioactivity (<0.01%ID/g from 2 h) was detected in brain; this is the reason why Figure 2 does not show levels in this organ.

Table 2 resumes C_{max}, AUC_{0-24} and MRT_{0-24} data obtained with the N3, N1.5 and P1.5 nanocarriers. The kidney and the bone marrow were the organs that exhibited greater exposition to NLCs, since the highest values of AUC_{0-24} were measured in these organs. Moreover, the positively charged formulation (P1.5) presented higher accumulation in these organs than the anionic nanoparticles (N3 and N1.5). The liver and the spleen presented also high radioactivity levels, being higher for the formulation with negative surface charge and smaller particle size (N3). The formulation that showed higher accumulation in the lung was the anionic formulation with greater size (N1.5). The organs that showed the lowest exposition to the nanoparticles were the pancreas, the small intestine, the heart and the thyroid, regardless of the formulation.

The radioactivity measured in thyroid after the administration of free $^{99m}TcO_4^-$ was significantly higher than that measured after the administration of the radiolabeled formulations. After the administration of free $^{99m}TcO_4^-$, radioactivity levels at 0.25 h, 1 h and 2 h were 15.96, 23.66 and 21.80 %ID/g, respectively. After the administration of the nanocarriers, radioactivity levels were in all cases lower than 1 %ID/g (figure 2). These results indicate that the radioactivity measured after the administration of the formulations corresponds to the radiolabeled nanoparticles.

Concerning the MRT_{0-24}, the kidney was the organ for which this value was the highest for the three formulations, and in the case of the cationic NLCs (P1.5) the value was also elevated in the bone marrow. The lowest value for the MRT_{0-24} was observed in the lung with the anionic formulation N1.5.

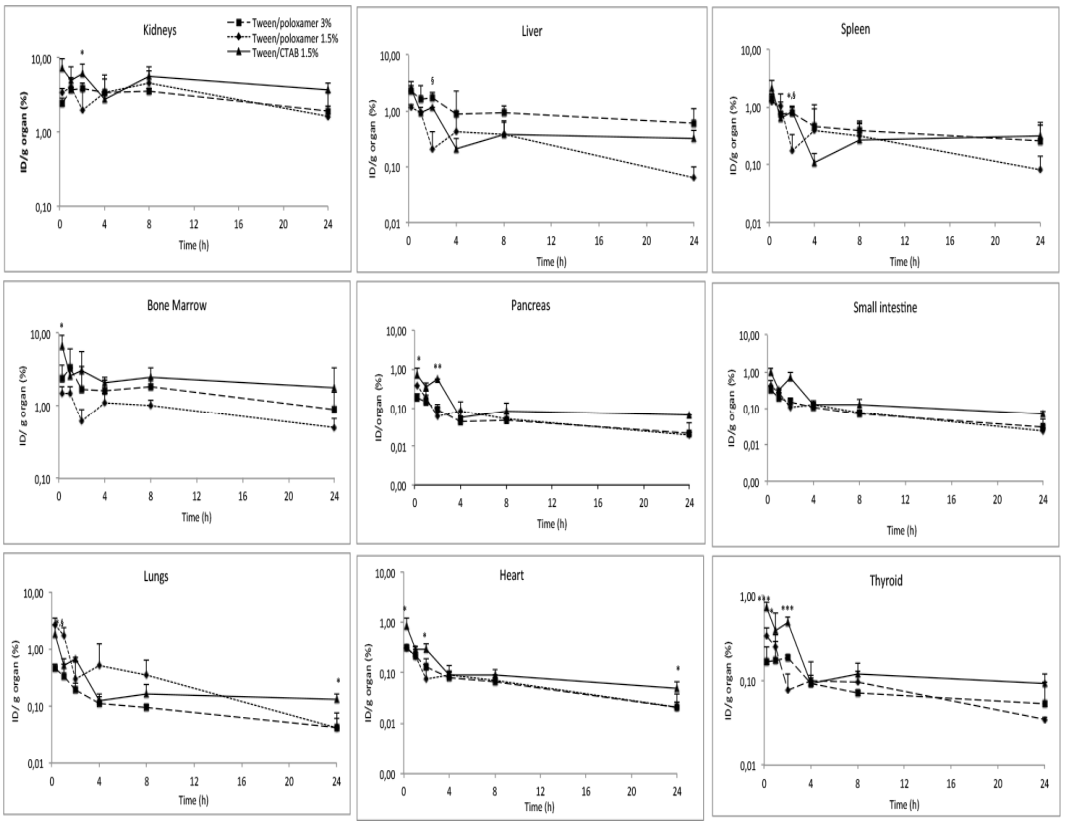

Figure 2 Biodistribution profile of ^{99m}Tc-NLCs in the removed organs after intravenous administration to rats.

Figure 3 shows the AUC_{tissue}/AUC_{blood} radioactivity ratio for the three formulations. As it can be observed, with all the three formulations the highest values were retrieved in the kidney and the bone marrow. The radioactivity ratio was higher than 1 in these organs and also in the liver, the spleen (except the P1.5 formulation), and the lung (except for the N3 formulation).

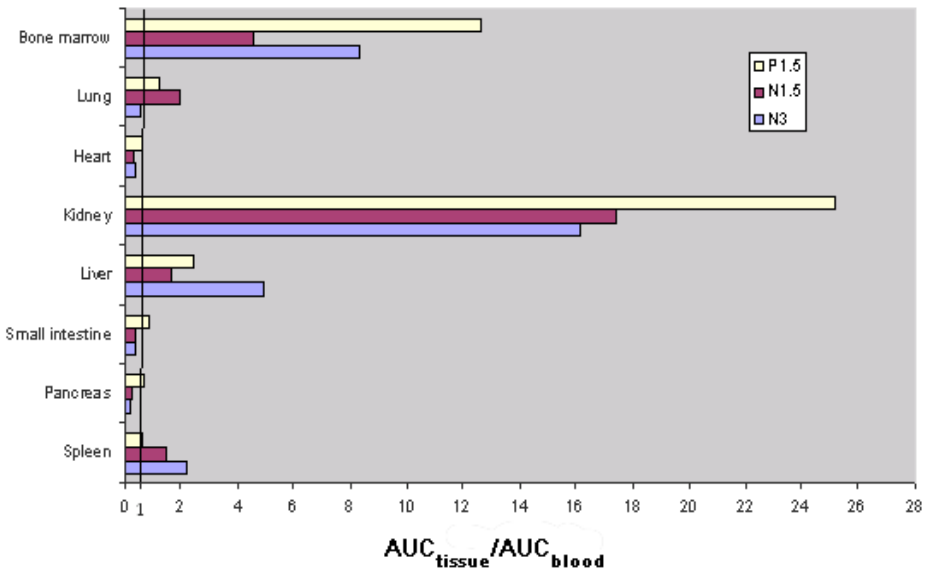

Figure 3. AUC_{tissue}/AUC_{blood} ratios for the assayed formulations.

4. Discussion

Particulate agents are useful as carrier systems of drugs, vaccines and imagining agents, among others. The knowledge of the biodistribution profile of the nanoparticles and, more specifically, how the biodistribution is influenced by their physicochemical properties, such as the size or the surface charge, can be very useful when attemping to design nanoparticle-based drugs. However, very few trends have been still identified [18]. In this study we elaborated NLCs differing on particle size, surface charge and surfactant content and administered them intravenously to rats. As expected, the application of the high pressure homogenization technique allowed us to obtain NLCs with a lower particle size and lower polidispersity index (Table 1). The higher particle size was obtained when the NLCs were

not subjected to the high pressure homogenization process, although the increment on particle size could also be due to the lower surfactant content. Regarding to the surfactants employed during the preparation of the NLCs, we obtained positively or negatively charged nanoparticles: the combination of Tween 80 and Poloxamer 188 provided negatively charged NLCs (N3 and N1.5), whereas the combination of Tween 80 and CTAB provided positively charged nanoparticles (P1.5). The different amount of surfactants in the negative formulations did not modify nanoparticle surface charge (-20±2 mV in the N3 formulation *vs.* -19±3 mV in the N1.5 formulation; $p>0.05$). On the contrary, the use of CTAB instead of Poloxamer 188 resulted on a significant increase on nanoparticle surface charge, from negative to positive (-19±3 mV in the N1.5 formulation vs. +44±5 mV in the P1.5 formulation; $^*p<0.05$).

After intravenously administered, the radiolabeled nanocarriers exhibited a long circulation time since radioactivity was detected in blood even 24 h post-injection. Actually, it is known that the solid state of the lipid matrix present in these nanoparticles at body temperature results in a much slower degradation, making NLCs attractive carriers for the formulation of long-acting controlled release preparations over extended periods of time [23]. The small particle size of our nanoparticles (from 150 nm to 424 nm), along with the presence of hydrophilic surfactants (Poloxamer 188 and Tween 80) could also justify the prolonged circulation time. Polyethylene glycol chains (PEG) in the Tween 80, and the Poloxamer 188 provide “stealth” properties to nanoparticles [24-26], which may justify the high MRT values obtained. Surface modification by pegylation is a well-established strategy for prolonging nanoparticle half-life, as it is known to decrease their recognition by the reticulo-endothelial system (RES) [27]. Gref et al. [28] were the first to report the advantages of pegylation on nanoparticles, resulting in a substantial increase in blood residence of nanoparticles. These authors observed that a PEG content in PLA nanoparticles as low as 0.5 wt % on the surface of the nanoparticles was able to significally reduce the total amount of blood protein absorbed when compared to nonpegylated PLA nanoparticles. The

effect of PEG was previously reported also for PEG-coated liposomes [29] and lipid nanocapsules [30, 31]. Due to all these properties, lipid-based nanoparticles help to stabilize drugs, such as peptides, proteins and nucleic acids, from plasma enzymes inactivation, providing an enhanced and significally prolonged biological activity [32-37].

No differences on the MRT values in blood among the NLCs were observed, in spite of the different particle size, surfactant content, and surface charge. However, cationic nanoparticles provided higher radioactivity levels during the first 2 h when compared to anionic nanoparticles and, consequently, higher AUC_{0-24} (Table 2). This may be due to a lower uptake of the positive nanoparticles by the RES organs, such as the liver or the spleen. The tissue/blood radioactivity ratio (Figure 3) confirmed the low uptake of the cationic nanocarriers by the spleen, and, in the case of the liver, these positively charged NLCs (P1.5) were less uptaken than negatively charged nanoparticles holding similar particle size (N3). These results are in accordance to previously reported studies where positively charged solid lipid nanoparticles exhibited a low uptake by the RES system [38, 39].

The highest radioactivity levels, expressed as %ID/g tissue, were observed in the kidney, followed by the bone marrow, the liver and the spleen (figure 2). In a previous study, pegylated liposomes were also detected mainly in these organs after the intravenous administration to mice [40]. The uptake into these organs is largely attributed to the macrophages residing in these tissues [17]. Taking into account the weight of the complete organ, the liver and the kidney accumulated more radioactivity, and therefore, higher amount of nanoparticles. Other authors also reported higher radioactivity levels in the kidney after intravenous administration of radiolabeled nanoparticles and liposomes [41-43]. The accumulation of the nanoparticles in the kidney could be related to their excretion in urine. The discontinuous endothelium is a characteristic of the liver and bone marrow and explain the high levels of radioactivity in these organs [17]. In our study, the distribution in bone marrow was clearly influenced by the particle size (figure 2), being higher for the smaller particles (N3

and P1.5). Snehalatha *et al.,* [42] found high levels of PLGA 85/15 nanoparticles (105 nm) in the bone following intravenous administration of ^{99m}Tc labeled nanoparticles to mice. In the authors opinion, the high radioactivity levels measured in the bone were attributed to nanoparticle uptake by the phagocytic reticulo-endothelial cells lining the vascular sinusoids of the bone marrow. As the particle size increases, more difficult is the access to bone marrow through the vascular sinusoids and explain the lower distribution of the formulation N1.5 in this tissue.

Overall, brain uptake was negligible when comparing with other organs (<0.01%ID/g). Thus, although lipid nanoparticles have been considered for brain targeting [44], certain factors such as particle size, surface properties (e.g surface charge) or the presence of hydrophilic surfactants in these nanoparticles (Tween 80 and Poloxamer 188) seem not to be suitable for brain targeting.

Nanoparticles were also found in the lung (Figure 2). The N1.5 formulation was the most extensively distributed in this organ, as indicated by the C_{max} and AUC_{0-24} (Table II). This phenomenon could be attributed to the fact that this nanocarrier presented a higher particle size and, thus, the retention in the capillaries and latter removal from the lung is likely to happen. The MRT value and the uptake of this formulation were lower in the liver and the spleen in comparison with the smaller particle size nanoparticles. Likewise, these low values could be explained by their retention and elimination in the lung.

When comparing NLCs of similar particle size and different surface charge (N3 and P1.5) both formulations were mainly located in the kidney and the bone marrow, although the positively charged nanocarriers in a higher extension (Figure 3). It can be also elucidated from Figure 3 that anionic nanoparticles were more uptaken by the RES (liver and spleen) than the cationic ones.

The MRT values in most tissues were closely to those in plasma, which indicated that unexpected accumulation should not occur in these tissues with repeated administration. Actually, prolonged circulation time also entails slow tissue accumulation of the nanoparticles and very slow drug release [17]. A rapid release

formulation (within a few hours) would be more desirable for the NLCs we have designed

Nanoparticles presenting an electrical charge, that can be either positive or negative, when intravenously administered, bind nonspecifically many products into their surface, especifically blood components. Protein binding has been pointed as a main cause of change in nanoparticle size and surface charge which leads to alterations in the biodistribution profiles and influences pathway-specific uptake following intravenous administration [4, 45]. The "nanoparticle-protein corona" concept is focused on the basis that certain serum proteins are wrapping nanoparticle surface, evoking conformational changes in the surface and enhancing phagocytosis by the RES [27, 41]. Therefore, the influence of particle size, surface charge and surfactant content on the biodistribution profile observed in our study will be also conditioned by differences in the binding pattern to blood components, which make difficult to stablish a relationship between the physicochemical properties of the nanoparticles and the biodistribution profile.

Taking into account the results obtained in our study, the potential clinical application of these nanocarriers could be focused on the preparation of long-acting controlled release formulations. The capacity to protect against plasma enzymes inactivation make these nanoparticles very useful for the administration of peptides, proteins and nucleic acids, prolonging their biological activity.

5.- Conclusions

After intravenous administration to rats, a long permanence of the nanocarriers in blood and tissues was observed. The particle size, surface charge and surfactant content of the nanoparticles affected to their tissue biodistribution profile; however, no differences in the MRT values in blood among the three formulations were found. The higher accumulation of radioactivity after the administration of the three formulations was observed in kidney, liver, bone marrow, and spleen. Comparing the nanoparticles presenting similar particle size and different surface charge, we observed a difference on the biodistribution profile. In the kidney there was a higher accumulation of the positive

formulation and, in the liver, negative nanoparticles were more uptaken than positive ones. The nanoparticles with the largest particle size showed a higher uptake in the lung and lower accumulation in liver and bone marrow, in comparison with the smaller ones.

6.-Acknowledgements

A. Beloqui wishes to thank the University of the Basque Country UPV/EHU for the fellowship grant. This work was partially supported by the Basque Government´s Department of Education, Universities and Investigation (IT-341-10) and by the Ministry of Education and Science (DCB2009-0067). We also acknowledge the Department of Nuclear Medicine at the *Hospital Universitario de Canarias* for their assistance in the biodistribution studies (Tenerife, Spain).

References

[1] Y.S.R. Krishnaiah, Pharmaceutical Technologies for Enhancing Oral Bioavailability of Poorly Soluble Drugs, J. Bioequiv. Availab. 2 (2010) 28-36.

[2] E.M. Merisko-Liversidge, G.G. Liversidge, Drug nanoparticles: formulating poorly water-soluble compounds, Toxicol. Pathol. 36 (2008) 43-48.

[3] L. Zhang, F.X. Gu, J.M. Chan, A.Z. Wang, R.S. Langer, O.C. Farokhzad, Nanoparticles in medicine: therapeutic applications and developments, Clin. Pharmacol. Ther. 83 (2008) 761-769.

[4] S. Hirn, M. Semmler-Behnke, C. Schleh, A. Wenk, J. Lipka, M. Schäffler, S. Takenaka, W. Möller, G. Schmid, U. Simon, W.G. Kreyling, Particle size-dependent and surface charge-dependent biodistribution of gold nanoparticles after intravenous administration, Eur. J. Pharm. Biopharm. 77 (2011) 407-416.

[5] F. Alexis, E. Pridgen, L.K. Molnar, O.C. Farokhzad, Factors Affecting the Clearance and Biodistribution of Polymeric Nanoparticles, Mol. Pharm. 5 (2008) 505-515.

[6] S. Acharya, S.K. Sahoo, PLGA nanoparticles containing various anticancer agents and tumour delivery by EPR effect, Adv. Drug Deliv. Rev. 63 (2011) 170-183.

[7] C. Prashant, M. Dipak, C.-T. Yang, K.-H. Chuang, D. Jun, S.-S. Feng, Superparamagnetic iron oxide – Loaded poly (lactic acid)-d-α-tocopherol polyethylene glycol 1000 succinate copolymer nanoparticles as MRI contrast agent, Biomaterials. 31 (2010) 5588-5597.

[8] A.A. Date, M.D. Joshi, V.B. Patravale, Parasitic diseases: Liposomes and polymeric nanoparticles versus lipid nanoparticles, Adv. Drug Deliv. Rev. 59 (2007) 505-521.

[9] L.F. Lai, H.X. Guo, Preparation of new 5-fluorouracil-loaded zein nanoparticles for liver targeting, Int. J. Pharm. 404 (2011) 317-323.

[10] Y. Gao, W. Gu, L. Chen, Z. Xu, Y. Li, The role of daidzein-loaded sterically stabilized solid lipid nanoparticles in therapy for cardio-cerebrovascular diseases, Biomaterials. 29 (2008) 4129-4136.

[11] S. Gelperina, O. Maksimenko, A. Khalansky, L. Vanchugova, E. Shipulo, K. Abbasova, R. Berdiev, S. Wohlfart, N. Chepurnova, J. Kreuter, Drug delivery to the brain using surfactant-coated poly(lactide-co-glycolide) nanoparticles: Influence of the formulation parameters, Eur. J. Pharm. Biopharm. 74 (2010) 157-163.

[12] A. del Pozo-Rodríguez, D. Delgado, M.Á. Solinís, J.L. Pedraz, E. Echevarría, J.M. Rodríguez, A.R. Gascón, Solid lipid nanoparticles as potential tools for gene therapy: In vivo protein expression after intravenous administration, Int. J. Pharm. 385 (2010) 157-162.

[13] D.E. Owens Iii, N.A. Peppas, Opsonization, biodistribution, and pharmacokinetics of polymeric nanoparticles, Int. J. Pharm. 307 (2006) 93-102.

[14] M.D. Joshi, R.H. Müller, Lipid nanoparticles for parenteral delivery of actives, Eur. J. Pharm. Biopharm. 71 (2009) 161-172.

[15] S.B. Lim, A. Banerjee, H. Önyüksel, Improvement of drug safety by the use of lipid-based nanocarriers, J. Control.Release 163 (2012) 34-45.

[16] A.M. Nyström, B. Fadeel, Safety assessment of nanomaterials: Implications for nanomedicine, J. Control. Release. 161 (2012) 403-8.

[17] S.-D. Li, L. Huang, Pharmacokinetics and Biodistribution of Nanoparticles, Mol. Pharma. 5 (2008) 496-504.

[18] P. Decuzzi, B. Godin, T. Tanaka, S.Y. Lee, C. Chiappini, X. Liu, M. Ferrari, Size and shape effects in the biodistribution of intravascularly injected particles, J. Control. Release. 141 (2010) 320-327.

[19] R.H. Müller, K. Mäder, S. Gohla, Solid lipid nanoparticles (SLN) for controlled drug delivery - a review of the state of the art, Eur. J. Pharm. Biopharm. 50 (2000) 161-177.

[20] G.B. Saha, Fundamentals of Nuclear Pharmacy, sixth ed., Springer, New York, 2010.

[21] Animals Guide for the Care and Use of Laboratory Animals, eigth ed., National Academies Press (US), Washington (DC), 2011.

[22] D. Dekanić, Bone marrow in male and female rats, Experientia. 34 (1978) 1313-1314.

[23] T.M. Göppert, R.H. Müller, Plasma protein adsorption of Tween 80- and poloxamer 188-stabilized solid lipid nanoparticles, J. Drug Target. 11 (2003) 225-231.

[24] S. Dufort, L. Sancey, J.L. Coll, Physico-chemical parameters that govern nanoparticles fate also dictate rules for their molecular evolution, Adv. Drug Deliv. Rev. 64 (2012) 179-189.

[25] J.M. Chae, S.M. Mo, I.J. Oh, Effects of poloxamer 188 on the characteristics of poly(lactide-co-glycolide) nano-particles, J. Nanosci. Nanotechnol. 10 (2010) 3224-3227.

[26] I. Ozcan, F. Segura-Sánchez, K. Bouchemal, M. Sezak, O. Ozer, T. Güneri, G. Ponchel, Pegylation of poly(γ-benzyl-L-glutamate) nanoparticles is efficient for avoiding mononuclear phagocyte system capture in rats, Int. J. Nanomedicine. 5 (2010) 1103-1111.

[27] R. Gref, M. Lück, P. Quellec, M. Marchand, E. Dellacherie, S. Harnish, T. Blunk, R.H. Müller, ´Stealth´corona-core nanoparticles surface modified by polyethylene glycol (PEG): influences of the corona (PEG chain length and surface density) and of the core composition on phagocytic uptake and plasma protein adsorption. Colloids Surf. B Biointerfaces 18 (2000) 301-313.

[28] G. Storm, S.O. Belliot, T. Daemen, D.D. Lasic, Surface modification of nanoparticles to oppose uptake by the mononuclear phagocyte system, Adv. Drug Deliv. Rev. 17 (1995) 31-48.

[29] D. Hoarau, P. Delmas, S.x.E. David, phanie, E. Roux, J.-C. Leroux, Novel Long-Circulating Lipid Nanocapsules, Pharm. Res. 21 (2004) 1783-1789.

[30] S. Ballot, N. Noiret, F. Hindré, B. Denizot, E. Garin, H. Rajerison, J.-P. Benoit, ^{99m}Tc/^{188}Re-labelled lipid nanocapsules as promising radiotracers for imaging and therapy: formulation and biodistribution, Eur. J. Nucl. Med. Mol. Imaging. 33 (2006) 602-607.

[31] A. Krishnadas, H. Önyüksel, I. rubinstein, Interactions of VIP, secretin and PACAP(1-38) with phospholipids: a biological paradox revisited, Curr. Pharm. Des. 9 (2003) 1005-1012.

[32] H. Önyüksel, S. Séjourné, H. Suzuki, I. Rubinstein, Human VIP-alpha: a long-acting, biocompatible and biodegradable peptide nanomedicine for essential hypertension, Peptides 27 (2006) 2271-2275.

[33] I. Rubinstein, H. Ikezaki, H. Önyüksel, Intratracheal and subcutaneous liposomal VIP normalizes arterial pressure in spontaneously hypertensive hamsters, Int. J. Pharm. 316 (2006) 144-147.

[34] A. Banerjee, H. Önyüksel, Human pancreatic polypeptide in a phospholiipid-based micellar formulation, Pharm. Res. 29 (2012) 1698-1711.

[35] A. Kuzmis, S.B. Lim, E. Desai, E. Jeon, B.S Lee, I. Rubinstein, H. Önyüksel, Micellar nanomedicine of human neuropeptide Y, Nanomedicine 7 (2011) 464-471.

[36] D. Delgado, A.R. Gascón, A. del Pozo-Rodríguez, E. Echevarria, A.P. Ruíz de Garibay, J.M. Rodríguez, M.A. Solinís, Dextran-protamine-solid lipid nanoparticles as a non-viral vector for gene therapy: in vitro characterization and in vivo transfection after intravenous administration to mice, Int. J. Pharm. 425 (2012) 35-43.

[37] L. Reddy, R. Sharma, K. Chuttani, A. Mishra, R. Murthy, Etoposide-incorporated tripalmitin nanoparticles with different surface charge: Formulation, characterization, radiolabeling, and biodistribution studies, AAPS J. 6 (2004) 55-64.

[38] L. Harivardhan Reddy, R.K. Sharma, K. Chuttani, A.K. Mishra, R.S.R. Murthy, Influence of administration route on tumor uptake and biodistribution of etoposide loaded solid lipid nanoparticles in Dalton's lymphoma tumor bearing mice, J. Control. Release. 105 (2005) 185-198.

[39] L.C. Chen, Y.H. Chen, I.H. Liu, C.L. Ho, W.C. Lee, C.H. Chang, K.L. Lang, G. Ting, T.W. Lee, J.H. Shien, Pharmacokinetics, dosimetry and comparative efficacy of 188Re-liposome and 5-FU in a CT26-luc lung-metastatic mice model, Nucl. Med. Biol. 39 (2012) 35-43.

[40] A.J. Cole, A.E. David, J. Wang, C.J. Galbán, V.C. Yang, Magnetic brain tumor targeting and biodistribution of long-circulating PEG-modified, cross-linked starch-coated iron oxide nanoparticles, Biomaterials. 32 (2011) 6291-6301.

[41] M. Snehalatha, K. Venugopal, R.N. Saha, A.K. Babbar, R.K. Sharma, Etoposide Loaded PLGA and PCL Nanoparticles II: Biodistribution and Pharmacokinetics after Radiolabeling with ^{99m}Tc, Drug Deliv. 15 (2008) 277-287.

[42] C. Yan, J. Gu, Y. Guo, D. Chen, In vivo biodistribution for tumor targeting of 5-fluorouracil (5-FU) loaded N-succinyl-chitosan (Suc-Chi) nanoparticles, Yakugaku Zasshi. 130 (2010) 801-804.

[43] I.P. Kaur, R. Bhandari, S. Bhandari, V. Kakkar, Potential of solid lipid nanoparticles in brain targeting, J. Control. Release. 127 (2008) 97-109.

[44] K. Xiao, Y. Li, J. Luo, J.S. Lee, W. Xiao, A.M. Gonik, R.G. Agarwal, K.S. Lam, The effect of surface charge on in vivo biodistribution of PEG-oligocholic acid based micellar nanoparticles, Biomaterials. 32 (2011) 3435-3446.

informa
healthcare

Journal of Microencapsulation, 2013, Under review

Fate of Nanostructured Lipid Carriers (NLCs) following the oral route: design, pharmacokinetics and biodistribution

Ana Beloqui[1], María Ángeles Solinís[1], Araceli Delgado[2], Carmen Évora[2], Arantxazu Isla[1], Alicia R. Gascón[1,*]

[1] Pharmacokinetics, Nanotechnology and Gene Therapy Group. Laboratory of Pharmacy and Pharmaceutical Technology, School of Pharmacy, University of the Basque Country (UPV/EHU), Vitoria-Gasteiz, Spain
[2] Department of Chemical Engineering and Pharmaceutical Technology, University of La Laguna, La Laguna, Tenerife, Spain

ABSTRACT

The aim of this study was to develop an NLC formulation containing spironolactone (SPN-NLCs), and to investigate its potential for the oral delivery of poorly water-soluble compounds. SPN-NLCs were orally administered to rabbits and the pharmacokinetics of spironolactone and its metabolites was evaluated. As reference formulation, we administered a syrup. Spironolactone was only detected in a few plasma samples; hence, metabolite levels were employed for the pharmacokinetic analysis. The absolute bioavailability of 7α-TMS was significantly higher with the syrup than those obtained with the SPN-NLCs (0.7 *vs* 0.4, $p<0.05$). However, no significant differences were observed in the bioavailability of canrenone, revealing a different canrenone/7α-TMS ratio depending on the administered formulation. Orally administered ^{99m}Tc-radiolabeled SPN-NLCs were mainly detected in the small intestine. These results suggest the retention of the nanocarriers in the underlying epithelium and further uptake by the epithelial cells.

Keywords: NLCs, nanoparticles, lipids, bioavailability, biodistribution, spironolactone

1. Introduction

Among the new chemical entities identified by current drug discovery techniques, over a 40% are poorly water soluble compounds (Dahan and Hoffman, 2007, Merisko-Liversidge and Liversidge, 2008, O'Driscoll and Griffin, 2008, Porter et al., 2008, Merisko-Liversidge et al., 2003, Merisko-Liversidge and Liversidge, 2011). From the early nineties onwards, many efforts have been made for the development of new technologies to overcome the crescent problem related with poorly water soluble drugs (Trevaskis et al., 2008, Hauss, 2007, Krishnaiah, 2010).

Lipid-based drug delivery systems have emerged during the last decade as promising vehicles for poorly water soluble compounds (O'Driscoll and Griffin, 2008, Porter et al., 2008, Porter et al., 2007, Trevaskis et al., 2008, Pouton and Porter, 2008, Jannin et al., 2008, Chen, 2008, Hauss, 2007, Dahan and Hoffman, 2008, Chakraborty et al., 2009, Pouton, 2006, Müllertz et al., 2010, Hauss, 2007b). Lipid formulations enhance drug absorption, and hence, drug bioavailability, through different mechanisms. Special attention should be paid to the ability of lipids to enhance drug solubilization in the gastrointestinal tract, promote intestinal lymphatic drug transport and modify enterocyte-based transport processes (Porter et al., 2007). Nanosized particles have been shown to present several advantages such as increasing solubility, enhancing dissolution rate and improving bioavailability (Teeranachaideekul et al., 2007, Müller et al., 2000, Florence, 2005). The combination of nanoparticulated devices with lipids resulted in the development of a new class of nanoparticles commonly known as solid lipid nanoparticles (SLNs) (Müller et al., 2000). SLNs are particles made from a lipid being solid at room temperature and also at body temperature. They combine advantages of different colloidal systems. Like emulsions or liposomes, they are physiologically compatible and, like polymeric nanoparticles, it is possible to modulate drug release from the lipid matrix. Moreover, SLNs possess certain advantages like the lack of organic solvent usage during the production process, when prepared by means of high pressure

homogenization techniques, and ease of scale production (Teeranachaideekul et al., 2007). However, they present associated disadvantages such as a relatively low loading capacity for several drugs, possible expulsion of the drug during storage and a high water content (Muchow et al., 2008).

A second generation of SLNs was developed to overcome these limitations: nanostructured lipid carriers (NLCs). In these nanoparticles the solid matrix is mixed with a liquid lipid (oil) to form an unstructured matrix full of imperfections, which flatters an increase in drug loading capacity of nanoparticles and avoids or reduces drug expulsion from the matrix during storage (Müller et al., 2002, Muchow et al., 2008, Müller et al., 2000).

Lipid nanoparticles are, therefore, one of the most promising delivery systems for the enhancement of bioavailability of highly lipophilic drugs (Venishetty et al., 2012) and are also an alternative drug delivery system to bypass the first pass metabolism (O'Driscoll and Griffin, 2008, Porter et al., 2008, Merisko-Liversidge and Liversidge, 2008, Venishetty et al., 2012) Spironolactone is a poorly soluble drug (class II according to the Biopharmaceutics Classification System) that undergoes efficient first-pass effect (Overdiek and Merkus, 1987). These characteristics make spironolactone a good candidate as for being formulated in lipid nanoparticles. Although the absorption of this drug may be improved by using syrups as suspending agents, this strategy is not alwas useful, as in the case of neonatal patients (Limayem Blouza et al. 2006).

The aim of this study was to develop an NLC formulation containing spironolactone, and to investigate its potential as an oral delivery system for poorly water-soluble compounds. *In vivo* studies were performed in order to evaluate the pharmacokinetics of the drug and the biodistribution of the nanoparticles.

2. Materials and methods

2.1 Materials

Spironolactone (SPN), lorazepam, pancreatin from porcine pancreas (4xUSP) and pepsin were purchased from Sigma-Aldrich Chemical Co. (Madrid, Spain). Canrenone and

lorazepam were obtained from LGC Standards (Barcelona, Spain) and 7α-thiomethylspironolactone (7α-TMS) from Toronto Research Chemicals Inc (Toronto, Canada). Precirol ATO®5 (Glyceryl palmitostearate) was kindly provided by Gattefossé (Madrid, Spain). Tween 80 was provided by Vencaser (Bilbao, Spain). Poloxamer 188 was a gift of BASF (Madrid, Spain). Miglyol 812 N/F (C8-C12 triglyceride) was purchased from Sasol (Germany). Methanol (gradient HPLC grade) was obtained from Scharlau (Barcelona, Spain). Formic acid was purchased from Panreac Quimica (Barcelona, Spain). Ultrapure water was obtained from a Milli-Q® Plus apparatus (Millipore). Other chemicals were all analytical grade. Plasma to prepare standard and quality controls for the HPLC-MS/MS analysis was provided by the Basque Biobank for Research-OEHUN (www.biobancovasco.org) and was processed following standard operation procedures with appropriate ethical approval.

2.2 Preparation of NLCs

SPN-NLCs were prepared by a high pressure homogenization technique (Müller et al., 2000). Briefly, precirol ATO®5 (5 g), Miglyol 812 (0.5 mL) and spironolactone (250 mg) were blended and melted at 75 °C to form a uniform and clear oil phase. Meanwhile, the aqueous phase was prepared by dispersing surfactants tween 80 (2%) and poloxamer 188 (1%) in water (50 mL) and heating to the same temperature as the lipid phase. The hot aqueous phase was then added to the oil phase and the mixture was sonicated during 15 seconds to form a hot pre-emulsion. This pre-emulsion was subsequently homogenized at 80°C and 500 Bar using a Stansted nG12500 homogenisizer (SFP, Essex, UK). The procedure was optimized, being necessary 10 homogenization cycles to obtain SPN-NLCs with a polydispersion index (P.I) lower than 0.2.

2.3 NLC characterization

2.3.1 Size and zeta potential measurements

Size of SPN-NLCs was determined by photon correlation spectroscopy (PCS) and zeta potential was measured by Laser Doppler Velocimetry (LDV) using a Malvern

Zetasizer Nano ZS (Malvern Instruments Ltd., Worcestershire, U.K). Samples were diluted in MilliQ™ water before measurement.

2.3.2 Morphology of NLCs

Morphology of SPN-NLCs was studied using a transmission electron microscopy (TEM, Philips EM208S). A negative staining technique with a 2% phosphotungstane acid solution was performed.

2.3.3 Drug encapsulation efficiency

Encapsulation efficiency (EE) of SPN-NLCs was calculated by determining the amount of free drug using a filtration technique. The SPN-NLCs suspension was placed in the upper chamber of Amicon® centrifugal filters (molecular weight cutoff, MWCO, 100,000 Da, Millipore, Spain) and centrifuged for 20 min at 3,000 rpm. The unencapsulated spironolactone in the filtrate was determined by HPLC-MS/MS. The total drug content in SPN-NLCs was determined by dissolving the SPN-NLCs in acetonitrile in order to release trapped spironolactone. The resulting solution was analyzed by HPLC-MS/MS. The drug loading content was the ratio of incorporated drug to lipid (w/w). The EE and drug loading were calculated by the following equations:

$$EE(\%) = \frac{W_{total} - W_{free}}{W_{total}} x100$$

$$\text{Drug loading}(\%) = \frac{W_{total} - W_{free}}{W_{lipid}} x100$$

where W_{total}, W_{free}, W_{lipid} were the weight of total drug in SPN-NLCs, the weight of unentrapped drug in ultrafiltrate and the weight of lipid added in system, respectively.

2.4 Lyophilization study

Lyophilization was performed for particle preservation during storage. SPN-NLCs were firstly frozen at -20°C and secondly at -80°C before the lyophilization step. After 24 h, frozen samples were lyophilized at -55°C and 0.2 mbar for 48 h (Telstar Cryodos freeze-dryer). Lyophilized samples were resuspended in Milli Q™ water, and then analyzed by usual inspection for freeze-drying appearance, rehydration rate and by measuring the mean particle size and zeta potential. Trehalose, sucrose and sorbitol, as most commonly used cryoprotectors (del Pozo-Rodríguez et

al., 2009, Mehnert and Mäder, 2001, Konan et al., 2002, Abdelwahed et al., 2006), were used at three different concentrations, 5, 10 and 15%, to evaluate the most suitable stabilizer for freeze drying our nanosuspensions.

2.5 In vitro dissolution assay

The *in vitro* dissolution assay was performed in simulated gastric fluid (SGF), with and without pepsin, and in simulated intestinal fluid (SIF) with and without pancreatin (European Pharmacopeia, 2007) using Quix-Sep® cells (Membrane Filtration Products Inc, TX, USA) at 37°C under magnetic stirring. A dialysis regenerated cellulose membrane having a MWCO between 6,000 and 8,000 Da was used. Previously we proved the stability of the drug in all dissolution media and that cellulose was not a rate limiting membrane for spironolactone. Membrane was first soaked in medium for 24 h before placing it in a Quix-Sep® cell. Five hundred µL of the SPN-NLCs suspension was placed in the cell and introduced into 250 mL of the medium. At fixed time intervals, samples were withdrawn from the medium and analyzed by HPLC-MS/MS using a previously validated method. The dissolution test was carried out under sink conditions.

2.6 In vivo studies

2.6.1 Pharmacokinetic studies in rabbits

2.6.1.1 Drug administration and sample collection

The *in vivo* pharmacokinetic study was carried out in male *New Zealand* rabbits (n=6) (Harlan Laboratories Models, S.L., Barcelona, Spain) in accordance with the Principles of Laboratory Animal Care (Guide for the Care and Use of Laboratory Animals,2011)

These rabbits were housed individually and fasted overnight with free access to water when orally administered. Three formulations were assayed: 1) spironolactone solution intravenously administered at a 0.5 mg/kg dose in the marginal ear vein of the rabbit (briefly, 10% EtOH, (v/v), 30% polyethylene glycol 400 (v/v) and 10% propylene glycol (v/v) in buffer solution were used to prepare the spironolactone solution (Langguth et al., 2005), 2) spironolactone suspension as

reference formulation (0.5% in simplex syrup) orally administered at a 2 mg/kg dose, and 3) spironolactone loaded NLCs at a 2 mg/kg dose.

Each animal received each formulation in a crossover study. A 7-day washout period was performed between the different treatments. At predefined times (pre-dose, 0.5, 1, 2, 3, 4, 6, 10 and 24 h) blood samples were collected from the other marginal ear vein of the rabbits in heparinized tubes. Blood samples were centrifuged at 3,000 rpm for 10 min at 4°C and the plasma was kept frozen at -80 °C until analysis.

2.6.1.2 Determination of SPN and its active metabolites, canrenone and 7α-TMS, by HPLC-MS/MS

HPLC-MS/MS determination of spironolactone and its active metabolites, canrenone and 7α-TMS, was performed with a Waters HT Alliance 2795 (Waters Corp., Milford, USA) coupled with a Micromass Quattro triple-quadrapole mass spectrometer operated in positive mode and the analytical method was validated (Food and Drug Administration, 2001). The system was controlled by Masslynx 4.1 software (Waters, UK). A reversed-phase HPLC column (Symmetry C18 4 µm, 4.6 x 150 mm) was used at room temperature. The mobile phase contained 60% methanol and 40% (v/v) of aqueous formic acid solution (0.1%). The flow rate was set at 1 mL/min in isocratic elution and it was split, with 0.50 mL entering the mass spectrometer. Electrospray ionization in the sample introduction and detection was operated in the multiple-reaction monitoring (MRM) mode. Nitrogen was used at flow rates of 600 L/h. Argon was used as collision gas at a pressure of 0.35 mL/h. The cone voltage and the collision energy were optimized for the MRM transitions. The chosen values were 30 eV for the collision energy and 40 V for the cone voltage. The optimum source and desolvation temperature were set at 150 and 350°C, respectively. Transition ions *m*/*z* 340,90→107,30 were selected for spironolactone, canrenone and 7α-TMS and 320,90→275,20 for lorazepam (used as internal standard). Liquid-liquid extraction was employed for the plasma sample preparation with dichloromethane. The injected sample volume was 25

μL and the autosampler was set at 4°C. The assay was linear over the concentration range of 2-80 ng/mL for spironolactone, and 2-200 ng/mL for canrenone and 7α-TMS. The intra- and inter-day coefficients of variation were both within ± 10%. The bias of the three analytes at three concentration levels (low, medium and high) was within ± 15%. The limit of quantification was considered the lowest level included in the calibration curve (2 ng/mL), where measures of intra-day coefficient of variation and bias were always lower than 20%. No interfering peaks were detected within the assay.

2.6.1.3 Pharmacokinetic analysis

Pharmacokinetic parameters were calculated by a non-compartment method using WinNonlin 4.1 (WinNonlin Professional version 4.1; Pharsight Corp.; Mountain View, California). The maximum plasma concentration (C_{max}) and the necessary time to reach C_{max} (T_{max}) were estimated directly from the observed concentration versus time profiles. The area under the curve of plasma concentration versus time up to the last quantificable time point, AUC_{0-t}, was obtained by the linear trapezoidal method. The AUC_{0-t} was extrapolated to infinity ($AUC_{0-\infty}$) by adding the quotient C_{last}/K_{el}, where C_{last} represents the last measured concentration and K_{el} represents the apparent terminal rate constant. K_{el} was calculated by the linear regression of the log-transformed concentrations of the drug in the terminal phase. The half-life of the terminal elimination phase was obtained using the relationship $t_{1/2}$= 0.693/ K_{el}. Mean residence time (MRT) was determined by division of AUMC (area under the first moment curve) by $AUC_{0-\infty}$. Absolute oral bioavailability (F) was calculated from plasma data of the two metabolites, as there were not detectable drug plasma levels, using the following relationship $F = [(dose_{IV} \times AUC_{0-\infty,oral})/(dose_{oral} \times AUC_{0-\infty,IV})] \times 100$.

2.6.2 Biodistribution studies in rats

2.6.2.1 Radiolabeling of SPN-NLCs

SPN-NLCs were labeled with ^{99m}Tc using $SnCl_2 \cdot H_2O$ as reducing agent and ascorbic acid as antioxidant (100 μL of a 1% and 5% solution, respectively), under nitrogen atmosphere. Labeling was carried out

adding 0.8 mL of saline solution containing 1-1.5 mC_i of ^{99m}Tc, derived from a commercial molybdenum generator, to a 3 mL volume of SPN-NLCs. The suspension was shaken for 10 min at 150 rpm. The labeled suspension was buffered with 100 μL of $NaHCO_3$ 0.5 M in order to achieve approximately a pH of 5, which is the pH of the original suspension.

2.6.2.2 Labeling efficiency

Labeling efficiency of the radiolabeled formulations was performed by instant thin layer chromatography (iTLC) using silica gel (SG)-coated strips (Varian Iberica, S.L.) with acetone as the mobile phase. Briefly, 5 μL of the labeled formulation was applied at 1 cm from the end of the strip and was allowed to migrate 8 cm from the point of application. The radioactivity was quantified by cutting the strip in two equal halves and counting in a gamma counter (Packard, Cobra II). Free $^{99m}TcO_4^-$ migrates with acetone to the front of the strip while the radiolabeled formulation remains at the application point. Radiolabeling efficiency was also confirmed by filtration: the radiolabeled SPN-NLCs suspension was placed in the upper chamber of Amicon® centrifugal filters (molecular weight cutoff, MWCO, 100,000 Da, Millipore, Spain) and centrifuged for 20 min at 3000 rpm. Free $^{99m}TcO_4^-$ was quantified in the filtrate. In all cases, the labeling efficacy was >90%. The stability of the labeled formulations was checked over a period of 24h by iTLC, as described above.

2.6.2.3 Biodistribution study performance

Biodistribution studies were carried out in triplicate in Sprague-Dawley male rats (250-300 g). Animals were obtained from the University of La Laguna (Spain). As previously, animals were handled in accordance with the Principles of Laboratory Animal Care (Guide for the Care and Use of Laboratory Animals, 2011). Each rat received 1 mL of the radiolabelled SPN-NLCs suspension (150-160 μCi) orally administered under fasted conditions. At prefixed times (0.25, 0.5, 1, 2, 4, 8 and 24 h) rats were sacrificed. Blood samples were collected (by cardiac puncture) and the heart, liver, lungs, kidneys, spleen, small intestine, thyroid, brain and one femur were removed. Organ and blood associated activity was counted using a gamma counter

(Packard, Cobra II). The radioactivity in the organ/tissues was expressed as the percent of the total measured radioactivity.

2.7 Statistical analysis

Statistical data were performed with SPSS 17.0.1 for Windows® (SPSS®, Chicago, USA) using the Student´s *t*-test.

Differences were considered statistically significant at $p<0.05$. Data are presented as mean ± standard deviation (S.D).

3. Results

3.1. NLC characterization

We obtained SPN-NLCs with a particle size of 150 ± 5 nm and a surface charge of -20 ± 2 mV with a P.I lower than 0.2. Figure 1 shows a SPN-NLC photograph obtained by TEM. Encapsulation efficiency was higher than 99% and the drug loading was 2.46%.

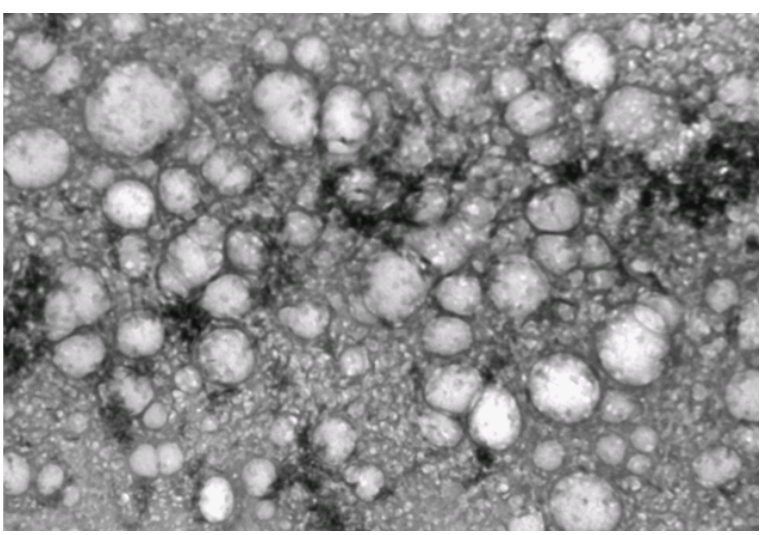

Fig 1. SPN-NLC photograph obtained by TEM.

3.2 Lyophilization study

Lyophilization of SPN-NLCs without cryoprotectors resulted in the aggregation of these particles forming a cake with rubbery aspect. When sorbitol and sucrose were used as stabilizers, the lyophilized samples showed a powdery aspect but redispersion in water was not feasible. By contrast, when lyophilization was carried out with trehalose as cryoprotector, aspect was powdery and redispersion in water was optimum. Figure 2 shows the increase in particle size of NLCs after lyophilization with the three cryoprotectors at 5% (A) and the influence of trehalose concentration on particle size variation (B). The increment in particle size was lower when using trehalose as cryoprotective agent in comparison with sorbitol or sucrose. No significant difference was observed in particle size when using different trehalose concentrations. In all cases, surface charge did not change and was around -20 mV.

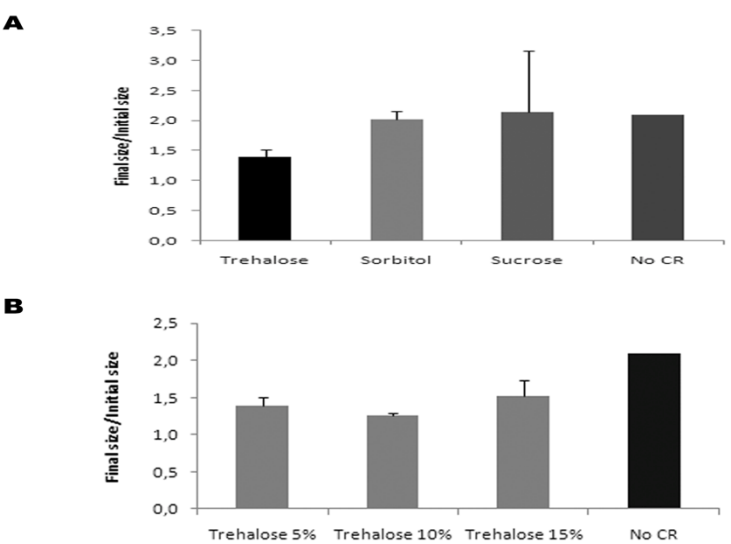

Fig 2. A) Changes on particle size of non-lyophilized and lyophilized NLCs in the presence of trehalose, sorbitol and sucrose cryoprotectors. B) Influence of trehalose concentration on particle size variation. FD: Freeze-drying; CR: cryoprotector

3.3 In vitro dissolution assay

Figure 3 shows spironolactone dissolution profiles in SGF with pepsin and in SIF with and without pancreatin. Drug released levels in SGF without pepsin were under the limit of quantification and, thus, data are not represented in the graph.

Spironolactone release appeared to be 0.5% in SGF after 2 hours and less than 5% in the SIF after 8 hours. As Figure 3 shows, the presence of enzymes in the SIF dissolution media did not modify the release profile.

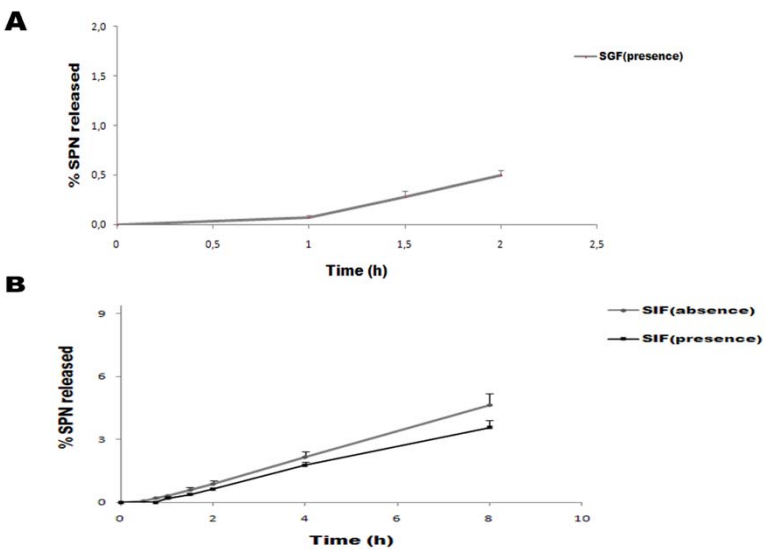

Fig 3. Dissolution profiles of spironolactone from NLCs after their incubation in SGF in the presence of pepsin (A) and SIF (B) medium in the presence and absence of pancreatin. SGF: simulated gastric fluid; SIF: simulated intestinal fluid; SPN: spironolactone

3.4 In vivo studies

3.4.1 Pharmacokinetic studies in rabbits

After the oral administration of the SPN-NLCs and the intravenous administration of spironolactone, the parent drug was only detected in a few plasma samples, and in most cases, levels were under the limit of quantification (2 ng/mL). Hence, plasma concentrations of its metabolites, canrenone and 7α-TMS, were used as surrogates for biopharmaceutical comparison of the administered formulations.

Figure 4 shows the mass chromatograms of drug-free plasma sample indicating that no endogenous peaks are present at the retention times of spironolactone and the two metabolites, canrenone and 7α-TMS. This figure also shows that the mass chromatograms of plasma spiked with 2 ng/mL of spironolactone, canrenone and 7α-TMS. Metabolites were properly separated under the above-mentioned conditions.

Figure 5 shows plasma concentration-time profile of both metabolites after intravenous administration of spironolactone (0.5 mg/kg). It is remarkable that 7α-TMS levels in plasma were higher than canrenone levels, with a concentration of 8.56 ng/mL for canrenone and 44.66 ng/mL for 7α-TMS at 0.5 h. In a study performed by Langguth *et al.* (Langguth et al., 2005) in rats, the authors also found higher 7α-TMS levels than canrenone levels.

Figure 6 shows plasma concentration-time profiles of both metabolites after oral administration (2 mg/kg) of spironolactone as syrup or as SPN-NLCs. In both cases, 7α-TMS plasma levels were also higher than canrenone levels.

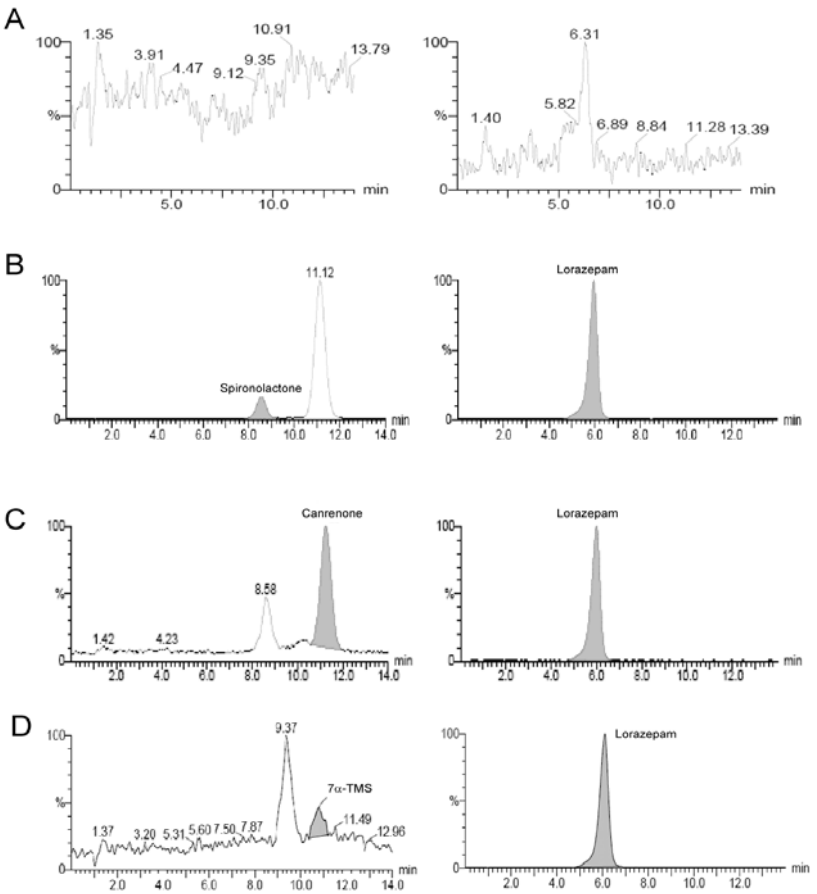

Fig 4. Chromatograms corresponding to drug-free plasma (A) and plasma spiked with 2 ng/mL of spironolactone (B), canrenone (C), and 7α-TMS (D). On the right the channel corresponding to the internal standard (lorazepam).

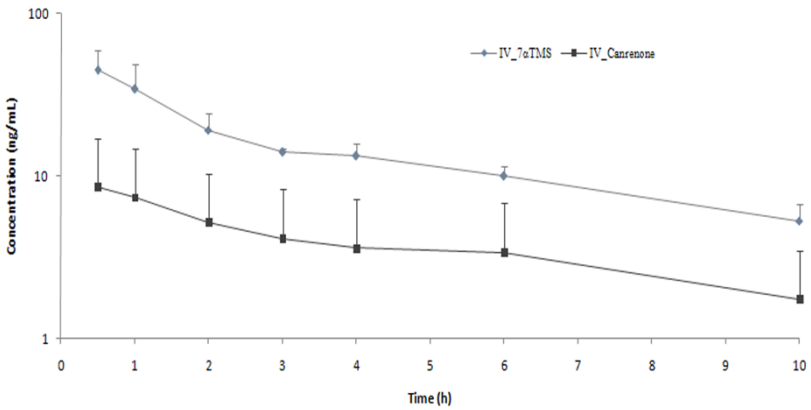

Fig 5. Concentration-time profiles of both spironolactone metabolites, canrenone and 7α-TMS, after intravenous administration of spironolactone.

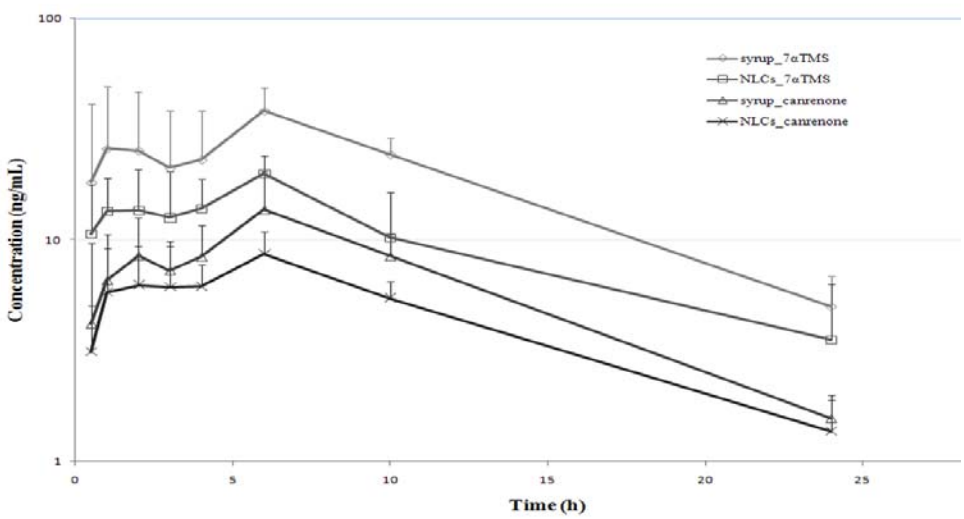

Fig 6. Concentration-time profiles of both metabolites, canrenone and 7α-TMS, after oral administration of SPN-NCLs and the syrup.

Table I shows the pharmacokinetic parameters (± SD) of canrenone and 7α-TMS calculated by a noncompartmental analysis. Absolute bioavailability (F) of spironolactone, measured in terms of canrenone, did not show significant differences between syrup (0.8) and SPN-NLCs (0.6) ($p>0.05$). However, F calculated from plasma levels of 7α-TMS was 0.7 for the syrup and 0.4 for NLCs ($p<0.05$).

		Syrup		NLCs		IV	
		Canrenone	7α-TMS	Canrenone	7α-TMS	Canrenone	7α-TMS
$t_{1/2}$	h	6.01 ± 1.07	5.97 ± 1.02	6.76 ± 1.06	8.09 ± 2.94	6.31 ± 2.64	4.56 ± 0.99
T_{max}	h	5.20 ± 1.79	5.80 ± 3.19	5.40 ± 1.34	4.88 ± 4.09	0.50 ± 0.00	0.50 ± 0.00
C_{max}	ng/mL	14.90 ± 6.07	44.26 ± 15.74	8.71 ± 2.23	21.76 ± 4.78	8.47 ± 2.74	36.54 ± 8.83
AUC_{0-t}	h ng/mL	163.59 ± 35.13	478.64 ± 98.37	113.05 ± 24.76	290.14 ± 74.94	38.77 ± 7.24	137.98 ± 18.48
$AUC_{0-\infty}$	h ng/mL	177.32 ± 34.57	523.92 ± 103.80	127.15 ± 32.43	348.73 ± 116.18	55.18 ± 8.43	172.68 ± 27.24
MRT	h	10.31 ± 1.42	10.58 ± 2.19	10.79 ± 1.92	12.79 ± 3.75	8.45 ± 2.77	5.92 ± 1.64
F		0.8 ± 0.2	0.7 ± 0.1*	0.6 ± 0.2	0.4 ± 0.2*		

Table I. Pharmacokinetic parameters of canrenone and 7 α-TMS obtained by a noncompartmental analysis.*$p<0.05$

3.4.2 Biodistribution studies in rats

Figure 7 shows the results obtained in the biodistribution study with the SPN-NLCs labeled with ^{99m}Tc. After oral administration to rats, radioactivity was mainly detected in the small intestine. In the liver and kidney, a significant level of radioactivity was also detected. Radioactivity was also detected in feces in to a significant degree (data not shown).

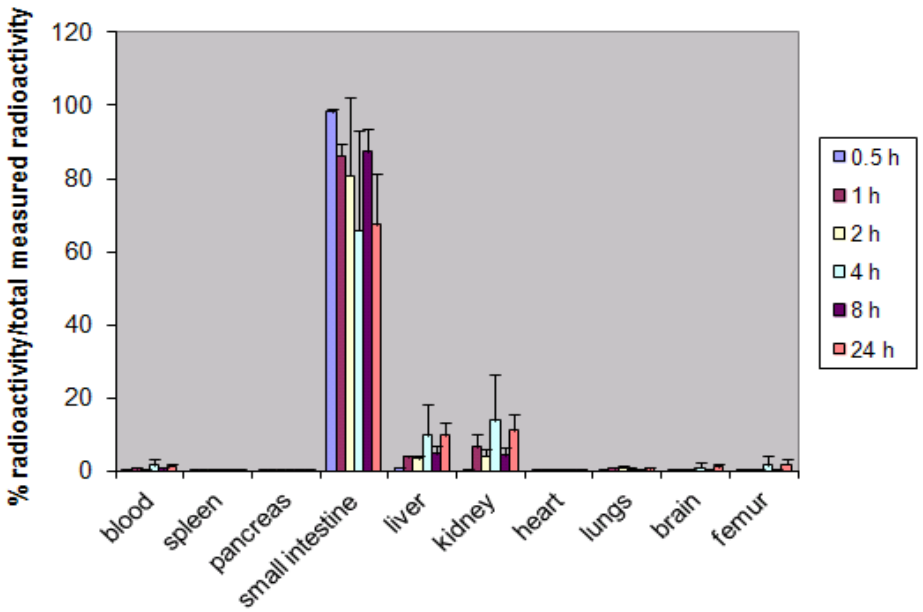

Fig 7. %radioactivity measure per organ/tissues after oral administration of SPN-NLCs labeled with ^{99m}Tc.

4. Discussion

The clinical use of many new chemical compounds is limited due to their poor water solubility. New lipid fomulations are emerging in order to solve this drawback and enhance drug absorption. In this study, we have developed a formulation based on NLCs for spironolactone delivery by a high pressure homogenization method. This procedure allowed us to obtain without the use of any organic solvent, spherical and homogeneous in size nanoparticles with an encapsulation efficiency above 99%. The lipids employed for the preparation of the SPN-NLCs, mygliol and precirol, are recognized as totally biocompatible, reducing the possibility of side effects appearance after the *in vivo* admistration. Tween 80 and Poloxamer 188 were used as surfactants. On the one hand, poloxamer is an sterically stabilizing polymer and due to the stearic hindrance, induces a slow degradation of the nanoparticles

(Müller et al., 2006). On the other, hand Tween 80 has been identified as a lymphotropic excipient due to the ability to solubilise lipophilic drugs, inhibit the P-gp and stimulate chylomicron production (Williams et al., 2012).

In order to improve the storage stability of the SPN-NLCs, they were liophylized. A cryoprotector agent was neccesary and 5% trehalose showed to be the most appropriate.

The *in vitro* dissolution study carried out under sink conditions showed a very slow release of spironolactone from the nanocarriers; this seems to indicate a high stability of the SPN-NLCs in the dissolution media. However, it has to be taken into account that under the conditions used for the test, it is unlikely to occur the hydrolysis of lipids due to the absence of bile salts (Bakala N´Goma et al., 2012).

Once the SPN-NLCs were characterized, we evaluated the pharmacokinetic behavior of the drug after oral administration to rabbits. As reference formulation, we prepared a spironolactone syrup for oral administration and a solution was administered intravenously. Only spironolactone metabolites, canrenone and 7α-TMS, could be quantified in collected samples. Plasma half-life of both metabolites did not show statistical differences between intravenous and oral administration of the drug, which demonstrates that the elimination rate of both metabolites was not affected by the absorption process. The levels of 7α-TMS, in comparison with canrenone levels, were higher in all cases regardless the formulation. The absolute bioavailability of 7α-TMS was significantly higher with the syrup than the absolute bioavailability obtained with the SPN-NLCs (0.7 *vs* 0.4, $p<0.05$). However, no statistically significant differences were observed in the bioavailability of canrenone among formulations. These results reveal a different canrenone/7α-TMS ratio depending on the administered formulation, which could be explain by differences in the absorption mechanism of the drug.

Spironolactone is a poor water soluble compound and, therefore, its absorption is limited by the dissolution in the gastrointestinal fluid. Lipids

from the formulation can promote the absorption of drugs through the formation of micelles. During the micelle formation process, the drug dissolved in the lipid is taken up in the micelles (solubilization) and the formed micelles interact with surface-active bile salts (e.g. sodium cholate) leading to the formation of so-called ´mixed micelles´ (Muchow et al., 2008). This process could promote the lymphatic absorption that avoids the first-pass metabolism to a certain degree, which could explain the differences in the metabolic profile of spironolactone between the syrup and the nanoparticles. However, although the primary mechanism by which lipid formulations improve the bioavailability of lipophilic drugs is the increase of the dissolution rate (Kesisoglou et al., 2007), the low amount of spironolactone released in the dissolution studies, along with the lower pasma levels of spironolactone metabolites obtained with the SPN-NLCs than with the syrup, suggest that this might not be the case for the SPN-NLCs. In our opinion, the high stability of SPN-NLCs in the gastrointestinal tract would lead to a low dissolution rate of the spironolactone from the nanoparticles *in vivo*. In a previous study, Müller *et al.* (Müller et al., 2006) formulated cyclosporine A into SLNs and orally administered them to pigs. The drug bioavailability obtained was low and the authors attributed it, among other factors, to a low dissolution rate of the drug/undissolved drug particles in the gut.

Since NLCs seem not to improve the dissolution rate of spironolactone, another mechanism should be involved in the absorption of the drug. It is well known that the NLCs may also be captured by the epithelial and M cells and further processed into blood circulation (Florence and Hussain, 2001). If this occurs, a high stability of the nanocarriers in the gastrointestinal tract is desirable. The mixture of Tween 80 and Poloxamer 188 in the SPN-NLCs lead to high stable nanoparticles and, as it was shown by the dissolution studies, spironolactone was hardly released. Therefore, and as it was previously discussed, the degradation velocity of lipid nanoparticles highly depends on its chemical composition, particularly on the stabilizer or the stabilizer mixture of the nanoparticles (Müller et al., 2006). In addition to the

composition, the particle size also affects the transport of nanocarriers through the biological barriers. The particle size of the SPN-NLCs was about 150 nm and it is known that particle size less than 300 nm is advisable for the intestinal transport (Charman and Stella, 1992). Therefore, the absorption of spironolactone may occur by the uptake of the SPN-NLCs by the intestinal cells. This fact could also justify the differences in the canrenone/7α-TMS ratio depending on the administered formulation, syrup or SPN-NLCs. When nanoparticles are processed inside the enterocyte, the drug absorption may be influenced by the lipids of the SPN-NLCs, which could favor the lymphatic pathway leading to differences in the metabolic profile.

In order to know if SPN-NLCs were able to be uptaken by the intestinal wall, a biodistribution study with ^{99m}Tc radiolabeled nanocarriers was carried out. The radiotracer technique was chosen as it is one of the most appropiate to investigate the absorption, distribution, metabolism and excretion (ADME) of these nanomaterials (Zhang et al., 2010). Following oral administration of radiolabeled SPN-NLCs, radioactivity was mainly detected in the small intestine (figure 7). The intestine of the rats was cleaned of all food and waste material and thus, the radioactivity measured in this organ corresponded to labeled nanoparticles trapped in the mucosa. The lack of radioactivity in the thyroid confirms the stability of the nanocarriers in the gastrointestinal tract; the opposite would lead to the absorption of the free ^{99m}Tc (Szymendera and Radwan, 1974; Saha, 2010) and the radioactivity levels in the thyroid would be significantly higher. The presence of the SPN-NLCs in the intestine along with the their adhesive properties (Chen et al., 2010), suggest a retention of the nanocarrier in the underlying epithelium. (Das and Chaudhury, 2010, Chen et al., 2010, Tarr and Yalkowsky, 1989). Therefore, the absorption of spironolactone and the change in its metabolic profile when comparing to the syrup (reference formulation) could be explained, at least in part, by the adhesion of SPN-NLCs to the gut wall and their subsequent uptake by the epithelial cells.

5. Conclusion

A new formulation based on NLCs for the oral administration of spironolactone was developed. Although the bioavilability of spironolactone was not enhanced when administered as SPN-NLCs, a shift in the metabolic profile was observed when compared to the reference formulation. Radioactivity studies indicated that the SPN-NLCs were trapped in the intestinal mucosa. However, and in order to optimize this formulation, further studies should be carried out for a better understanding of the transport across the gastrointestinal wall.

6. Acknowledgements

A. Beloqui whishes to thank the University of the Basque Country (UPV/EHU) for her fellowship grant. This work was partially supported by the Basque Government´s Department of Education, Universities and Investigation (IT-341-10) and by the Ministry of Education and Science (DCB2009-0067). We thank the Department of Nuclear Medicine at the *Hospital Universitario de Canarias* (Tenerife, Spain) for their assistance in the biodistribution studies. Authors also acknowledge the technical support and advice provided by SGIker (UPV/EHU, MICINN, GV/EJ, ESF) on transmission electron microscopy.

References

Abdelwahed W, Degobert G, Stainmesse S, Fessi H. 2006. Freeze-drying of nanoparticles: Formulation, process and storage considerations. *Adv Drug Deliv Rev,* 58, 1688-1713.

Bakala N´Goma JC, Amara S, Dridi K, Jannin V, Carrière F. 2012. Understanding lipid-digestion processes in the GI tract before designing lipid-based drug-delivery systems. *Ther Deliv*, 3,105-124.

Chakraborty S, Shukla D, Mishra B, Singh S. 2009. Lipid - An emerging platform for oral delivery of drugs with poor bioavailability. *Eur J Pharm Biopharm,* 73, 1-15.

Charman WN, Stella V. J. 1992. *Lymphatic transport of drugs*, CRC Press.

Chen CC, Tsai TH, Huang ZR, Fang JY. 2010. Effects of lipophilic emulsifiers on the oral administration of lovastatin from nanostructured lipid carriers: Physicochemical characterization and pharmacokinetics. *Eur J Pharm Biopharm*, 74, 474-82

Chen M. 2008. Lipid excipients and delivery systems for pharmaceutical development: a regulatory perspective. *Adv Drug Deliv Rev,* 60, 768-77.

Dahan A, Hoffman A. 2007. The effect of different lipid based formulations on the oral absorption of lipophilic drugs: the ability of in vitro lipolysis and consecutive ex vivo intestinal permeability data to predict in vivo bioavailability in rats. *Eur J Pharm Biopharm,* 67, 96-105.

Dahan A, Hoffman A. 2008. Rationalizing the selection of oral lipid based drug delivery systems by an in vitro dynamic lipolysis model for improved oral bioavailability of poorly water soluble drugs. *J Control Release,* 129, 1-10.

Das S, Chaudhury A. 2010. Recent Advances in Lipid Nanoparticle Formulations with Solid Matrix for Oral Drug Delivery. *AAPS PharmSciTech*.

Del pozo-Rodríguez A, Solinís MA, Gascón AR, Pedraz JL. 2009. Short- and long-term stability study of lyophilized solid lipid nanoparticles for gene therapy. *Eur J Pharm Biopharm,* 71, 181-189.

European Pharmacopeia. (2007). Dissolution test for solid dosage forms.

Florence AT. 2005. Nanoparticle uptake by the oral route: Fulfilling its potential? *Drug Discov Today: Technologies,* 2, 75-81.

Florence AT, Hussain N. 2001. Transcytosis of nanoparticle and dendrimer delivery systems: evolving vistas. *Adv Drug Deliv Rev,* 50, S69-S89.

Guide for the Care and Use of Laboratory Animals. (2011). Washington (DC), National Academies Press (US).

Hauss DJ. 2007. Oral lipid-based formulations. *Adv Drug Deliv Rev,* 59, 667-676.

Jannin V, Musakhanian J, Marchaud D. 2008. Approaches for the development of solid and semi-solid lipid-based formulations. *Adv Drug Deliv Rev,* 60, 734-746.

Kesisoglou F, Panmai S, Wu Y. 2007. Nanosizing - Oral formulation development and biopharmaceutical evaluation. *Adv Drug Deliv Rev,* 59, 631-644.

Konan YN, Gurny R, Allémann E. 2002. Preparation and characterization of sterile and freeze-dried sub-200 nm nanoparticles. *Int J Pharm,* 233, 239-252.

Krishnaiah YSR. 2010. Pharmaceutical Technologies for Enhancing Oral Bioavailability of Poorly Soluble Drugs. *J Bioequiv Availab,* 2, 28-36.

Langguth P, Hanafy A, Frenzel D, Grenier P, Nhamias A, Ohlig T, Vergnault G, Spahn-Langguth H. 2005. Nanosuspension formulations for low-soluble drugs: pharmacokinetic evaluation using spironolactone

as model compound. *Drug Dev Ind Pharm,* 31, 319-29.

Limayem Blouza I, Charcosset C, Sfar S, Fessi H. 2006. Preparation and characterization of spironolactone-loaded nanocapsules for paediatric use. *Int J Pharm,* 325, 124-31.

Mehnert W, Mäder K. 2001. Solid lipid nanoparticles: production, characterization and applications. *Adv Drug Deliv Rev,* 47, 165-96.

Merisko-Liversidge E, Liversidge G. 2008. Drug nanoparticles: formulating poorly water-soluble compounds. *Toxicol Pathol,* 36, 43-8.

Merisko-Liversidge E, Liversidge GG. 2011. Nanosizing for oral and parenteral drug delivery: A perspective on formulating poorly-water soluble compounds using wet media milling technology. *Adv Drug Deliv Rev,* 63, 427-440.

Merisko-Liversidge E, Liversidge GG, Cooper ER. 2003. Nanosizing: a formulation approach for poorly-water-soluble compounds. *Eur J Pharm Sci,* 18, 113-120.

Muchow M, Maincent P, Müller R. 2008. Lipid nanoparticles with a solid matrix (SLN, NLC, LDC) for oral drug delivery. *Drug Dev Ind Pharm,* 34, 1394-405.

Müller R., Mäder K, Gohla S. 2000. Solid lipid nanoparticles (SLN) for controlled drug delivery - a review of the state of the art. *Eur J Pharm Biopharm,* 50, 161-77.

Müller RH, Radtke M, Wissing SA. 2002. Nanostructured lipid matrices for improved microencapsulation of drugs. *Int J Pharm,* 242, 121-128.

Müller RH, Runge S, Ravelli V, Mehnert W, Thünemann AF, SOUTO EB. 2006. Oral bioavailability of cyclosporine: Solid lipid nanoparticles (SLN®) versus drug nanocrystals. *Int J Pharm,* 317, 82-89.

Müllertz A, Ogbonna A, Ren S, Rades T. 2010. New perspectives on lipid and surfactant based drug delivery systems for oral delivery of poorly soluble drugs. *J Pharm Pharmacol,* 62, 1622-36.

O'Driscoll CM, Griffin BT. 2008. Biopharmaceutical challenges associated with drugs with low aqueous solubility--The potential impact of lipid-based formulations. *Adv Drug Deliv Rev,* 60, 617-624.

Overdiek HW, Merkus FW. 1987. The metabolism and biopharmaceutics of spironolactone in man. *Rev Drug Metab Drug Interact,* 5, 273-302.

Porter C, Trevaskis N, Charman W. 2007. Lipids and lipid-based formulations: optimizing the oral delivery of lipophilic drugs. *Nat Rev Drug Discov,* 6, 231-48.

Porter CJH, Pouton CW, Cuine JF, Charman WN. 2008. Enhancing intestinal drug solubilisation using lipid-based delivery

systems. *Adv Drug Deliv Rev,* 60, 673-691.

Pouton CW. 2006. Formulation of poorly water-soluble drugs for oral administration: Physicochemical and physiological issues and the lipid formulation classification system. *Eur J Pharm Sci,* 29, 278-287.

Pouton CW, Porter CJH. 2008. Formulation of lipid-based delivery systems for oral administration: Materials, methods and strategies. *Adv Drug Deliv Rev,* 60, 625-637.

Saha GB. 2010. Fundamentals of Nuclear Pharmacy. Sixth edition. New York, USA: Springer.

Szymendera J, Radwan M. Intestinal absorption of pertechnetate: calculation by the oral-intravenous plasma activity quotients and inverse convolution method. J Nucl Med, 1974;15:314-316.

Tarr BD, Yalkowsky SH. 1989. Enhanced Intestinal Absorption of Cyclosporine in Rats Through the Reduction of Emulsion Droplet Size. *Pharm Res,* 6, 40-43.

Teeranachaideekul V, Müller RH, Junyaprasert VB. 2007. Encapsulation of ascorbyl palmitate in nanostructured lipid carriers (NLC)--Effects of formulation parameters on physicochemical stability. *IntJ Pharm,* 340, 198-206.

Trevaskis NL., Charman WN, Porter CJH. 2008. Lipid-based delivery systems and intestinal lymphatic drug transport: A mechanistic update. *Adv Drug Deliv Rev,* 60, 702-716.

Venishetty VK, Chede R, Komuravelli R, Adepu L, Sistla R, Diwan PV. 2012. Design and evaluation of polymer coated carvedilol loaded solid lipid nanoparticles to improve the oral bioavailability: A novel strategy to avoid intraduodenal administration. *Colloids Surf B Biointerfaces,* 95, 1-9.

Williams H, Sassene P, Kleberg K, Bakala N´Goma JC, Calderone M, Jannin V, Igonin A, Partheli A, Marchaud D, Vertommen J, Maio M, Blundell R, Benameur H, Carrière F, Müllertz A, Porter CJH, Pouton CW. 2012. Toward the establishment od standarized in vitro tests for lipid-based formulations, part 1: method parameterisation and comparison of in vitro digestion profiles across a range of representative formulations. *J Pharm Sci*, 101, 3360-3380.

Zhang X, Yin J, Kang C, Li J, Zhu Y, Li W, Huang Q, Zhu Z. 2010. Biodistribution and toxicity of nanodiamonds in mice after intratracheal instillation. *Toxicol Lett,* 198, 237-243.

Journal of Controlled Released 166 (2013) 115-123

Mechanism of transport of saquinavir-loaded nanostructured lipid carriers across the intestinal barrier

Ana Beloqui[1,2], María Ángeles Solinís[1], Alicia R. Gascón[1], Ana del Pozo-Rodríguez[1], Anne des Rieux[2*], Véronique Préat[2*]

[1] Pharmacokinetics, Nanotechnology and Gene Therapy Group. Laboratory of Pharmacy and Pharmaceutical Technology, School of Pharmacy, University of the Basque Country UPV/EHU, Vitoria-Gasteiz, Spain
[2] Université Catholique de Louvain, Louvain Drug Research Institute, Pharmaceutics and Drug Delivery, Brussels, Belgium

ABSTRACT

The aims of this work were (i) to evaluate the potential of nanostructured lipid carriers (NLCs) as a tool to enhance the oral bioavailability of poorly soluble compounds using saquinavir (SQV), a BCS class IV drug and P-gp substrate as a model drug, and (ii) to study NLC transport mechanisms across the intestinal barrier. Three different NLC formulations were evaluated. SQV transport across Caco-2 monolayers was enhanced up to 3.5-fold by NLCs compared to SQV suspension. M cells did not enhance the transport of NLCs loaded with SQV. The size and amount of surfactant in the NLCs influenced SQV permeability, the transcytosis pathway and the efflux of SQV by P-gp. An NLC of size 247 nm and 1.5% (w/v) surfactant content circumvented P-gp efflux and used both caveolae- and clathrin-mediated transcytosis, in contrast to the other NLC formulation, which used only caveolae-mediated transcytosis. By modifying critical physicochemical parameters of the NLC formulation, we were thus able to overcome the P-gp drug efflux and alter the transcytosis mechanism of the nanoparticles. These findings support the use of NLCs approaches for oral delivery of poorly water-soluble P-gp substrates.

Keywords: endocytosis, transcytosis, nanoparticle, P-gp substrate, Caco-2, M cell

1. Introduction

Most of newly discovered chemical entities are poorly soluble in water [1-4]. Enhancing the oral bioavailability of these poorly water-soluble compounds is of great interest to the scientific community and a key area of pharmaceutical research. One of the most widely studied strategies in this regard is nanotechnology [2, 5-8], because of the ability of nanoparticles to pass multiple biological barriers and to release a therapeutic compound within the optimal dosage range. Polymeric nanoparticles [9], lipid nanocarriers [10-12], micelles [13, 14], nanosuspensions [5, 15] appear to be promising tools for delivery of poorly soluble drugs, yet few have been commercialized.

Among the wide variety of current nanocarriers, solid lipid nanoparticles (SLNs) present certain advantages compared to other colloidal systems, including that they can be prepared without an organic solvent and using suitable large scale production method (e.g., high pressure homogenization) [16]. However, SLNs have a relatively low loading capacity for several drugs compared to other nanocarrier systems, are associated with possible expulsion of the drug during storage, and have a high water content. Nanostructured lipid carriers (NLCs) are a second generation of SLNs, which have a solid matrix mixed with a liquid lipid (oil) to form an unstructured matrix that helps increase the drug loading capacity of nanoparticles and avoids or reduces drug expulsion from the matrix during storage [17, 18].

Nanoparticle size and surface properties, among other physicochemical properties of nanoparticles, strongly influence the mechanisms involved in nanoparticle cell internalization [19-21]. The non-phagocytic pathways, involving clathrin-mediated endocytosis, caveolae-mediated endocytosis and macropinocytosis, are the most common mechanisms of nanoparticle absorption/transcytosis by the oral route [22]. Nevertheless, designing tunable nanocarriers in order to control the endocytic pathway remains a challenge. Increasing our understanding of the mechanisms and processes involved in nanoparticle transport across the intestinal barrier and the factors limiting their transport across this barrier could help improve the formulations to enhance drug

absorption [23-26]. Improved knowledge of these processes can help them fulfill their potential as tools for delivery of poorly water-soluble drugs by the oral route and provide new insights in their potential application for the treatment of different pathologies using this route.

The aim of this work was, first, to evaluate NLCs as tools to enhance the oral bioavailability of poorly water-soluble compounds using saquinavir (SQV), a class IV drug in the Biopharmaceutical Classification System (BCS), and a P-glycoprotein (P-gp) substrate, as a model drug and, second, to study NLC transport mechanisms across the intestinal barrier. We evaluated SQV transport and then conducted a mechanistic study of NLC transport across an *in vitro* Caco-2 model, simulating the enterocyte barrier, and a Caco-2/Raji cell M inverted culture model simulating, the intestinal follicle-associated epithelium (FAE model) [27]. The influence of controversial parameters that could affect nanoparticle transport, such as the size and the surfactant content of the aforementioned nanoparticles, was investigated and their contribution to nanoparticle endocytosis and transcytosis evaluated using endocytosis inhibitors. Finally, the ability of these nanocarriers to overcome P-gp efflux was also assessed.

2. Materials and methods

2.1. Materials

Saquinavir mesylate (SQV) was kindly provided by Roche (Mannheim, DE). Verapamil, chlorpromazine, nystatin, methyl-ß-cyclodextrin (MßCD), lovastatin, coumarin-6, Rose Bengal and propidium iodide (PI) were purchased from Sigma-Aldrich (St. Louis, MO). Precirol ATO®5 was kindly provided by Gattefossé (Madrid, SP). Tween 80 was purchased from Vencaser (Bilbao, SP). Poloxamer 188 was a gift from BASF (Madrid, Spain). Miglyol 812 N/F was purchased from Sasol (Hamburg, DE). Potassium dihydrogen phosphate (KH_2PO_4) and disodium hydrogen phosphate (Na_2HPO_4) were obtained from Merck (Darmstadt, DE). Acetonitrile (gradient HPLC grade) was purchased from VRW (Leuven, BE).

2.2. Preparation of the formulations

2.2.1 NLC preparation

SQV-NLCs were prepared using the high pressure homogenization technique [28]. Briefly, Precirol ATO®5 (5 g), Miglyol 812 (0.5 mL) and SQV (50 mg) were blended and melted at 75 ºC until a uniform and clear oil phase was obtained. The aqueous phase was prepared by dispersing Tween 80 (2%) (w/v) and poloxamer 188 (1%) (w/v) or Tween 80 (1%) (w/v) and poloxamer 188 (0.5%) (w/v) in water (50 mL) and heating to the same temperature as the lipid phase. The hot aqueous phase was then added to the oil phase and the mixture was sonicated for 15 seconds to form a hot pre-emulsion, which was subsequently homogenized at 80°C and 500 Bar using a Stansted nG12500 homogenizer (SFP, Essex, UK) for ten homogenization cycles. To obtain NLCs with an increased particle size, one of the batches was not homogenized and the pre-emulsion was used.

To track the entry of nanoparticles into the cells, SQV-NLCs were labeled with the fluorescent dye coumarin-6. Briefly, 5 mg of coumarin-6 were incorporated in the lipid phase of the formulation and the preparation continued as aforementioned.

2.2.2 SQV suspension

To evaluate free SQV transport compared to nanoparticle transport, an SQV suspension was prepared. SQV (50 mg) was dispersed in a transport buffer (Hank´s Balance Solution Buffer, HBSS) (50 mL). The concentration of SQV was calculated by dissolving the SQV suspension in acetonitrile and analyzing the resultant solution by HPLC.

2.3. NLC characterization

2.3.1 Size and zeta potential measurements

The size of the NLCs was determined using photon correlation spectroscopy (PCS) and the zeta potential was measured using Laser Doppler Velocimetry (LDV) with a Malvern Zetasizer Nano ZS (Malvern Instruments Ltd., Worcestershire, U.K). Samples were diluted in MilliQ™ water before measurement.

2.3.2 Surface hydrophobicity of nanoparticles

The surface hydrophobicity of the NLCs was evaluated using the Rose Bengal method [29]. Briefly, increasing nanoparticle concentrations were diluted to a constant 20 μg/mL Rose Bengal solution. The surface of the nanoparticles and the aqueous phase were considered as two phases. The absorption of the hydrophobic dye to the nanoparticle surface was measured by calculating the partitioning coefficient (PQ). The PQ values were plotted versus the increasing nanoparticle concentrations. The surface hydrophobicity of the nanoparticles was quantified by the slope of the line. The slope increases with increasing surface hydrophobicity.

2.3.3 Drug encapsulation efficiency

The encapsulation efficiency (EE) of SQV-NLCs was calculated by determining the amount of free drug using a filtration technique. The SQV-NLCs suspension was placed in the upper chamber of Amicon® centrifugal filters (molecular weight cutoff, MWCO, 100,000 Da, Millipore, Spain) and centrifuged for 20 min at 1500 g. The unencapsulated SQV in the filtrate was determined using HPLC. The total drug content in the SQV-NLCs was determined by dissolving the SQV-NLCs in acetonitrile to release trapped SQV. The resulting solution was analyzed using HPLC. The drug loading content was the ratio of incorporated drug to lipid (w/w).

Encapsulation efficiency and drug loading, each determined in triplicate, were calculated as follows:

$$EE(\%) = \frac{Amount\ of\ SQV\ in\ NLCs}{Initial\ amount\ of\ SQV} x100$$

$$\text{Drug loading}(\%) = \frac{Amount\ of\ SQV\ in\ NLCs}{Amount\ of\ lipid\ in\ NLCs} x100$$

Coumarin-6 encapsulation was assessed by ultracentrifuging coumarin-6-SQV-loaded NLC suspension (1,500 g, 20 min) using Millipore (Madrid, Spain) Amicon® ultra centrifugal filters (molecular weight cutoff, MWCO, 100,000 Da). Free coumarin-6 present in the filtrate was then measured using fluorimetry (SFM 25 fluorometer, Konton Instruments).

2.3.4. Determination of saquinavir by HPLC

HPLC for SQV was performed with a Waters 1525 HPLC Binary Pump (Waters Corp., Milford, USA). The detector was a Waters 2487. The system was controlled by Breeze software (Waters, UK). A Nucleodur 100-5 C18 5 μm (4 mm x 125 mm) was used at room temperature. The mobile phase contained 46% acetonitrile and 54% (v/v) of 70mM KH_2PO_4 adjusted to pH 5 with 80 mM Na_2HPO_4, as previously reported by Albert et al. [30]. The flow rate was set at 1 mL/min in isocratic elution and the injected sample volume was 50 μL, except for the analysis of SQV under certain inhibitors for which a sample volume of 100 μL was necessary to reach the limit of quantification. The assay was linear over the SQV concentration range of 0.025-15 μg/mL. The intra- and inter-day coefficients of variation were both within ± 5%. The limits of detection (LOD) and of quantification (LOQ) of SQV were 0.0125 μg/mL and 0.025 μg/mL, respectively. No interfering peaks were detected within the assay.

2.4. In vitro dissolution assay

The *in vitro* dissolution assay was performed in HBSS (transport buffer during the *in vitro* assays) using Quix-Sep® cells (Membrane Filtration Products.Inc, TX, USA) at 37°C under magnetic stirring. A dialysis regenerated cellulose membrane with an MWCO between 6,000 and 8,000 Da was used. The membrane was first soaked in medium for 24 h before placing it in a Quix-Sep® cell. Five hundred microliters of the SQV-NLCs suspension was placed in the cell and introduced into 200 mL of HBSS. After 2 h, samples were withdrawn from the medium and analyzed by HPLC using the abovementioned method. The dissolution test was carried out in triplicate for each formulation under sink conditions.

In addition, in order to assess the stability of the nanoparticles in the gastrointestinal tract, the *in vitro* dissolution assay was performed in simulated gastric fluid (SGF) and in simulated intestinal fluid (SIF) as described in the European Pharmacopeia (European Pharmacopeia, 2010) and performed as abovementioned. Samples were withdrawn after 2 h and 8 h in SGF and SIF, respectively.

2.5. In vitro culture studies

2.5.1 *Cell cultures: Caco-2 and FAE monolayers*

All cell culture media and reagents were purchased from Invitrogen (Merelbeke, BE). Caco-2 cells (clone 1) were kindly provided by Dr Maria Rescigno, University of Milano-Bicocca (Milano, Italy) [31] and used from passage *x*+12 to *x*+30. Human Burkitt´s lymphoma Raji B cell line was purchased from American Type Culture Collection (Manassas, VA, USA) and used between passages 102-110. Caco-2 cells were grown in DMEM supplemented with 10% (v/v) inactivated fetal bovine serum, 1% (v/v) non-essential amino-acids, and 1% (v/v) L-glutamine, at 37ºC under a 10% CO_2/90% air atmosphere. Caco-2 cells were grown on inserts in the same medium, but further supplemented with 1% (v/v) of penicillin-streptomycin (PEST). Raji cells were grown in a suspension culture, cultivated in RPMI medium supplemented with 10% (v/v) inactivated fetal bovine serum, 1% (v/v) non-essential amino-acids, 1% (v/v) L-glutamine, and 1% (v/v) PEST, at 37ºC in a 5% CO_2/95% air atmosphere.

Caco-2 cells were seeded at a density of $5x10^5$ cells/well on Transwell® polycarbonate inserts (12 mm insert diameter, 3 μm pore size) (Corning Costar, Cambridge, U.K.) and cultivated over 21 days. The medium was replaced every second day. The inverted FAE model was obtained by co-culturing Raji and Caco-2 as previously reported by des Rieux et al. [27, 32]. Briefly, after 3 to 5 days of Caco-2 seeding, inserts were inverted, a piece of silicone tube was placed into the inserts and maintained until day 21 in large petri dishes. The medium was replaced every other day, until day 9-11 when Raji cells were then added to the basolateral compartment for the conversion of Caco-2 cells into M cells at a density of $2.5x10^5$ cells/well.

2.5.2 Cytotoxicity studies

Cell viability was assessed after the co-incubation of 20,000 Caco-2 cells/well on a 96-well tissue culture plate (Costar® Corning® CellBIND Surface) with the aforementioned formulations by the 3-(4,5-dimethylthiazol-2-yl)-2,5 diphenyltetrazolium bromide (Sigma-Aldrich, BE) assay (MTT assay) and the

measurement of lactate dehydrogenase (LDH) activity released from the cytosol of damaged cells (LDH assay) (Roche Diagnostics Belgium, Vilvoorde, BE) following manufacturer's instructions [33].

The IC_{50}s for the different formulations were calculated using the GraphPad Prism 5 program (CA, USA). All MTT assays were repeated in triplicate.

The LDH release induced by the different nanoparticles did not exceed 25%, even for the highest concentration.

The integrity of the monolayer was also corroborated by measuring the trans-epithelial electrical resistance (TEER) before and after the transport studies on day 21. The measurements were carried out at 37°C using an epithelial voltohm meter (EVOM, World Precision Instruments, Berlin, DE). TEER values over 200 Ω cm^2 for Caco-2 monolayers and over 100 Ω cm^2 for Caco-2/Raji coculture were used. TEER values were not significantly different to initial values unless otherwise stated.

2.5.3 Evaluation of SQV permeability across intestinal in vitro models

The permeability of SQV across gastrointestinal *in vitro* models was evaluated by comparing free SQV with SQV-NLC formulations, in Caco-2 and Caco-2/Raji co-culture cells.

The experiments were conducted at 37ºC or 4ºC by adding a volume of 400 µL at 44 µg/mL SQV concentration in HBSS on the apical side and 1 mL of HBSS on the basolateral side. After 2h of incubation, samples were collected from the basolateral side and SQV concentration was measured by HPLC: The apparent permeability coefficient (P_{app}, cm s^{-1}) was calculated according to the following equation [23, 34]:

$$P_{app} = dQ/dt \times 1/AC_0$$

where dQ/dt is the transport rate (µg/s), C_0 is the initial drug concentration on the apical side (µg/mL), and A is the surface area of the membrane filter (cm^2).

After transport experiments, cell monolayers were washed twice in cold HBSS and fixed in paraformaldehyde (PFA) 4% for subsequent staining.

For the assessment of FAE model functionality in each experiment transport studies were conducted under the aforementioned conditions

with commercial fluorescent carboxylated nanoparticles (0.2 μm) (Gentaur, BE) [26, 35]. A nanoparticle suspension (400 μL) with final concentration of 4.5 × 10^9 nanoparticles/ml was added on the apical side and inserts were incubated at 37ºC for 2 h. After this incubation time, basolateral solutions were then sampled and the number of transported nanoparticles measured using a flow cytometer (BD FACSCalibur). Nanoparticle transport was expressed as mean ± S.D.

2.5.4 Mechanisms of transport of SQV-NLCs across Caco-2 cells

In order to evaluate the endocytosis mechanisms involved in SQV-NLC transport across Caco-2 cells, the monolayers were pre-incubated for 1 h at 37ºC with 400 μL of a solution consisting of different concentrations of endocytosis inhibitors in transport buffer. After 1 h, SQV-NLC were added into the inhibitor solution on the apical side and co-incubated for 2 h. Chlorpromazine 10 μg/mL was used as an inhibitor of receptor-mediated and clathrin-mediated endocytosis [23, 34]. The endocytic pathway of caveolae/lipid raft mediated endocytosis was inhibited with nystatin 50 μg/mL [36, 37]. MßCD 10 mM in the presence of lovastatin 1 μg /mL, an inhibitor of *de novo* synthesis of cholesterol [38], was used for the inhibition of caveolae and clathrin-mediated pathways by cholesterol depletion [38].

As mentioned previously, SQV is a well-known P-gp substrate [39, 40]. To evaluate the role of SQV-NLCs in the inhibition of P-gp, cells were pretreated with a solution of 100 μM verapamil, a well-known P-gp inhibitor [40, 41], for 1h and nanoparticles were subsequently added on the apical side and incubated for 2 h in the presence of verapamil. The evaluation of SQV suspension P_{app} was also carried out under P-gp inhibition to confirm that SQV was a P-gp substrate in our Caco-2 cell model.

In all the assays carried out in the presence of inhibitors, several inserts were kept as controls and the transport studies were carried out in transport buffer instead of in inhibitor solutions.

2.5.5 Intracellular uptake of nanoparticles by Caco-2 cells

Entry of nanoparticles into Caco-2 cells was studied quantitatively by flow cytometry and qualitatively by confocal laser scanning microscopy (CLSM), for which coumarin-6 (λ_{em}= 505 nm) loaded nanoparticles were employed.

For the flow cytometry study, Caco-2 cells were seeded in 24-well cell culture plates at a density of $5x10^5$ cells per well and allowed to adhere for 48 h until confluency. As for the transport studies, cells were co-incubated with 400 μL of a coumarin-6 loaded nanoparticles suspension in transport buffer (17.5 μL per 100 μL of buffer). After 2 h of incubation with fluorescent nanoparticles, cells were washed three times with PBS and detached from the plates by trypsinization. Cells were then centrifuged at 1,500 x g, the supernatant was discarded, the cells were resuspended in PBS and fluorescence was measured using a BD FACSCalibur flow cytometer and BD CellQuest software (Becton Dickinson Biosciences, San Jose, CA, US). Cell fluorescence was quantified by measuring the fluorescence of coumarin-6 at 525 nm (FL1). To avoid fluorescence overestimation inside the cells from free dye entry, coumarin-6 was added as a solution (100 μg/mL) and prepared as described by Rivolta et al. [42]. For cell viability measurements, the propidium iodide reagent was employed. The reagent was added to each sample at a final concentration of 10 μg/mL, and, after 10 min of incubation, the fluorescence corresponding to dead cells was measured at 620 nm (FL2). For each sample, 10,000 events were collected. The data were subsequently analyzed using the FlowJo data analysis software package (TreeStar, USA). In the case of inhibition studies, cells were pre-treated 1 h with the inhibitors used for the transport mechanisms studies (section 2.5.4).

For the CLSM study, the Transwell® inserts fixed in PFA 4% were gently washed in HBSS. Actin was stained with 200 μL of rhodamine-phalloidine (1:50) in buffered HBSS+0.2% (v/v) Triton X-100 for 10 min in the dark to reveal cell borders, as described by des Rieux et al. [26]. Cell nuclei were stained with DAPI (1:20). Subsequently, inserts were washed in HBSS, cut and mounted on glass slides. Images were captured using a Zeiss™ confocal microscope (LSM

150). Data were analyzed by the Axio Vision software (vs 4.8) to obtain *y-z, x-z* and *x-y* views of the cells monolayers.

2.6. Statistical analysis

Statistical analysis was performed using the GraphPad Prism 5 program (CA, USA). Normal distribution was assessed with the Shapiro-Wilk normality test. One-way ANOVA in multiple comparisons followed by Tukey´s post-hoc test were applied according to the result of the Bartlett's test of homogeneity of variances for the 37°C and 4°C transport comparison. All other analysis were performed using a *S*tudent´s t-test. Differences were considered statistically significant at $*p<0.05$. Results are expressed as mean ± SD.

3. Results and discussion

3.1 NLC characterization

Three lipid formulations differing in particle size and surfactant content, all negatively charged. Particle characterization and compositions of the different formulations are summarized in Table 1.

The composition of these nanoparticles was based on results from previous studies on lipid nanoparticles carried out in our laboratory [43].

Table 1. Summary of formulation composition and particle size, zeta potential and polydispersity index (P.I.) per formulation (n=3; data are expressed as mean ± SD).

		NLC formulations		
		A	**B**	**C**
Composition	**Tween 80 (g)**	1	0.5	0.5
	Poloxamer 188 (g)	0.5	0.25	0.25
	Precirol ATO® 5 (g)	5	5	5
	Mygliol 812N/F (mL)	0.5	0.5	0.5
	SQV (mg)	50	50	50
	H_2O (mL)	50	50	50
	Homogenization	Yes	Yes	No
Characterization	**Size (nm)**	165±6	247±4	1,090±6
	Zeta (mV)	-21±8	-33±7	-31±5
	P.I.	0.16	0.35	0.6
	Surface hydrophobicity (slope)	0.054	0.040	0.008
	EE (%)	99±0.2	99±0.02	99±0.14
	Drug loading (%)	0.90±0.00	0.90±0.00	0.90±0.00

All the formulations had an EE of ~100% and drug loading of ~1%. Reduction in the amount of surfactant present in the formulation led to an increased particle size (165±6 nm vs 247±4 nm for formulations A and B, respectively). Moreover, when formulation B was prepared without further homogenization (formulation C), the particle size varied from the nanometer to the micrometer range (247±4 nm *vs* 1090±6 nm for formulations B and C, respectively), highlighting the importance of the preparation method in obtaining different nanoparticle size. Although SQV is considered a model drug, the low drug loading of SQV (~0.90%; therapeutic dose 1g twice a day) compromises the foreseen application of these nanocarriers to reach an efficient therapeutic dose (e.g. budesonide, 9 mg once a day in Crohn´s disease).

There were no differences in nanoparticle parameters and EE of SQV when incorporating coumarin-6 (5 mg) into the formulations (data not shown). There was a difference in nanoparticle surface hydrophobicity between the three formulations: formulation A had a greater slope

and, thus, greater hydrophobicity compared to formulations B and C. Formulations B and C had the same amount of surfactant but formulation B had greater hydrophobicity than formulation C, which can be explained by the different surface areas of the two formulations [29].

3.2 In vitro dissolution assays

An *in vitro* dissolution study was performed to ensure that SQV was not released from the NLC formulations during the *in vitro* transport studies. The amount of drug released from the NLCs into the transport buffer medium (HBSS) during 2 h of incubation at 37ºC was analyzed by HPLC (n=3). For the three formulations, SQV release was less than 0.4% indicating that the differences in the subsequent data were not the result of greater dissolution (maximum solubility of SQV mesylate in HBSS ~50 μg/mL [43]).

Moreover, for the three formulations, the drug released from NLCs in SGF media after 2 h of incubation at 37ºC was below the LOD (LOD<0.0125μg/mL) (n=3). SQV release was below the LOD after 2 h and less than 5% in SIF media after 8 h of incubation 37ºC (n=3).

3.3 In vitro evaluation of SQV transport across the intestinal barrier

3.3.1 SQV permeability evaluation across enterocyte-like and M cells-like models

The main aim of the present study was to evaluate the potential of NLCs as suitable carriers for poorly water-soluble drugs using SQV as a BCS class IV model drug. For this purpose, we evaluated the permeability of SQV across the enterocyte-like model (Caco-2 monolayers) and the FAE model (Caco-2/Raji cell monolayers). We confirmed the conversion of Caco-2 cells into M-cells in the FAE model by measuring the number of commercial carboxylated particles transported using a flow cytometer. After 2 h of incubation, the number of transported nanoparticles was significantly higher in the M-cell model than in the Caco-2 model (82,633±6,443 nanoparticles, versus 108±91, respectively; n=4, $p<0.05$).

We compared the permeability values obtained for each nanoparticle formulation with the permeability values of free SQV as a suspension.

Figure 1 represents the P_{app} data obtained for the assayed formulations after 2 h of incubation in the enterocyte-like Caco-2 model and the FAE model.

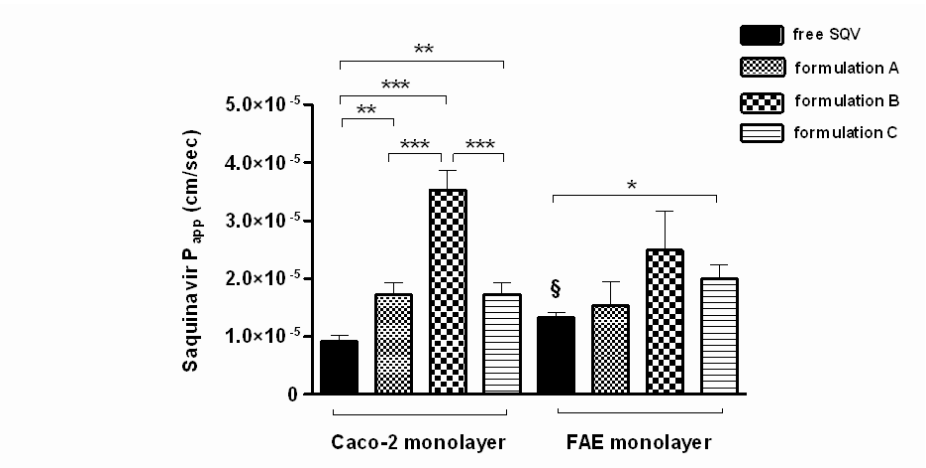

Fig 1. Saquinavir (SQV) P_{app} values obtained after 2 h of incubation of the three NLC formulations (A,B and C) with a SQV suspension in the Caco-2 model and the FAE model. (n=9, mean ± S.D, *p<0.05, **p<0.01, ***p<0.001).§p<0.05 versus Caco-2 monolayers.

In the Caco-2 model, the increase in SQV P_{app} values for the nanoparticle formulations compared to free SQV, is highlighted. It is remarkable to note the 3.5-fold increase in the SQV P_{app} with formulation B compared to free SQV ($p<0.001$), and the 2-fold increase compared with the two other NLC formulations (A and C) ($p<0.01$). These SQV P_{app} values are greater than previously reported values obtained across Caco-2 monolayers and ex vivo transport studies using different strategies for enhancing SQV permeability [45, 46]. These data confirm that NLCs are suitable carriers for enhancing the permeability of poorly water-soluble drugs.

The size of the nanoparticles did not influence SQV P_{app} values in the Caco-2 model, because there was no significant difference between the P_{app} values of formulation A (165±6 nm) and C (1,090±6 nm) ($1.73 \times 10^{-5}\pm2.23 \times 10^{-6}$ cm/sec versus $1.73 \times 10^{-5}\pm2.09 \times 10^{-6}$ cm/sec, respectively; n=9, $p>0.05$). However, in the M cell

model, there was a significant increase in the P_{app} of formulation C compared to free SQV ($p<0.05$), which was not observed with formulations A or B ($p>0.05$). The use of microparticles for targeting M cells has been studied previously by other authors [47, 48].

In contrast to polymeric nanoparticles [32], the permeability of the drug from the submicron NLCs was not increased in M cells. Hence, the subsequent evaluation of the transport mechanisms and the intracellular uptake was evaluated only in the Caco-2 cell model.

3.3.2 Intracellular uptake in Caco-2 cells

In Figure 2 we can see the flow cytometry results (Figure 2A) and the CLSM images (Figure 2B and 2C) corresponding to the cellular uptake of the nanoparticle formulations and free coumarin-6. Cell viability was assessed by staining dead cells with PI and was greater than 90% in all cases unless otherwise stated. Untreated cells were used as controls.

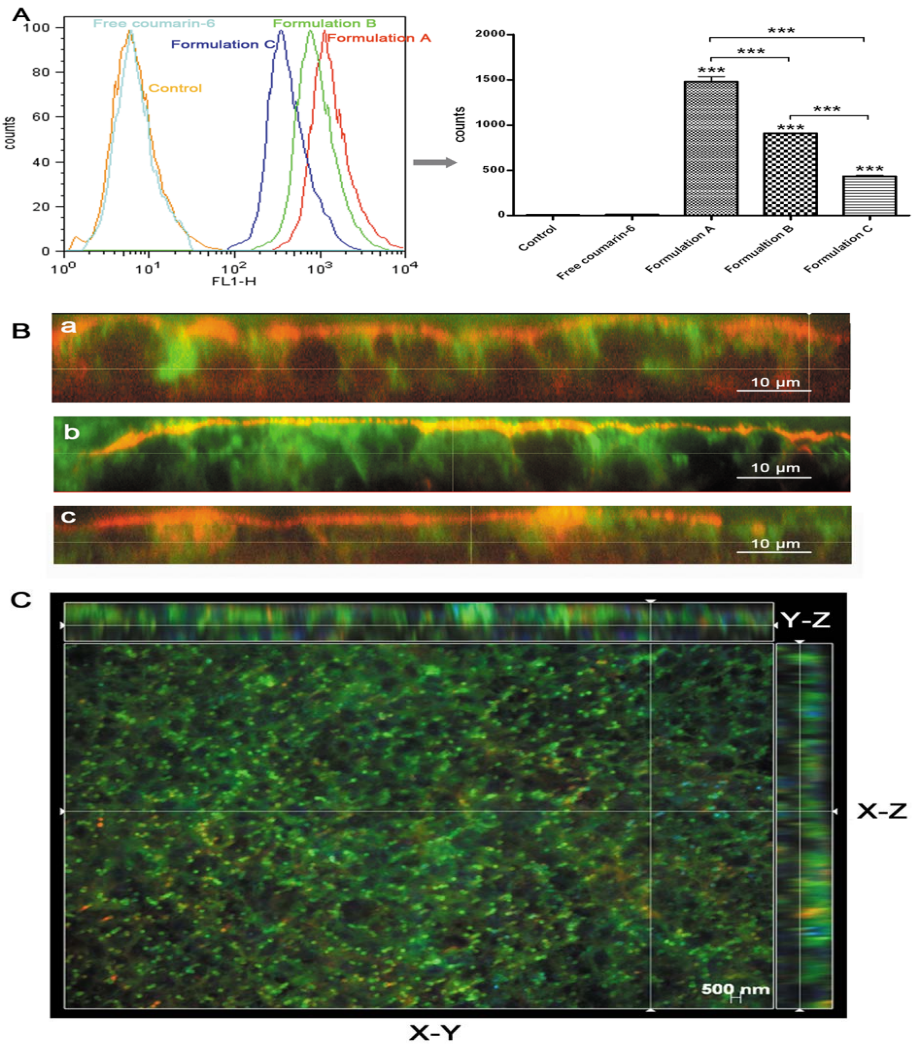

Fig 2. Flow cytometry analysis of the cellular uptake study of coumarin-6 NLCs (green) in Caco-2 cells (A) and CLSM images (B and C) of the inserts after 2 h of incubation with the nanoparticles. A) Nanoparticles and free coumarin-6 entrance into the cell measured by flow cytometry. Untreated cells are shown as control (n=3; ***p<0.001). B) a, b and c correspond to *y-z* sections of CLSM images of the inserts for formulations A, B and C, respectively. Cell membranes are stained in red with rhodamine-phalloidine and cell nuclei in blue with DAPI. C) *y-z*, *x-y* and *x-z* sections of formulation A CLSM images with which the higher uptake rate was recorded.

The cellular uptake of NLCs was size-dependent (formulation A> B> C; n=3, ***p<0.001; Figure 2A). This finding is consistent with Rejman et al. [19] who also reported a tendency to decreased internalization with increased particle size. These authors studied the pathway of entry and subsequent fate of commercial latex nanoparticles inside the cell and concluded that particles with a diameter <200 nm enter the cell via clathrin-mediated endocytosis whereas larger particles (200 nm-1 μm) enter preferentially via caveolae-mediated endocytosis. Moreover, the surface hydrophobicity of the nanoparticles may also determine nanoparticle entrance into Caco-2 cell because the larger uptake into the cells is correlated with the higher nanoparticle surface hydrophobicity (formulation A>B>C) [27]. Gaumet et al. [21] found that the surface hydrophilicity of polymeric nanoparticles was a critical factor for nanoparticle uptake and Liang et al. [49] reported that gold nanoparticles were more efficiently taken up with increasing hydrophobic interactions with the membrane of Caco-2 cells. In our study, nanoparticle size and surface hydrophobicity were major factors influencing NLC entrance into the cell.

The P_{app} values for SQV formulated in NLCs did not correlate with their intracellular uptake. Formulation B exhibited higher SQV P_{app} values than did formulations A and C but did not have a greater intracellular uptake. Figure 2B shows that NLCs penetrated inside the Caco-2 cells whatever the formulation.

3.3.3 Mechanistic study of SQV-NLC transport across Caco-2 cells

3.3.3.1 Influence of temperature on NLC transport

The second objective of the present study was to evaluate the mechanisms of transport used by the different NLC formulations to estimate whether the differences on permeability were due to different entry pathways. For this purpose, we first focused on the type of transport: passive or active. Although lipid nanoparticles are known to enter into cells in an active endocytic manner [34], we assessed this phenomenon in Caco-2 and FAE monolayers. It is well-established that at 4ºC pinocytic/endocytic uptake is inactivated [50]. Figure 3 illustrates

the influence of temperature on the transport of nanoparticles and SQV suspension across Caco-2 and FAE monolayers.

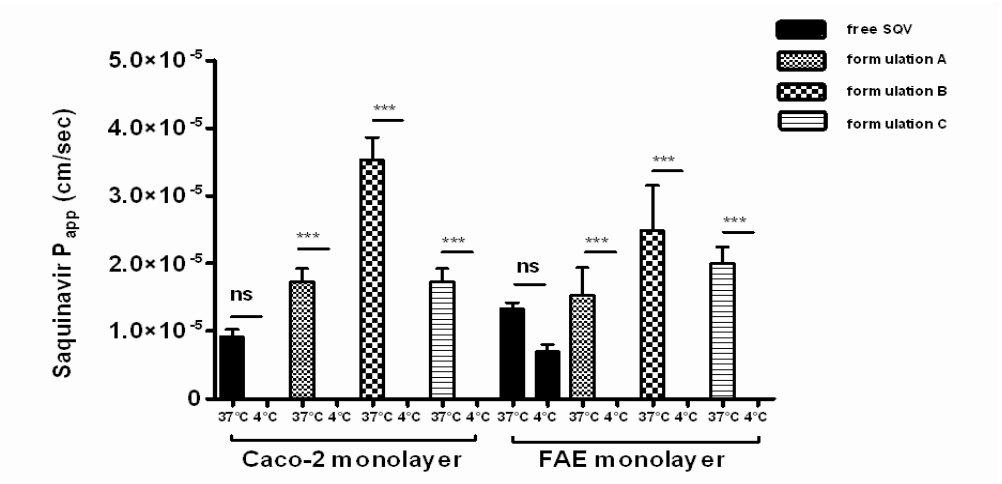

Fig 3. Influence of temperature on nanoparticle and free SQV transport in Caco-2 and FAE monolayers after 2 h of incubation at 37ºC and 4ºC. (n=9; ***p<0.001) (ns: no significant difference).

In all cases, nanoparticles penetrated enterocyte and M cell-like models in an active manner, whereas the suspension entered the cells passively. In most cases, SQV was not detected on the basolateral side after nanoparticle incubation at 4ºC (LOD<0.0125µg/mL).

3.3.3.2 Characterization of NLC endocytosis mechanisms

Taking the aforementioned results together, we can conclude that NLCs predominantly enter cells by endocytosis. Different mechanisms of nanocarrier internalization in cells have been described: macropinocytosis, clathrin-mediated endocytosis, caveolae-mediated endocytosis and clathrin- and caveolae-independent endocytosis [22]. To evaluate the endocytic mechanism used by NLCs, transport studies were undertaken in the presence of different inhibitors. We quantified the intracellular uptake by

FACs and the permeability of SQV across Caco-2 cells by HPLC after the transport study.

Figure 4 represents the intracellular uptake of coumarin-6-SQV-loaded NLCs in Caco-2 cells after 2 h of incubation along with chlorpromazine, an inhibitor of clathrin-mediated endocytosis [23,34], nystatin, an inhibitor of caveolae/lipid raft-mediated endocytosis [36,37] and MßCD+lovastatin, an inhibitor of both clathrin- and caveolae-mediated endocytosis [38].

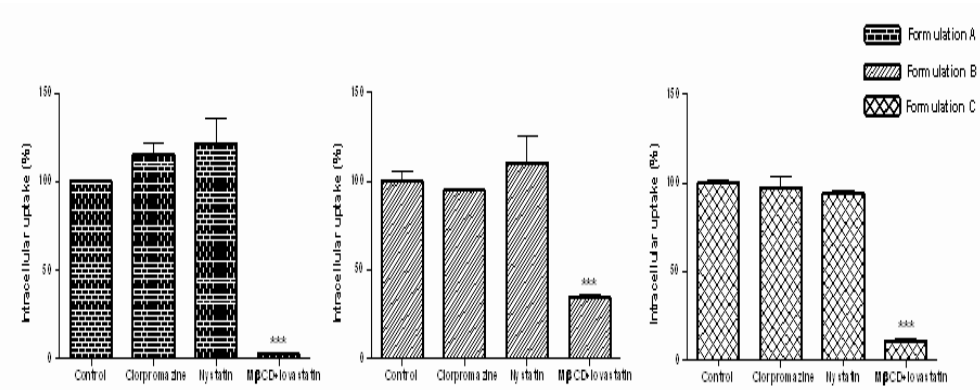

Fig 4. Intracellular uptake, measured by FACS, of coumarin-6-SQV-loaded NLCs in Caco-2 cells after 2 h of incubation with inhibitors. Formulations under no inhibition were considered as controls and represent P_{app} values of 100%. (n=3, ***p<0.001).

There was no significant difference in the presence of clathrin- or caveolae-mediated endocytosis inhibitors (chlorpromazine and nystatin, respectively) regardless of the nanoparticle formulation. In contrast, there was a significant difference when the cells were incubated in the presence of MßCD and lovastatin. It has to be remembered that, by sequestering cholesterol, we not only disrupt caveolae integrity but also other endocytic mechanisms involving cholesterol [51, 52], so that clathrin- and caveolae-independent cholesterol-dependent mechanisms may be involved in NLC endocytosis [53]. Furthermore, clathrin-independent endocytosis has been related to so called *lipid rafts*, lipid-based cholesterol-enriched microdomains present on certain cell surfaces. Whether caveolae and rafts share a common pathway remains

controversial [54-56], but both are undoubtedly sensitive to cholesterol depletion and share common machinery. Paillard et al. [57] also reported a significant decreased internalization of lipid nanocapsules under MßCD and lovastation inhibition regardless of nanoparticle size, suggesting that endogenous cholesterol was involved in lipid nanoparticle internalization. Although no significant differences were found regarding nystatin inhibition or chlorpromazine, during the intracellular uptake study, one should take into account the fact that the internalization process occurs under distinct mechanisms acting in parallel and, thus, the different endocytic pathways might tend to compensate each other [58]. This factor could explain, in part, why there were no significant differences in the endocytosis when incubating the nanocarriers with one of these specific inhibitors, but their involvement in nanoparticle internalization should not be totally discarded.

C viability was greater than 99% when compared to untreated cells in all cases except for formulation A co-incubated with MßCD + lovastatin for which viability was 65% (data not shown).

3.3.3.3 Transcytosis

It is important to distinguish between the mechanisms of endocytosis and transcytosis. Endocytosis involves the uptake or internalization of the nanoparticles inside the cells, whereas transcytosis is the transport across the cell from one membrane to the opposite. To evaluate the transcytosis of NLC formulations in the enterocyte-like model, we incubated the nanocarriers in the Caco-2 cells monolayers along with the clathrin-and caveolae-mediated inhibitors, chlorpromazine and nystatin, respectively. After 2 h of incubation, SQV P_{app} was estimated and results were expressed as percentage of control values. The P_{app} value of SQV-loaded NLCs under no inhibition was considered as 100% (control). Figure 5 features a diagram of SQV P_{app} after 2 h of incubation of SQV-loaded nanoparticles with chlorpromazine (Figure 5A) or nystatin (Figure 5B). Permeability decreased significantly with caveolae/lipid rafts depletion in the presence of nystatin regardless of the formulation (Figure 5B). Simionescu

et al. [59] suggest that endocytosis and transcytosis share the same mechanisms (receptor-independent and receptor-mediated) and caveolae. Hence, regarding the results obtained under caveolae/lipid raft inhibiton and the existence of a caveolae transcytotic pool, caveolae vesicle-mediated transcytosis appears to be involved in SQV transcytosis across Caco-2 cells regardless of the nanocarrier. The same decreased permeability was observed under clathrin depletion exclusively in the case of formulation B (Figure 5A), which means that clathrin is also involved in SQV transcytosis with this formulation. Roger et al. [24] also reported a clathrin- and caveolae-mediated internalization of paclitaxel-loaded lipid nanocapsules involved in the transcellular transport of the drug across Caco-2 cells, but in our study, in the case of NLCs, this was not a steady phenomenon and depended on nanoparticle size and the amount of surfactant employed in the formulation.

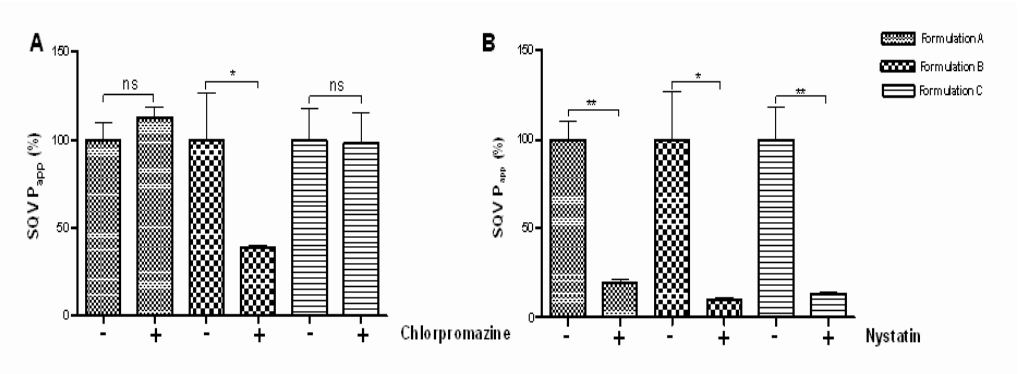

Fig 5. Comparison of SQV Papp values under clathrin (A) and caveolae (B) inhibition (chlorpromazine 10 µg/mL and nystatin 50 µg/mL, respectively) with untreated cell values (n=3-5; *p<0.05, **p<0.01, ns: no significant difference). ”-“ absence of an inhibitor,“+” under inhibition.

We relate the entry pathway of the nanocarriers with the transcytosis of the drugs itself, but we do not provide information about the fate of the nanoparticle inside of the cells as we did not assess the presence of the nanoparticles in the receiver compartment.

3.3.3.4 Evaluation of the contribution of P-gp inhibition to enhancement of SQV permeability

SQV is known to be a P-gp substrate [39]. To evaluate whether the NLCs inhibited the P-gp drug efflux, we conducted SQV permeability studies in Caco-2 cells under verapamil inhibition, a well-known P-gp inhibitor [41].

Figure 6 shows SQV P_{app} values after 2 h of incubation in the presence of 100 μM verapamil, inhibiting P-gp, or in a transport buffer, without P-gp inhibition.

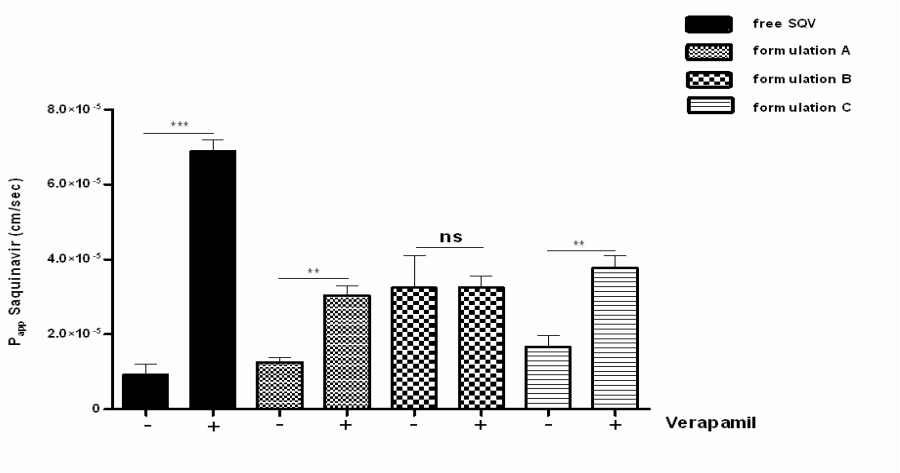

Fig 6. shows the SQV P_{app} values for free SQV and the nanoparticles after 2 h of incubation with 100 μM verapamil, a P-gp inhibitor (n=9; ns: no significance;**p<0.01, ***p<0.001). Formulations with no inhibition were considered as controls (n=3). "-" absence of verapamil,"+" under verapamil inhibition.

Our results confirm that SQV is a P-gp substrate. Indeed, incubating a SQV suspension with verapamil for 2 h significantly increased permeability (***p<0.001). Formulations A and C also exhibited greater permeability when the P-gp efflux was inhibited. In contrast, there was no difference in the permeability rates with formulation B regardless of the presence or absence of verapamil, suggesting that this formulation circumvented the P-gp efflux and, thus, enhanced SQV permeability. A shift in the internalization mechanism could explain how formulation B overcomes

the P-gp efflux. In this study, we have already reported clathrin-mediated transcytosis in addition to caveolae-mediated transcytosis for formulation B, which were not present with formulations A and C. This finding could explain the ability of formulation B to circumvent the P-gp drug efflux. P-gp is localized in caveolae [60], where it is co-localized with Cav-1 [61], the principal component of caveolae. Several immune-precipitation studies have suggested an interaction between P-gp and Cav-1, which could modulate P-gp transport activity. Barakat et al. [62] reported that decreased P-gp/Cav-1 interactions led to increased P-gp transport activity. Thus, one might hypothesize that, as clathrin-mediated endocytosis could contribute to the entrance of formulation B into the cell, there may be decreased competition for the caveolae pathway and, hence, increased P-gp/Cav-1 interaction and decreased P-gp activity. This ability of formulation B to overcome P-gp efflux could explain the 2-fold permeability increase found with formulation B in comparison to formulations A and C. Interestingly, the same formulation prepared by a different method and with a different size (247±4 nm versus 1,090±6 nm; formulation B and C respectively) did not have the same ability to overcome the P-gp, highlighting the importance not only of the composition but also of the method employed for the preparation as it provided a different particle size.

Figure 7 features a schematic representation of the NLC A, B and C transport across Caco-2 cells.

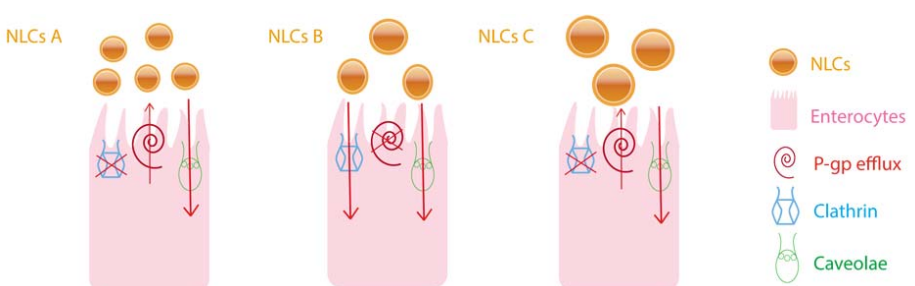

Fig 7. Scheme of the transport mechanisms used by the different NLC formulations.

Previous studies reported competition between lipid nanocapsules and P-gp for paclitaxel transport across Caco-2 cells describing P-gp inhibition by the nanoparticles themselves and suggesting that P-gp may not only be involved in drug efflux but also in the regulation of endocytosis [41]. However, the mechanisms used by these nanoparticles to inhibit the P-gp remained unclear. The mechanistic study allowed us to demonstrate the contribution of clathrin-mediated transcytosis of NLCs to circumvent P-gp, which resulted in a 2-fold increase in permeability of SQV, and highlights the importance of lipid nanoparticle size and composition on their ability to overcome the P-gp efflux.

These findings add to the large number of approaches for delivery of P-gp substrates using nano-technology [63].

5. Conclusion

In this study, we evaluated three different NLC formulations and assessed their potential to increase drug permeability using SQV (a BCS class IV drug and P-gp substrate) as a model drug. NLCs enhanced SQV permeability up to 3.5-fold. SQV transport across the intestinal barrier was influenced by the size of the NLCs and the amount of surfactant used for their formulation. Transport of NLCs was not increased by M cells, in contrast to drug suspension. Formulation B (247 nm and 1.5% (w/v) of surfactant content) circumvented the P-gp efflux and used both a caveolae- and clathrin-mediated transcytosis, in contrast to formulations A and C, which followed caveolae-mediated transcytosis. By modifying critical physicochemical parameters of the formulation we were able to overcome the P-gp drug efflux and alter the transcytosis mechanism of the nanoparticles. To our knowledge, this is the first time that a mechanistic study of NLC transport across intestinal *in vitro* models has been described. Our findings are encouraging for the delivery of class IV drugs and P-gp substrates by the oral route and support further nanotechnology approaches on this regard.

6. Acknowledgements

A. Beloqui wishes to thank the University of the Basque Country UPV/EHU for the fellowship grants (*Personal Investigador en Formación*

2008 and *Ayudas para la movilidad y divulgación de resultados de investigación en la Universidad del País Vasco, movilidad de investigadores en estancias 2011*). This work was partially supported by the Basque Government´s Department of Education, Universities and Investigation (IT-341-10) and *Fonds de la Recherche Scientifique Medical* (FRSM, Belgium).

References

[1] A. Dahan, A. Hoffman, The effect of different lipid based formulations on the oral absorption of lipophilic drugs: the ability of in vitro lipolysis and consecutive ex vivo intestinal permeability data to predict in vivo bioavailability in rats, Eur. J. Pharm. Biopharm. 67 (2007) 96-105.

[2] E.M. Merisko-Liversidge, G.G. Liversidge, Drug nanoparticles: formulating poorly water-soluble compounds, Toxicol. Pathol. 36 (2008) 43-48.

[3] C.M. O'Driscoll, B.T. Griffin, Biopharmaceutical challenges associated with drugs with low aqueous solubility--The potential impact of lipid-based formulations, Adv. Drug Deliv. Rev. 60 (2008) 617-624.

[4] Y. Kawabata, K. Wada, M. Nakatani, S. Yamada, S. Onoue, Formulation design for poorly water-soluble drugs based on biopharmaceutics classification system: basic approaches and practical applications, Int. J. Pharm. 420 (2011) 1-10.

[5] E. Merisko-Liversidge, G.G. Liversidge, Nanosizing for oral and parenteral drug delivery: A perspective on formulating poorly-water soluble compounds using wet media milling technology, Adv. Drug Deliv. Rev. 63 (2011) 427-440.

[6] O.C. Farokhzad, R. Langer, Impact of nanotechnology on drug delivery, ACS Nano. 3 (2009) 16-20.

[7] J. Shi, A.R. Votruba, O.C. Farokhzad, R. Langer, Nanotechnology in drug delivery and tissue engineering: from discovery to applications, Nano Lett. 10 (2010) 3223-3230.

[8] P. Couvreur, Nanoparticles in drug delivery: Past, present and future, Adv. Drug Deliv. Rev. (2012). In Press. http://dx.doi.org/10.1016/j.addr.2012.04.010

[9] C.E. Mora-Huertas, H. Fessi, A. Elaissari, Polymer-based nanocapsules for drug delivery, Int. J.Pharm. 385 (2010) 113-142.

[10] A. Elgart, I. Cherniakov, Y. Aldouby, A.J. Domb, A. Hoffman, Lipospheres and pro-nano lipospheres for delivery of poorly water soluble compounds, Chem. Phys. Lipids. 165 (2012) 438-453.

[11] N.T. Huynh, C. Passirani, P. Saulnier, J.P. Benoit, Lipid nanocapsules: A new platform for nanomedicine, Int. J. Pharm. 379 (2009) 201-209.

[12] H. Harde, M. Das, S. Jain, Solid lipid nanoparticles: an oral bioavailability enhancer vehicle, Expert Opin. Drug Deliv. 8 (2011) 1407–1424.

[13] G. Gaucher, P. Satturwar, M.-C. Jones, A. Furtos, J.-C. Leroux, Polymeric micelles for oral drug delivery, Eur. J. Pharm. Biopharm. 76 (2010) 147-158.

[14] V.P. Sant, D. Smith, J.-C. Leroux, Enhancement of oral bioavailability of poorly water-soluble drugs by poly(ethylene glycol)-block-poly(alkyl acrylate-co-methacrylic acid) self-assemblies, J. Control. Release. 104 (2005) 289-300.

[15] X. Pu, J. Sun, M. Li, Z. He, Formulation of nanosuspensions as a new approach for the delivery of poorly soluble drugs, Curr. Nanosci. 5 (2009) 417-427.

[16] P. Parhi, P. Suresh, Preparation and characterization of solid lipid nanoparticles- a review, Curr. Drug Discov. Technol. 9 (2012) 2–16.

[17] R.H. Müller, M. Radtke, S.A. Wissing, Nanostructured lipid matrices for improved microencapsulation of drugs, Int. J. Pharm. 242 (2002) 121-128.

[18] M. Muchow, P. Maincent, R. Muller, Lipid nanoparticles with a solid matrix (SLN, NLC, LDC) for oral drug delivery, Drug Dev. Ind. Pharm. 34 (2008) 1394-1405.

[19] J. Rejman, V. Oberle, I.S. Zuhorn, D. Hoekstra, Size-dependent internalization of particles via the pathways of clathrin- and caveolae-mediated endocytosis, Biochem. J. 377 (2004) 159-169.

[20] O. Harush-Frenkel, E. Rozentur, S. Benita, Y. Altschuler, Surface charge of nanoparticles determines their endocytic and transcytotic pathway in polarized MDCK cells, Biomacromolecules. 9 (2008) 435-443.

[21] M. Gaumet, R. Gurny, F. Delie, Interaction of biodegradable nanoparticles with intestinal cells: the effect of surface hydrophilicity, Int. J. Pharm. 390 (2010) 45-52.

[22] H. Hillaireau, P. Couvreur, Nanocarriers' entry into the cell:

relevance to drug delivery, Cell. Mol. Life Sci. 66 (2009) 2873-2896.

[23] F. Mathot, A. des Rieux, A. Ariën, Y.J. Schneider, M. Brewster, V. Préat, Transport mechanisms of mmePEG750P(CL-co-TMC) polymeric micelles across the intestinal barrier, J. Control. Release. 124 (2007) 134-143.

[24] E. Roger, F. Lagarce, E. Garcion, J.P. Benoit, Lipid nanocarriers improve paclitaxel transport throughout human intestinal epithelial cells by using vesicle-mediated transcytosis, J. Control. Release. 140 (2009) 174-181.

[25] I. Behrens, A.I. Pena, M.J. Alonso, T. Kissel, Comparative uptake studies of bioadhesive and non-bioadhesive nanoparticles in human intestinal cell lines and rats: the effect of mucus on particle adsorption and transport, Pharm. Res. 19 (2002) 1185-1193.

[26] A.des Rieux, E.G.E. Ragnarsson, E. Gullberg, V. Préat, Y.-J. Schneider, P. Artursson, Transport of nanoparticles across an in vitro model of the human intestinal follicle associated epithelium, Eur. J. Pharm. Sci. 25 (2005) 455-465.

[27] A. des Rieux, V. Fievez, I. Théate, J. Mast, V. Préat, Y.-J. Schneider, An improved in vitro model of human intestinal follicle-associated epithelium to study nanoparticle transport by M cells, Eur. J. Pharm. Sci. 30 (2007) 380-391.

[28] R. Müller, K. Mäder, S. Gohla, Solid lipid nanoparticles (SLN) for controlled drug delivery - a review of the state of the art, Eur. J. Pharm. Biopharm. 50 (2000) 161-177.

[29] R.H. Müller, D. Rühl, M. Lück, B.R. Paulke, Influence of fluorescent labelling of polystyrene particles on phagocytic uptake, surface hydrophobicity, and plasma protein adsorption, Pharm. Res. 14 (1997) 18-24.

[30] V. Albert, P. Modamio, C.F. Lastra, E.L. Mariño, Determination of saquinavir and ritonavir in human plasma by reversed-phase high-performance liquid chromatography and the analytical error function, J. Pharm. Biomed. Anal. 36 (2004) 835-840.

[31] M. Rescigno, M. Urbano, B. Valzasina, M. Francolini, G. Rotta, R. Bonasio, F. Granucci, J.-P. Kraehenbuhl, P. Ricciardi-Castagnoli, Dendritic cells express tight junction proteins and penetrate gut epithelial monolayers to sample bacteria, Nat. Immunol. 2 (2001) 361-367.

[32] A. des Rieux, V. Fievez, M. Momtaz, C. Detrembleur, M. Alonso-Sande, J. Van Gelder, A. Cauvin, Y.-J. Schneider, V.

Préat, Helodermin-loaded nanoparticles: characterization and transport across an in vitro model of the follicle-associated epithelium, J. Control. Release. 118 (2007) 294-302.

[33] P.B. Memvanga, V. Préat, Formulation design and in vivo antimalarial evaluation of lipid-based drug delivery systems for oral delivery of β-arteether, Eur. J. Pharm. Biopharm. 82 (2012) 112-119

[34] E. Roger, F. Lagarce, E. Garcion, J.P. Benoit, Lipid nanocarriers improve paclitaxel transport throughout human intestinal epithelial cells by using vesicle-mediated transcytosis, J. Control. Release. 140 (2009) 174-181.

[35] E. Gullberg, M. Leonard, J. Karlsson, A.M. Hopkins, D. Brayden, A.W. Baird, P. Artursson, Expression of specific markers and particle transport in a new human intestinal M-cell model, Biochem. Biophys. Res. Commun. 279 (2000) 808-813.

[36] Z. Zhang, F. Gao, H. Bu, J. Xiao, Y. Li, Solid lipid nanoparticles loading candesartan cilexetil enhance oral bioavailability: in vitro characteristics and absorption mechanism in rats, Nanomedicine. 8 (2012) 740-747

[37] S. Matveev, X. Li, W. Everson, E.J. Smart, The role of caveolae and caveolin in vesicle-dependent and vesicle-independent trafficking, Adv. Drug Deliv. Rev. 49 (2001) 237-250.

[38] S.K. Rodal, G. Skretting, O. Garred, F. Vilhardt, B. van Deurs, K. Sandvig, Extraction of cholesterol with methyl-beta-cyclodextrin perturbs formation of clathrin-coated endocytic vesicles, Mol. Biol. Cell. 10 (1999) 961-974.

[39] B.J. Aungst, P-glycoprotein, secretory transport, and other barriers to the oral delivery of anti-HIV drugs, Adv. Drug Deliv. Rev. 39 (1999) 105-116.

[40] S.J. Mouly, M.F. Paine, P.B. Watkins, Contributions of CYP3A4, P-glycoprotein, and serum protein binding to the intestinal first-pass extraction of saquinavir, J. Pharmacol. Exp. Ther. 308 (2004) 941-948.

[41] E. Roger, F. Lagarce, E. Garcion, J.P. Benoit, Reciprocal competition between lipid nanocapsules and P-gp for paclitaxel transport across Caco-2 cells, Eur. J. Pharm. Sci. 40 (2010) 422-429.

[42] I. Rivolta, A. Panariti, B. Lettiero, S. Sesana, P. Gasco, M.R. Gasco, M. Masserini, G. Miserocchi, Cellular uptake of coumarin-6 as a model drug loaded in solid lipid nanoparticles, J. Physiol. Pharmacol. 62 (2011) 45-53.

[43] A. del Pozo-Rodríguez, D. Delgado, M.Á. Solinís, J.L. Pedraz, E. Echevarría, J.M. Rodríguez, A.R. Gascón, Solid lipid nanoparticles as potential tools for gene therapy: In vivo protein expression after intravenous administration, Int. J. Pharm. 385 (2010) 157-162.

[44] J. Weiss, J. Burhenne, K.D. Riedel, W.E. Haefeli, Poor solubility limiting significance of in-vitro studies with HIV protease inhibitors, AIDS. 16 (2002) 674-676.

[45] F. Föger, K. Kafedjiiski, H. Hoyer, B. Loretz, A. Bernkop-Schnürch, Enhanced transport of P-glycoprotein substrate saquinavir in presence of thiolated chitosan, J. Drug Target. 15 (2007) 132-139.

[46] S.M. Pathak, P. Musmade, S. Dengle, A. Karthik, K. Bhat, N. Udupa, Enhanced oral absorption of saquinavir with Methyl-Beta-Cyclodextrin—preparation and in vitro and in vivo evaluation, Eur. J. Pharm. Sci. 41 (2010) 440-451.

[47] T.H. Ermak, P.J. Giannasca, Microparticle targeting to M cells, Adv. Drug Deliv. Rev. 34 (1998) 261-283.

[48] B. D'Souza, T. Bhowmik, R. Shashidharamurthy, C. Oettinger, P. Selvaraj, M. D'Souza, Oral microparticulate vaccine for melanoma using M-cell targeting, J. Drug Target. 20 (2011) 166-173.

[49] M. Liang, I.C. Lin, M.R. Whittaker, R.F. Minchin, M.J. Monteiro, I. Toth, Cellular uptake of densely packed polymer coatings on gold nanoparticles, ACS Nano. 4 (2009) 403-413.

[50] H. Tomoda, Y. Kishimoto, Y.C. Lee, Temperature effect on endocytosis and exocytosis by rabbit alveolar macrophages, J. Biol. Chem. 264 (1989) 15445-15450.

[51] S. Mayor, R.E. Pagano, Pathways of clathrin-independent endocytosis, Nat. Rev. Mol. Cell. Biol. 8 (2007) 603-612.

[52] Z.-J. Cheng, R.D. Singh, D.K. Sharma, E.L. Holicky, K. Hanada, D.L. Marks, R.E. Pagano, Distinct mechanisms of clathrin-independent endocytosis have unique sphingolipid requirements, Mol. Bio. Cell. 17 (2006) 3197-3210.

[53] G. Sahay, D.Y. Alakhova, A.V. Kabanov, Endocytosis of nanomedicines, J. Control. Release. 145 (2010) 182-195.

[54] I.R. Nabi, P.U. Le, Caveolae/raft-dependent endocytosis, J. Cell Biol. 161 (2003) 673-677.

[55] M. Kirkham, R.G. Parton, Clathrin-independent endocytosis: new insights into caveolae and non-caveolar lipid raft carriers, Biochim. Biophys. Acta. 1745 (2005) 273-286.
[56] R.G. Parton, A.A. Richards, Lipid Rafts and Caveolae as Portals for endocytosis: new Insights and common mechanisms, Traffic. 4 (2003) 724-738.

[57] A. Paillard, F. Hindré, C. Vignes-Colombeix, J.P. Benoit, E. Garcion, The importance of endo-lysosomal escape with lipid nanocapsules for drug subcellular bioavailability, Biomaterials. 31 (2010) 7542-7554.

[58] A. del Pozo-Rodríguez, S. Pujals, D. Delgado, M.A. Solinís, A.R. Gascón, E. Giralt, J.L. Pedraz, A proline-rich peptide improves cell transfection of solid lipid nanoparticle-based non-viral vectors, J. Control. Release. 133 (2009) 52-59.

[59] M. Simionescu, D. Popov, A. Sima, Endothelial transcytosis in health and disease, Cell Tissue Res. 335 (2009) 27-40.

[60] K. Yunomae, H. Arima, F. Hirayama, K. Uekama, Involvement of cholesterol in the inhibitory effect of dimethyl-β-cyclodextrin on P-glycoprotein and MRP2 function in Caco-2 cells, FEBS Lett. 536 (2003) 225-231.

[61] A. Garrigues, A.E. Escargueil, S. Orlowski, The multidrug transporter, P-glycoprotein, actively mediates cholesterol redistribution in the cell membrane, Proc Natl. Acad. Sci. U.S.A. 99 (2002) 10347-10352.

[62] S. Barakat, M. Demeule, A. Pilorget, A. Régina, D. Gingras, L.G. Baggetto, R. Béliveau, Modulation of p-glycoprotein function by caveolin-1 phosphorylation, J. Neurochem. 101 (2007) 1-8.

[63] R. Nieto Montesinos, A. Béduneau, Y. Pellequer, A. Lamprecht, Delivery of P-glycoprotein substrates using chemosensitizers and nanotechnology for selective and efficient therapeutic outcomes, J. Control. Release. 161 (2012) 50-61.

DISCUSSION

TECHNOLOGICAL FACTORS AFECTING NLCs FATE AFTER INTRAVENOUS ADMINISTRATION TO RATS

Nanoparticles for medical applications are frequently administered via parenteral administration. Nanomedicines are not different from other pharmaceutical products insofar as the safety of any new drug or drug carrier always has to be carefully assessed, through pre-clinical and clinical trials, prior to its approval by the regulatory agencies[1]. Although the potential of lipid nanoparticles for the intravenous delivery of drugs has been stated, there is still a necessity of *in vivo* studies establishing their parenteral acceptability for their further commercialization[2]. The biodistribution of nanoparticles is mainly determined by their chemical and physical properties, such as size, charge, and surface chemistry. In this study, the tissue distribution of three lipid formulations based on nanostructured lipid carriers (NLCs) after intravenous administration to rats was evaluated. The ultimate scope of this work was to gain insight into how the biodistribution is affected by these physicochemical properties in order to better optimize new formulations for specific biomedical applications.

We prepared three formulations based on NLCs and we evaluated the kinetic biodistribution profile of the NLCs by radiolabeling them with ^{99m}Tc and tracking them *in vivo* upon intravenous injection to rats in order to assess their potential clinical use.

Physicochemical properties of nanoparticles like the size or the surface charge are determinant parameters that highly influence nanoparticle biodistribution[3]. However, very few trends have been still identified[4]. In an attempt to make a step forward towards a better understanding of particle size and surface charge influence on lipid nanoparticle biodistribution, we elaborated NLC differing on these parameters (Table I).

Table I. Characterization of the nanoparticles evaluated in the study. The amounts of Mygliol (1% w/v) and Precirol ATO®5 (10% w/v) were the same in the preparation of all the formulations. Data are expressed as mean ± S.D. (n=3; S.D: standard deviation). § Higher than N3 and N1.5 ($p<0.05$). * Higher than N3 and P1.5 ($p<0.001$). ¥ Higher than N3 ($P<0.05$).

	N3	**N1.5**	**P1.5**
Tween 80 (% w/v)	2	1	1
Poloxamer 188 (% w/v)	1	0.5	-
CTAB (% w/v)		-	0.5
Zeta (mV)	-20±2	-19±3	+44±5§
Size (nm)	150±6	424±16*	180±7
PI	0.2±0.03	0.4±0.04¥	0.3±0.01

As expected, the application of the high pressure homogenization technique allowed us to obtain NLCs with a lower particle size and lower polidispersity index. The higher particle size was obtained when the NLCs were not subjected to the homogenization process, although the increment on particle size could also be due to the lower surfactant content. Regarding to the surfactants employed during the preparation of the NLCs, we obtained positively or negatively charged nanoparticles: the combination of Tween 80 and Poloxamer 188 provided negatively charged NLCs (N3 and N1.5), whereas the combination of Tween 80 and CTAB provided positively charged nanoparticles (P1.5).

After intravenously administered, the radiolabeled nanocarriers exhibited a long circulation time since radioactivity was detected in blood even 24 h post-injection (Figure 1).

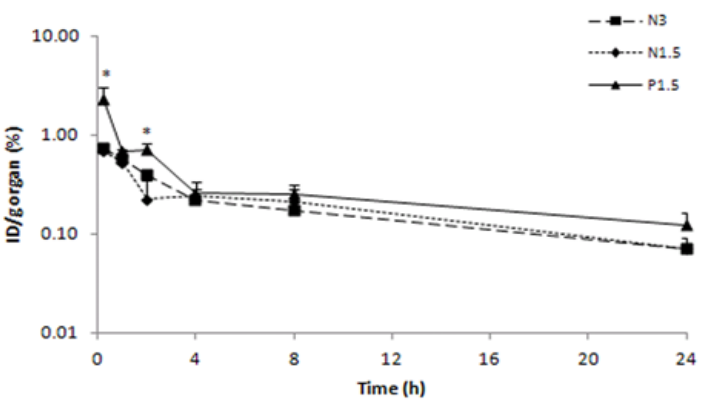

Figure 1. Biodistribution profile of ^{99m}Tc-NLCs in blood after intravenous administration to rats. *P1.5 higher than N3 and N1.5 ($p<0.05$).

It is known that the solid state of the lipid matrix present in these nanoparticles at body temperature results in a much slower degradation, making NLCs attractive carriers for the formulation of long-acting controlled release preparations over extended periods of time[5]. The small particle size of our nanoparticles (from 150 nm to 424 nm), along with the presence of hydrophilic surfactants (Poloxamer 188 and Tween 80) could also justify the prolonged

circulation time. Polyethylene glycol chains (PEG) in the Tween 80, and the Poloxamer 188 provide "stealth" properties to nanoparticles[6-8], which may justify the high MRT values obtained. Surface modification by pegylation is a well-established strategy for prolonging nanoparticle half-life, as it is known to decrease their recognition by the reticulo-endothelial system (RES)[9]. *Gref et al*.[10] were the first to report the advantages of pegylation on nanoparticles, resulting in a substantial increase in blood residence of nanoparticles. These authors observed that a PEG content in PLA nanoparticles as low as 0.5 wt % on the surface of the nanoparticles was able to significally reduce the total amount of blood protein absorbed when compared to nonpegylated PLA nanoparticles. The effect of PEG was previously reported also for PEG-coated liposomes[11] and lipid nanocapsules[12,13]. Due to all these properties, lipid-based nanoparticles help to stabilize drugs, such as peptides, proteins and nucleic acids, from plasma enzymes inactivation, providing an enhanced and significally prolonged biological activity[14-18].

No differences on the MRT values in blood among the NLCs were observed, in spite of the different particle size, surfactant content, and surface charge. However, cationic nanoparticles provided higher radioactivity levels during the first 2 h when compared to anionic nanoparticles and, consequently, higher AUC_{0-24} (Table II). This may be due to a lower uptake of the positive nanoparticles by the RES organs, such as the liver or the spleen. The tissue/blood radioactivity ratio (Figure 3) confirmed the low uptake of the cationic nanocarriers by the spleen, and, in the case of the liver, these positively charged NLCs (P1.5) were less uptaken than negatively charged nanoparticles holding similar particle size (N3). These results are in accordance to previously reported studies where positively charged solid lipid nanoparticles exhibited a low uptake by the RES system[19,20].

Table II. Pharmacokinetic parameters (C_{max}, AUC_{0-24}, MRT_{0-24}) estimated for the ^{99m}Tc-NLCs (N3, N1.5 and P1.5) after intravenous administration to rats.

		C_{max}	AUC_{0-24}	MRT_{0-24}
		%ID/g	h %ID/g	h
N3	Blood	0.73	4.48	7.02
	Spleen	1.40	10.05	8.92
	Pancreas	0.19	1.16	7.54
	Small intestine	0.32	1.84	7.19
	Liver	2.33	22.05	9.32
	Kidney	3.90	72.29	9.87
	Heart	0.30	1.68	6.56
	Lung	0.45	2.51	7.13
	Bone marrow	3.38	37.46	9.21
N1.5	Blood	0.69	4.61	7.44
	Spleen	1.18	6.94	6.81
	Pancreas	0.37	1.40	6.57
	Small intestine	0.41	1.98	6.22
	Liver	1.15	7.38	6.57
	Kidney	4.59	77.97	9.38
	Heart	0.31	1.63	6.74
	Lung	2.70	9.02	4.94
	Bone marrow	1.49	20.47	9.41
P1.5	Blood	2.26	7.41	6.61
	Spleen	2.10	2.87	9.90
	Pancreas	0.74	3.04	6.75
	Small intestine	0.93	4.17	6.65
	Liver	2.57	11.25	8.69
	Kidney	7.41	112.93	10.76
	Heart	0.85	2.85	6.71
	Lung	1.78	5.69	7.37
	Bone marrow	6.75	56.80	10.20

The highest radioactivity levels, expressed as %ID/g tissue, were observed in the kidney, followed by the bone marrow, the liver and the spleen (figure 2). In a previous study, pegylated liposomes were also detected mainly in these organs after the intravenous administration to mice[21]. The uptake into these organs is largely attributed to the macrophages residing in these tissues[22]. Taking into account the weight of the complete organ, the liver and the kidney accumulated more

radioactivity, and therefore, higher amount of nanoparticles. Other authors also reported higher radioactivity levels in the kidney after intravenous administration of radiolabeled nanoparticles and liposomes[23-26]. The accumulation of the nanoparticles in the kidney could be related to their excretion in urine. The discontinuous endothelium is a characteristic of the liver and bone marrow and explain the high levels of radioactivity in these organs[22]. In our study, the distribution in bone marrow was clearly influenced by the particle size (figure 2), being higher for the smaller particles (N3 and P1.5). *Snehalatha et al.*[23], found high levels of PLGA 85/15 nanoparticles (105 nm) in the bone following intravenous administration of ^{99m}Tc labeled nanoparticles to mice. In the authors opinion, the high radioactivity levels measured in the bone were attributed to nanoparticle uptake by the phagocytic reticulo-endothelial cells lining the vascular sinusoids of the bone marrow. As the particle size increases, more difficult is the access to bone marrow through the vascular sinusoids and explain the lower distribution of the formulation N1.5 in this tissue.

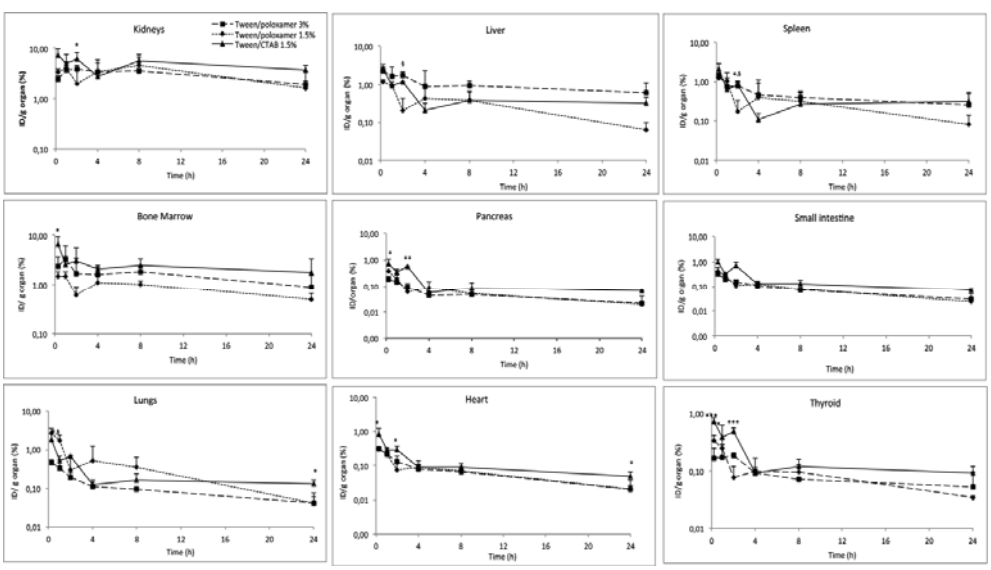

Figure 2. Biodistribution profile of ^{99m}Tc-NLCs in the removed organs after intravenous administration to rats. n=3; *p<0.05, **p<0.01; ***p<0.001 for P.1.5 higher than N3 and N1.5; §p<0.05 for N3 vs. N1.5 formulation.

Overall, brain uptake was negligible when comparing with other organs (<0.01%ID/g). Thus, although lipid nanoparticles have been considered for brain targeting[27], certain factors such as particle size, surface properties (e.g surface charge) or the presence of hydrophilic surfactants in these nanoparticles (Tween 80 and Poloxamer 188) seem not to be suitable for brain targeting.

Nanoparticles were also found in the lung (Figure 2). The N1.5 formulation was the most extensively distributed in this organ, as indicated by the C_{max} and AUC_{0-24} (Table II). This phenomenon could be attributed to the fact that this nanocarrier presented a higher particle size and, thus, the retention in the capillaries and latter removal from the lung is likely to happen. The MRT value and the uptake of this formulation were lower in the liver and the spleen in comparison with the smaller particle size nanoparticles. Likewise, these low values could be explained by their retention and elimination in the lung.

When comparing NLCs of similar particle size and different surface charge (N3 and P1.5) both formulations were mainly located in the kidney and the bone marrow, although the positively charged nanocarriers in a higher extension (Figure 3). It can be also elucidated from Figure 3 that anionic nanoparticles were more uptaken by the RES (liver and spleen) than the cationic ones.

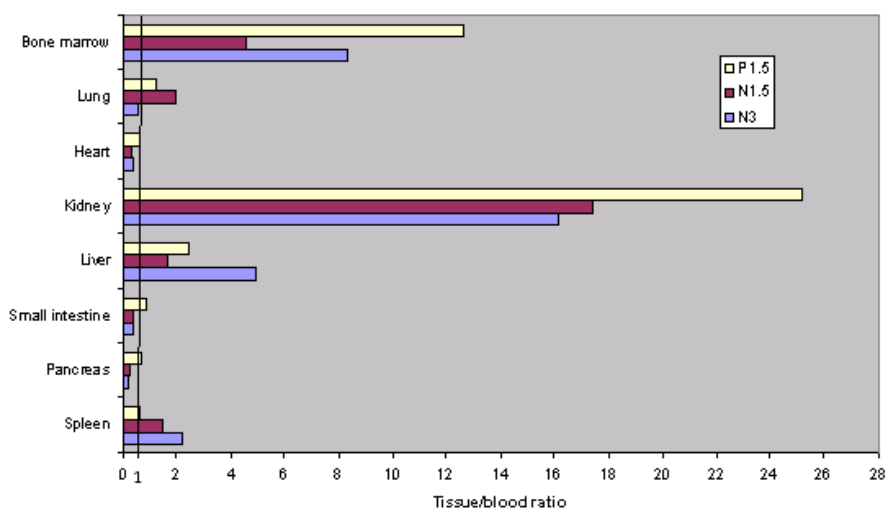

Figure 3. AUC_{tissue}/AUC_{blood} ratios for the assayed formulations

The MRT values in most tissues were closely to those in plasma, which indicated that unexpected accumulation should not occur in these tissues with repeated administration. Actually, prolonged circulation time also entails slow tissue accumulation of the nanoparticles and very slow drug release[22]. A rapid release formulation (within a few hours) would be more desirable for the NLCs we have designed.

Nanoparticles presenting an electrical charge, that can be either positive or negative, when intravenously administered, bind nonspecifically many products into their surface, especifically blood components. Protein binding has been pointed as a main cause of change in nanoparticle size and surface charge which leads to alterations in the biodistribution profiles and influences pathway-specific uptake following intravenous administration[28,29]. The “nanoparticle-protein corona” concept is focused on the basis that certain serum proteins are wrapping nanoparticle surface, evoking conformational changes in the surface and enhancing phagocytosis by the RES[9,30]. Therefore, the influence of particle size, surface charge and surfactant content on the biodistribution profile observed in our study will be also conditioned by differences in the binding pattern to blood components, which make difficult to stablish a relationship between the physicochemical properties of the nanoparticles and the biodistribution profile.

Taking into account the results obtained in our study, the potential clinical application of these nanocarriers could be focused on the preparation of long-acting controlled release formulations. The capacity to protect against plasma enzymes inactivation make these nanoparticles very useful for the administration of peptides, proteins and nucleic acids, prolonging their biological activity.

NANOSTRUCTURED LIPID CARRIERS (NLCs) FOR THE ORAL ADMINISTRATION OF SPIRONOLACTONE

Due to the increasing number of insoluble compounds among the newly discovered chemical entities, many efforts have been made for the efficient delivery of poorly water-soluble compounds. The enhancement of the oral bioavailability of these drugs remains a challenge in the drug delivery field. The administration of insoluble drugs as lipid-based formulations has been exploited as an alternative to conventional formulations. The combination of lipid-based formulations with nanotechnology provides additional advantages to the first ones as not only the lipids present in the formulation could help solubilizing the drug, but also lipid nanoparticles provide protection of the drug from the gastrointestinal degradation and the ability to target the drug to the specific site of effect by overcoming the biological barriers. Thus, we carried out a pharmacokinetic and biodistribution study of one of the previously studied NLC formulation following the oral route.

In this study, we have developed a formulation based on NLCs for spironolactone delivery by a high pressure homogenization method. This procedure allowed us to obtain without the use of any organic solvent, spherical and homogeneous in size nanoparticles with an encapsulation efficiency above 99%. The lipids employed for the preparation of the SPN-NLCs, mygliol and precirol, are recognized as totally biocompatible, reducing the possibility of side effects appearance after the *in vivo* admistration. Tween 80 and Poloxamer 188 were used as surfactants. On the one hand, poloxamer is an sterically stabilizing polymer and due to the stearic hindrance, induces a slow degradation of the nanoparticles [31]. On the other hand, Tween 80 has been identified as a lymphotropic excipient due to the ability to solubilise lipophilic drugs, inhibit the P-gp and stimulate chylomicron production[32].

In order to improve the storage stability of the SPN-NLCs, they were liophylized. A cryoprotector agent was neccesary and 5% trehalose showed to be the most appropriate.

The *in vitro* dissolution study carried out under sink conditions showed a very slow release of spironolactone from the nanocarriers and indicated a high stability of the SPN-NLCs in the dissolution media.

Once the SPN-NLCs were characterized, we evaluated the pharmacokinetic behavior of the drug after oral administration to rabbits. As reference formulation, we prepared a spironolactone syrup for oral administration and a solution was administered intravenously. Only spironolactone metabolites, canrenone and 7α-TMS, could be quantified in collected samples (Table III). Plasma half-life of both metabolites did not show statistical differences between intravenous and oral administration of the drug, which demonstrates that the elimination rate of both metabolites was not affected by the absorption process. The levels of 7α-TMS, in comparison with canrenone levels, were higher in all cases regardless the formulation. The absolute bioavailability of 7α-TMS was significantly higher with the syrup than the absolute bioavailability obtained with the SPN-NLCs (0.7 *vs* 0.4, $p<0.05$). However, no statistically significant differences were observed in the bioavailability of canrenone among formulations. These results reveal a different canrenone/7α-TMS ratio depending on the administered formulation, which could be explain by differences in the absorption mechanism of the drug.

		Syrup		NLCs		IV	
		Canrenone	**7α-TMS**	**Canrenone**	**7α-TMS**	**Canrenone**	**7α-TMS**
$t_{1/2}$	h	6.01 ± 1.07	5.97 ± 1.02	6.76 ± 1.06	8.09 ± 2.94	6.31 ± 2.64	4.56 ± 0.99
T_{max}	h	5.20 ± 1.79	5.80 ± 3.19	5.40 ± 1.34	4.88 ± 4.09	0.50 ± 0.00	0.50 ± 0.00
C_{max}	ng/mL	14.90 ± 6.07	44.26 ± 15.74	8.71 ± 2.23	21.76 ± 4.78	8.47 ± 2.74	36.54 ± 8.83
AUC_{0-t}	h ng/mL	163.59 ± 35.13	478.64 ± 98.37	113.05 ± 24.76	290.14 ± 74.94	38.77 ± 7.24	137.98 ± 18.48
$AUC_{0-\infty}$	h ng/mL	177.32 ± 34.57	523.92 ± 103.80	127.15 ± 32.43	348.73 ± 116.18	55.18 ± 8.43	172.68 ± 27.24
MRT	h	10.31 ± 1.42	10.58 ± 2.19	10.79 ± 1.92	12.79 ± 3.75	8.45 ± 2.77	5.92 ± 1.64
F		0.8 ± 0.2	0.7 ± 0.1*	0.6 ± 0.2	0.4 ± 0.2*		

Table III. Pharmacokinetic parameters of canrenone and 7α-TMS obtained by a noncompartmental analysis.*p<0.05.

Spironolactone is a poor water soluble compound and, therefore, its absorption is limited by the dissolution in the gastrointestinal fluid. Lipids from the formulation can promote the absorption of drugs through the formation of micelles. During the micelle formation process, the drug dissolved in the lipid is taken up in the micelles (solubilization) and the formed micelles interact with surface-active bile salts (e.g. sodium cholate) leading to the formation of so-called ´mixed micelles´[33]. This process could promote the lymphatic absorption that avoids the first-pass metabolism to a certain degree, which could explain the differences in the metabolic profile of spironolactone between the syrup and the nanoparticles. However, although the primary mechanism by which lipid formulations improve the bioavailability of lipophilic drugs is the increase of the dissolution rate[34], the low amount of spironolactone released in the dissolution studies, along with the lower pasma levels of spironolactone metabolites obtained with the SPN-NLCs than with the syrup, suggest that this might not be the case for the SPN-NLCs. In our opinion, the high stability of SPN-NLCs in the gastrointestinal tract would lead to a low dissolution rate of the spironolactone from the nanoparticles *in vivo*. In a previous

study, *Müller et al.*[31] formulated cyclosporine A into SLNs and orally administered them to pigs. The drug bioavailability obtained was low and the authors attributed it, among other factors, to a low dissolution rate of the drug/undissolved drug particles in the gut.

Since NLCs seem not to improve the dissolution rate of spironolactone, another mechanism should be involved in the absorption of the drug. It is well known that the NLCs may also be captured by the epithelial and M cells and further processed into blood circulation[35]. If this occurs, a high stability of the nanocarriers in the gastrointestinal tract is desirable. The mixture of Tween 80 and Poloxamer 188 in the SPN-NLCs lead to high stable nanoparticles and, as it was shown by the dissolution studies, spironolactone was hardly released. Therefore, and as it was previously discussed, the degradation velocity of lipid nanoparticles highly depends on its chemical composition, particularly on the stabilizer or the stabilizer mixture of the nanoparticles[31]. In addition to the composition, the particle size also affects the transport of nanocarriers through the biological barriers. The particle size of the SPN-NLCs was about 150 nm and it is known that particle size less than 300 nm is advisable for the intestinal transport[36]. Therefore, the absorption of spironolactone may occur by the uptake of the SPN-NLCs by the intestinal cells. This fact could also justify the differences in the canrenone/7α-TMS ratio depending on the administered formulation, syrup or SPN-NLCs. When nanoparticles are processed inside the enterocyte, the drug absorption may be influenced by the lipids of the SPN-NLCs, which could favor the lymphatic pathway leading to differences in the metabolic profile.

In order to know if SPN-NLCs were able to be uptaken by the intestinal wall, a biodistribution study with ^{99m}Tc radiolabeled nanocarriers was carried out. The radiotracer technique was chosen as it is one of the most appropiate to investigate the absorption, distribution, metabolism and excretion (ADME) of these nanomaterials[37]. Following oral administration of radiolabeled SPN-NLCs, radioactivity was mainly detected in the small intestine (figure 4). The intestine of the rats was cleaned of all food and waste material and thus, the radioactivity measured in this organ corresponded to labeled nanoparticles trapped in the mucosa. The lack of radioactivity in the thyroid confirms the stability of the nanocarriers in the gastrointestinal tract; the opposite would lead to the absorption of the free

^{99m}Tc[38,39]and the radioactivity levels in the thyroid would be significantly higher. The presence of the SPN-NLCs in the intestine along with the their adhesive properties[40], suggest a retention of the nanocarrier in the underlying epithelium[40-42].

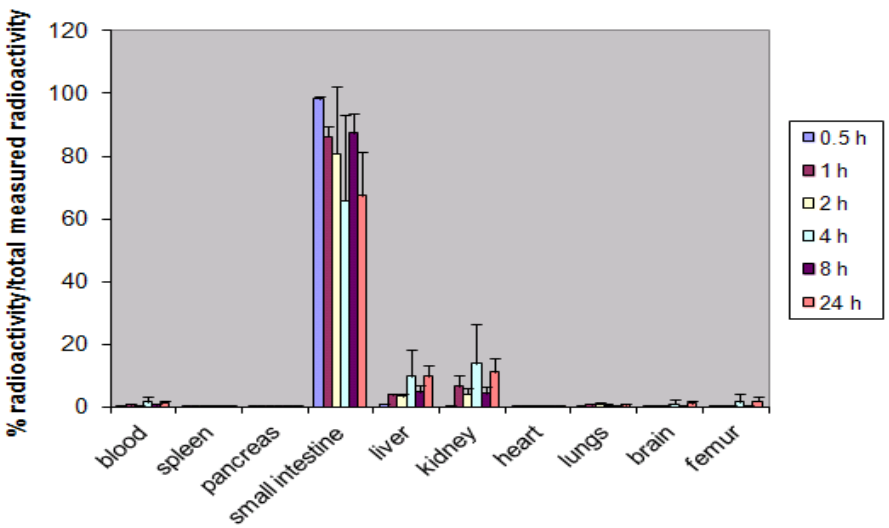

Figure 4. %radioactivity measure per organ/tissues after oral administration of SPN-NLCs labeled with ^{99m}Tc.

Therefore, the absorption of spironolactone and the change in its metabolic profile when comparing to the syrup (reference formulation) could be explained, at least in part, by the adhesion of SPN-NLCs to the gut wall and their subsequent uptake by the epithelial cells.

MECHANISM OF TRANSPORT OF SAQUINAVIR-LOADED NLCs ACROSS THE INTESTINAL BARRIER

In order to understand the processes involved on the NLC transport across the intestinal barrier, a mechanistic study was performed. Moreover, we also evaluated critical physicochemical properties that could highly interfere on nanoparticle uptake and drug permeability. In this case, we used saquinavir, a BSC class IV drug, a poorly water-soluble drug and P-gp substrate as model drug.

Three lipid formulations differing in particle size and surfactant content were obtained, all negatively charged. Particle characterization and compositions of the different formulations are summarized in Table V. The composition of these nanoparticles was based on results from previous studies on lipid nanoparticles carried out in our laboratory[43].

Table V. Summary of formulation composition and particle size, zeta potential and polydispersity index (P.I.) per formulation (n=3; data are expressed as mean ± SD).

		NLC formulations		
		A	**B**	**C**
Composition	**Tween 80 (g)**	1	0.5	0.5
	Poloxamer 188 (g)	0.5	0.25	0.25
	Precirol ATO® 5 (g)	5	5	5
	Mygliol 812N/F (mL)	0.5	0.5	0.5
	SQV (mg)	50	50	50
	H_2O (mL)	50	50	50
	Homogenization	Yes	Yes	No
Characterization	**Size (nm)**	165±6	247±4	1,090±6
	Zeta (mV)	-21±8	-33±7	-31±5
	P.I.	0.16	0.35	0.6
	Surface hydrophobicity (slope)	0.054	0.040	0.008
	EE (%)	99±0.2	99±0.02	99±0.14
	Drug loading (%)	0.90±0.00	0.90±0.00	0.90±0.00

All the formulations had an EE of ~100% and drug loading of ~0.90%. Reduction in the amount of surfactant present in the formulation lead to an increased particle size (165±6 nm *vs* 247±4 nm for formulations A and B, respectively). Moreover, when formulation B was prepared without further homogenization (formulation C), the particle size varied from the nanometer to the micrometer range (247±4 nm vs 1090±6 nm for formulations B and C, respectively), highlighting the importance of the preparation method in obtaining different nanoparticle size. Although SQV is considered a model drug, the low drug loading of SQV (~0.90%; therapeutic dose 1g twice a day) compromises the foreseen application of these nanocarriers to reach an efficient therapeutic effect of the drug and it would be desirable to encapsulate more potent drugs with a lower therapeutic dose (e.g. budesonide, 9 mg once a day in Crohn's disease).

There were no differences in nanoparticle parameters and EE of SQV when incorporating coumarin-6 (5 mg) into the formulations (data not shown). There was a difference in nanoparticle surface hydrophobicity between the three formulations: formulation A had a higher slope and, thus, higher hydrophobicity compared to formulations B and C. Formulations B and C had the same amount of surfactant but formulation B had higher hydrophobicity than formulation C, which can be explained by the different surface areas of the two formulations[44].

An *in vitro* dissolution study was performed to ensure that SQV was not released from the NLC formulations during the *in vitro* transport studies. The amount of drug released from the NLCs into the transport buffer medium (HBSS) during 2 h of incubation at 37ºC was analyzed by HPLC (n=3). For the three formulations, SQV release was less than 0.4% indicating that the differences in the subsequent data were not the result of greater dissolution (maximum solubility of SQV mesylate in HBSS ~50 μg/mL[45]). Moreover, for the three formulations, the drug released from NLCs in SGF media after 2 h of incubation at 37ºC was below the LOD (LOD<0.0125μg/mL) (n=3). SQV release was below the LOD after 2h and less than 5% in SIF media after 8 h of incubation 37ºC (n=3).

The main aim of the present study was to evaluate the potential of NLCs as suitable carriers for poorly water-soluble drugs using SQV as a BCS class IV model drug. For this purpose, the permeability of SQV across the enterocyte-like model (Caco-2 monolayers) and the FAE monolayers (Caco-2/Raji cell coculture) was evaluated. The conversion of Caco-2 cells into M-cells in the FAE model was confirmed by measuring the number of commercial carboxylated particles transported using a flow cytometer. After 2 h of incubation, the number of transported nanoparticles was significantly higher in the FAE model than in the Caco-2 model (82,633±6,443 nanoparticles, versus 108±91, respectively; n=4, $p<0.05$).

The permeability values obtained for each nanoparticle formulation was compared with the permeability values of free SQV as a suspension. Figure 5 represents the P_{app} of SQV data obtained for the assayed formulations after 2 h of incubation in Caco-2 monolayers and in FAE monolayers.

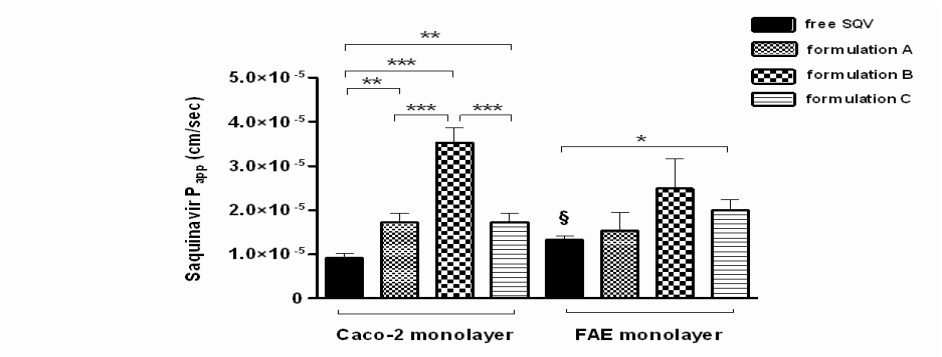

Figure 5. Saquinavir (SQV) P_{app} values obtained after 2 h of incubation of the three NLC formulations (A, B and C) and a SQV suspension in the Caco-2 monolayers and the FAE monolayers. (n=9, mean ± S.D, *p<0.05, **p<0.01, ***p<0.001).§p<0.05 versus Caco-2 monolayers.

In the Caco-2 model, the increase in SQV P_{app} values for the nanoparticle formulations compared to free SQV, is highlighted. It is remarkable to note the 3.5-fold increase in the SQV P_{app} with formulation B compared to free SQV ($p<0.001$), and the 2-fold increase compared with the two other NLC formulations (A and C) ($p<0.01$). These SQV P_{app} values are greater than previously reported values obtained across Caco-2 monolayers and ex vivo transport studies using different strategies for enhancing SQV permeability[46,47]. These data confirm that NLCs are suitable carriers for enhancing the permeability of poorly water-soluble drugs. There was a significant difference between the P_{app} values of formulation B (247±4 nm) and C (1,090±6 nm) ($3.52\text{x}10^{-5}\pm3.34\text{x}10^{-6}$cm/s versus $1.73\text{x}10^{-5}\pm2.09\text{x}10^{-6}$ cm/s, respectively; n=9, ***$p<0.001$).

In the M cell model, there was a significant increase in the P_{app} of formulation C compared to free SQV in suspension ($p<0.05$), which was not observed for formulations A or B ($p>0.05$). Enhanced microparticles uptake by M cells has been previously reported[48,49]. In contrast to polymeric nanoparticles[50], the permeability of the drug from the submicron NLCs was not increased in M cells. Hence, the subsequent evaluation of the transport mechanisms and the intracellular uptake was evaluated only in the Caco-2 cell model.

The diffusion of the particles through the mucus could also affect their transport[51]. Peyer's patches, in particular M cells, are less protected by the mucus barrier but account for only 1% of total surface area. The mucus penetrating properties of lipid-based nanoparticles, including NLCs, have not been extensively studied. NLCs are small enough (formulation A and B) to avoid being blocked sterically in the mucin mesh. However, as the mucus is rich in lipids, mucoadhesion of the NLCs could be promoted by their hydrophobic surface even if the surfactant coating could make their surface partly hydrophilic and more mucus penetrating. Mucus interaction with NLCs should be investigated.

Figure 6 shows the flow cytometry results (Figure 6A) and the CLSM images (Figure 6B and 6C) corresponding to the cellular uptake of the nanoparticle formulations and free coumarin-6. Cell viability was assessed by staining dead cells with PI and was greater than 90% in all cases unless otherwise stated. Untreated cells were used as controls.

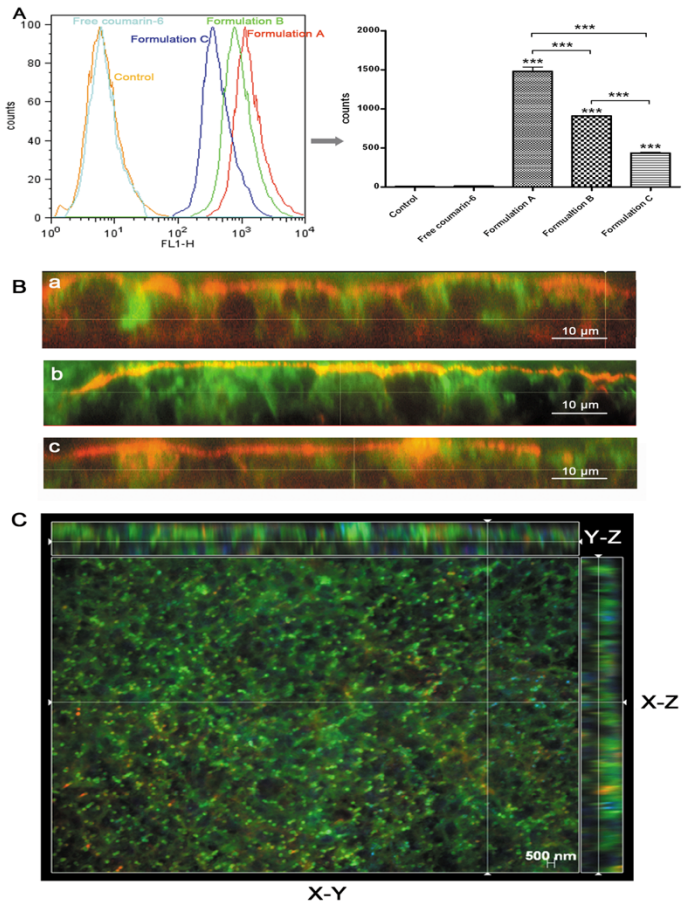

Figure 6. Cellular uptake of coumarin-6 NLCs (green) in Caco-2 cells, measured by flow cytometry, (A) and CLSM images (B and C) of the inserts after 2 h of incubation with the nanoparticles. A) Nanoparticles and free coumarin-6 entrance into the cell measured by flow cytometry. Untreated cells are shown as control (n=3; ***p<0.001). B) a, b and c correspond to *y-z* sections of CLSM images of the inserts for formulations A, B and C, respectively. Cell membranes are stained in red with rhodamine-phalloidine and cell nuclei in blue with DAPI. C) *y-z*, *x-y* and *x-z* sections of formulation A CLSM images with which the higher uptake rate was recorded.

The cellular uptake of NLCs was size-dependent (formulation A> B> C; n=3, ***p<0.001; Figure 2A). This finding is consistent with *Rejman et al*.[52] who also reported a tendency to decreased internalization with increased particle size. These authors studied the pathway of entry and subsequent fate of commercial latex nanoparticles inside the cell and concluded that particles with a diameter <200 nm enter the cell via clathrin-mediated endocytosis whereas larger particles (200 nm-1 μm) enter preferentially via caveolae-mediated endocytosis. Moreover, the surface hydrophobicity of the nanoparticles may also determine nanoparticle entrance into Caco-2 cell because the larger uptake into the cells is correlated with the higher nanoparticle surface hydrophobicity (formulation A>B>C) [53]. *Gaumet et al.* [54] found that the surface hydrophilicity of polymeric nanoparticles was a critical factor for nanoparticle uptake and *Liang et al.* [55] reported that gold nanoparticles were more efficiently taken up with increasing hydrophobic interactions with the membrane of Caco-2 cells. In our study, nanoparticle size and surface hydrophobicity were major factors influencing NLC entrance into the cell.

The P_{app} values for SQV formulated in NLCs did not correlate with their intracellular uptake. Formulation B exhibited higher SQV P_{app} values than did formulations A and C but did not have a higher intracellular uptake. Figure 2B shows that NLCs penetrated inside the Caco-2 cells whatever the formulation.

Another objective of the present study was to evaluate the mechanisms of transport used by the different NLC formulations to estimate whether the differences on permeability were due to different entry pathways. For this purpose, we first focused on the type of transport: passive or active. Although lipid nanoparticles are known to enter into cells in an active endocytic manner[56], we assessed this phenomenon in Caco-2 cells and the FAE model. It is well-established that at 4ºC pinocytic/endocytic uptake is inactivated[57]. Figure 7 illustrates the influence of temperature on the transport of SQV-loaded nanoparticles and SQV suspension across Caco-2 and FAE monolayers. In most cases, SQV was not detected in the basolateral side after nanoparticle incubation at 4ºC (LOD<0.0125μg/mL). These data suggest that SQV loaded in NLCs might mainly permeate Caco-2 cells and FAE monolayers in an active manner.

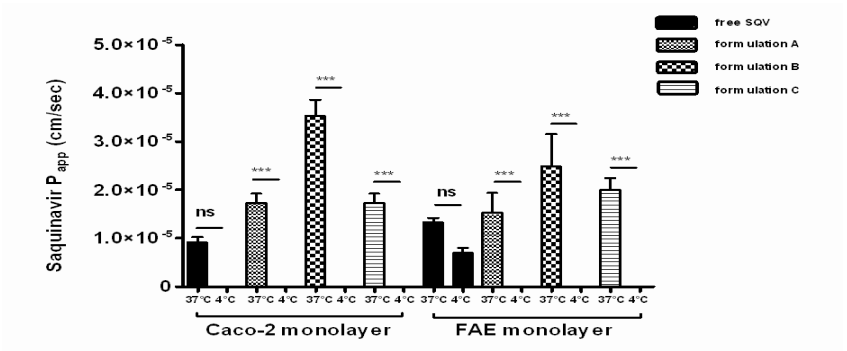

Figure 7. Influence of temperature on nanoparticle and free SQV transport in Caco-2 and FAE monolayers after 2 h of incubation at 37ºC and 4ºC. (n=9; ***p<0.001) (ns: no significant difference).

Taking the aforementioned results together, we can conclude that NLCs predominantly enter cells by endocytosis. Different mechanisms of nanocarrier internalization in cells have been described: macropinocytosis, clathrin-mediated endocytosis, caveolae-mediated endocytosis and clathrin- and caveolae-independent endocytosis[58]. To evaluate the endocytic mechanism used by NLCs, transport studies were undertaken in the presence of different inhibitors. We quantified the intracellular uptake, measured by flow citometry, and the permeability of SQV across Caco-2 cells by HPLC after the transport study.

Figure 8 represents the intracellular uptake of coumarin-6-SQV-loaded NLCs in Caco-2 cells after 2 h of incubation along with chlorpromazine, an inhibitor of clathrin-mediated endocytosis[56,59], nystatin, an inhibitor of caveolae/lipid raft-mediated endocytosis[60,61] and methyl-β-cyclodextrin (MßCD) + lovastatin, an inhibitor of both clathrin- and caveolae-mediated endocytosis[62].

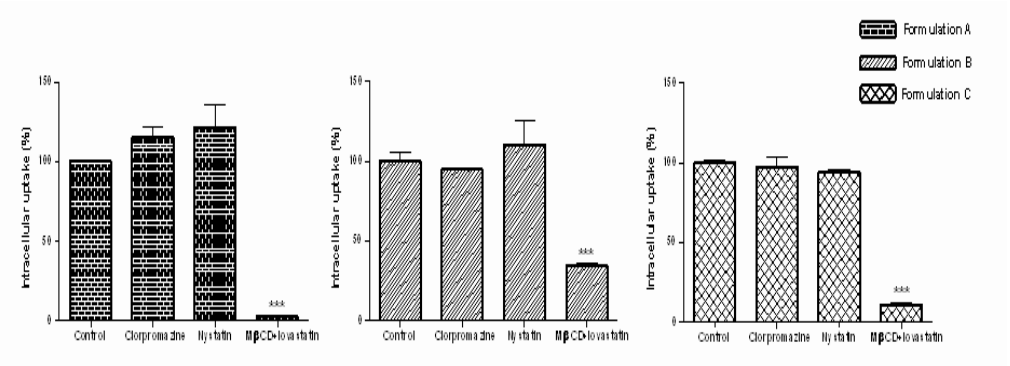

Figure 8. Intracellular uptake, measured by flow citometry, of coumarin-6-SQV-loaded NLCs in Caco-2 cells after 2 h of incubation with inhibitors. Formulations under no inhibition were considered as controls and represent P_{app} values of 100%. (n=3, ***p<0.001).

There was no significant difference in the presence of clathrin- or caveolae-mediated endocytosis inhibitors (chlorpromazine and nystatin, respectively) regardless of the nanoparticle formulation. In contrast, there was a significant difference when the cells were incubated in the presence of MßCD and lovastatin. It has to be remembered that, by sequestering cholesterol, is not only caveolae integrity disrupted but also other endocytic mechanisms involving cholesterol [63,64], so that clathrin- and caveolae-independent cholesterol-dependent mechanisms may be involved in NLC endocytosis[65]. Furthermore, clathrin-independent endocytosis has been related to so called *lipid rafts*, lipid-based cholesterol-enriched microdomains present on certain cell surfaces. Whether caveolae and rafts share a common pathway remains controversial[66-68], but both are undoubtedly sensitive to cholesterol depletion and share common machinery. *Paillard et al.* [69] also reported a significant decreased internalization of lipid nanocapsules under MßCD and lovastation inhibition regardless of nanoparticle size, suggesting that endogenous cholesterol was involved in lipid nanoparticle internalization. Although no significant differences were found regarding nystatin inhibition or chlorpromazine, during the intracellular uptake study, one should take into account the fact that the internalization process occurs under distinct mechanisms acting in parallel and, thus, the different endocytic pathways might tend to compensate each other [70]. This factor could explain, in part, why there were no significant differences in the

endocytosis when incubating the nanocarriers with one of these specific inhibitors, but their involvement in nanoparticle internalization should not be totally discarded. Cell viability was greater than 99% when compared to untreated cells in all cases except for formulation A co-incubated with MßCD + lovastatin for which viability was 65% (data not shown).

It is important to distinguish between the mechanisms of endocytosis and transcytosis. Endocytosis involves the uptake or internalization of the nanoparticles inside the cells, whereas transcytosis is the transport across the cell from one membrane to the opposite. To evaluate the transcytosis of NLC formulations in the Caco-2 cell model, the nanocarriers were incubated in the Caco-2 cells monolayers along with the clathrin-and caveolae-mediated inhibitors, chlorpromazine and nystatin, respectively. After 2 h of incubation, SQV P_{app} was estimated and results were expressed as percentage of control values. The P_{app} value of SQV-loaded NLCs under no inhibition was considered as 100% (control). Figure 5 features a diagram of SQV P_{app} after 2 h of incubation of SQV-loaded nanoparticles with chlorpromazine (Figure 9A) or nystatin (Figure 9B). SQV P_{app} was also evaluated under MßCD and lovastatin inhibition. The presence of these inhibitors induced TEER values of the monolayers less than 200 Ω cm^2 after the transport study. Therefore, because we could not guarantee the integrity of the monolayer, these results were excluded and transcytosis was characterized exclusively under nystatin and chlorpromazine inhibition. Permeability decreased significantly with caveolae/lipid rafts depletion in the presence of nystatin regardless of the formulation (Figure 9B). *Simionescu et al.*[71] suggest that endocytosis and transcytosis share the same mechanisms (receptor-independent and receptor-mediated) and caveolae. Hence, regarding the results obtained under caveolae/lipid raft inhibiton and the existence of a caveolae transcytotic pool, caveolae vesicle-mediated transcytosis appears to be involved in SQV transcytosis across Caco-2 cells regardless of the nanocarrier. The same decreased permeability was observed under clathrin depletion exclusively in the case of formulation B (Figure 9A), which means that clathrin is also involved in SQV transcytosis with this formulation. *Roger et al.*[72] also reported a clathrin- and caveolae-mediated internalization of paclitaxel-loaded lipid nanocapsules involved in the transcellular transport of the drug across Caco-2 cells, but in our study, in the case of NLCs, this was not a steady

phenomenon and depended on nanoparticle size and the amount of surfactant employed in the formulation.

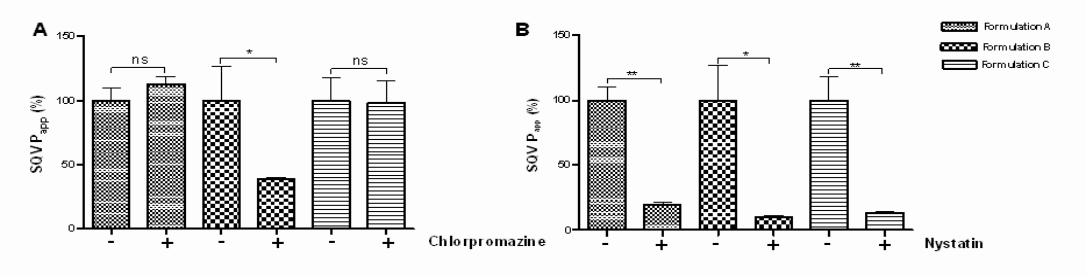

Figure 9. Comparison of SQV Papp values under clathrin (A) and caveolae (B) inhibition (chlorpromazine 10 μg/mL and nystatin 50 μg/mL, respectively) with untreated cell values (n=3-5; *p<0.05, **p<0.01, ns: no significant difference). "-" absence of an inhibitor,"+" under inhibition.

We relate the entry pathway of the nanocarriers with the transcytosis of the drugs itself, but we do not provide information about the fate of the nanoparticle inside of the cell as we did not assess the presence of the nanoparticles in the receiver compartment.

SQV is known to be a P-gp substrate[73]. To evaluate whether the NLCs inhibited the P-gp drug efflux, we conducted SQV permeability studies in Caco-2 cells under verapamil inhibition, a well-known P-gp inhibitor[74].

Figure 10 shows SQV P_{app} values after 2 h of incubation in the presence of 100 μM verapamil, inhibiting P-gp, or in a transport buffer, without P-gp inhibition.

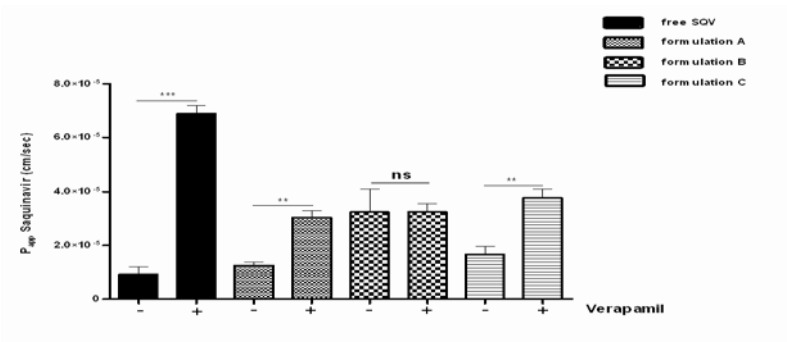

Figure 10. SQV P_{app} values for free SQV and the nanoparticles after 2 h of incubation with 100 μM verapamil, a P-gp inhibitor (n=9; ns: no significance;**p<0.01, ***p<0.001). Formulations with no inhibition were considered as controls (n=3). "-" absence of verapamil,"+" under verapamil inhibition.

Our results confirm that SQV is a P-gp substrate. Indeed, incubating a SQV suspension with verapamil for 2 h significantly increased permeability (***p<0.001). Formulations A and C also exhibited greater permeability when the P-gp efflux was inhibited. In contrast, there was no difference in the permeability rates with formulation B regardless of the presence or absence of verapamil, suggesting that this formulation circumvented the P-gp efflux and, thus, enhanced SQV permeability. A shift in the internalization mechanism could explain how formulation B overcomes the P-gp efflux. In this study, it was already reported a clathrin-mediated transcytosis in addition to a caveolae-mediated transcytosis for formulation B, which were not present with formulations A and C. This finding could explain the ability of formulation B to circumvent the P-gp drug efflux. P-gp is localized in caveolae[75], where it is co-localized with Cav-1[76], the principal component of caveolae. Several immunoprecipitation studies have suggested an interaction between P-gp and Cav-1, which could modulate P-gp transport activity. *Barakat et al.*[77] reported that decreased P-gp/Cav-1 interactions led to increased P-gp transport activity. Thus, one might hypothesize that, as clathrin-mediated endocytosis could contribute to the entrance of formulation B into the cell, there may be decreased competition for the caveolae pathway and, hence, increased P-gp/Cav-1 interaction and decreased P-gp activity. This ability of formulation B to overcome P-gp efflux could explain the 2-fold permeability increase found with formulation B in comparison to formulations A

and C. Interestingly, the same formulation prepared by a different method and with a different size (247±4 nm versus 1,090±6 nm; formulation B and C respectively) did not have the same ability to overcome the P-gp, highlighting the importance not only of the composition but also of the method employed for the preparation as it provided a different particle size.

Figure 11 features a schematic representation of the NLC A, B and C transport across Caco-2 cells.

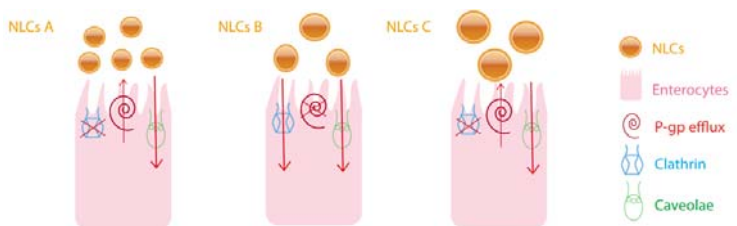

Figure 11. Scheme of the transport mechanisms used by the different NLC formulations.

Previous studies reported competition between lipid nanocapsules and P-gp for paclitaxel transport across Caco-2 cells describing P-gp inhibition by the nanoparticles themselves and suggesting that P-gp may not only be involved in drug efflux but also in the regulation of endocytosis [74]. However, the mechanisms used by these nanoparticles to inhibit the P-gp remained unclear. The mechanistic study allowed us to demonstrate the contribution of clathrin-mediated transcytosis of NLCs to circumvent P-gp, which resulted in a 2-fold increase in permeability of SQV, and highlights the importance of lipid nanoparticle size and composition on their ability to overcome the P-gp efflux.

These findings add to the large number of approaches for delivery of P-gp substrates using nanotechnology[78].

REFERENCES

1. Nyström, A.M. & Fadeel, B. Safety assessment of nanomaterials: Implications for nanomedicine. *J Control Release* **161**, 40-408 (2012).
2. Joshi, M.D. & Müller, R.H. Lipid nanoparticles for parenteral delivery of actives. *Eur J Pharm Biophars* **71**, 161-172 (2009).
3. Alexis, F., Pridgen, E., Molnar, L.K. & Farokhzad, O.C. Factors Affecting the Clearance and Biodistribution of Polymeric Nanoparticles. *Mol Pharm* **5**, 505-515 (2008).
4. Decuzzi, P*., et al.* Size and shape effects in the biodistribution of intravascularly injected particles. *J Control Release* **141**, 320-327 (2010).
5. Lim, S.B., Banerjee, A. & Önyüksel, H. Improvement of drug safety by the use of lipid-based nanocarriers. *J Control Release* **163**, 34-45 (2012).
6. Göppert, T.M. & Müller, R.H. Plasma protein adsorption of Tween 80- and poloxamer 188-stabilized solid lipid nanoparticles. *J Drug Target* **11**, 225-231 (2003).
7. Dufort, S., Sancey, L. & Coll, J.L. Physico-chemical parameters that govern nanoparticles fate also dictate rules for their molecular evolution. *Adv Drug Deliv Rev* **64**, 179-189 (2012).
8. Chae, J.M., Mo, S.M. & Oh, I.J. Effects of poloxamer 188 on the characteristics of poly(lactide-co-glycolide) nanoparticles. *J Nanosci Nanotechnol* **10**, 3224-3227 (2010).
9. Ozcan, I*., et al.* Pegylation of poly(γ-benzyl-L-glutamate) nanoparticles is efficient for avoiding mononuclear phagocyte system capture in rats. *Int J Nanomedicine* **5**, 1103-1111 (2010).
10. Gref, R*., et al.* 'Stealth' corona-core nanoparticles surface modified by polyethylene glycol (PEG): influences of the corona (PEG chain length and surface density) and of the core composition on phagocytic uptake and plasma protein adsorption. *Colloids Surf B Biointerfaces* **18**, 301-313 (2000).
11. Storm, G., Belliot, S.O., Daemen, T. & Lasic, D.D. Surface modification of nanoparticles to oppose uptake by the mononuclear phagocyte system. *Adv Drug Deliv Rev* **17**, 31-48 (1995).
12. Hoarau, D*., et al.* Novel Long-Circulating Lipid Nanocapsules. *Pharm Res* **21**, 1783-1789 (2004).
13. Ballot, S*., et al.* ^{99m}Tc/^{188}Re-labelled lipid nanocapsules as promising radiotracers for imaging and therapy: formulation and biodistribution. *Eur J Nucl Med Mol Imaging* **33**, 602-607 (2006).

14. Krishnadas, A., Onyüksel, H. & Rubinstein, I. Interactions of VIP, secretin and PACAP(1-38) with phospholipids: a biological paradox revisited. *Curr Pharm Des* **9**, 1005-1012 (2003).
15. Onyüksel, H., Séjourné, F., Suzuki, H. & Rubinstein, I. Human VIP-alpha: a long-acting, biocompatible and biodegradable peptide nanomedicine for essential hypertension. *Peptides* **27**, 2271-2275 (2006).
16. Banerjee, A. & Onyuksel, H. Human pancreatic polypeptide in a phospholipid-based micellar formulation. *Pharm Res* **29**, 1698-1711 (2012).
17. Kuzmis, A*., et al.* Micellar nanomedicine of human neuropeptide Y. *Nanomedicine* **7**, 464-471 (2011).
18. Delgado, D*., et al.* Dextran-protamine-solid lipid nanoparticles as a non-viral vector for gene therapy: in vitro characterization and in vivo transfection after intravenous administration to mice. *Int J Pharm* **425**, 35-43 (2012).
19. Reddy, L., Sharma, R., Chuttani, K., Mishra, A. & Murthy, R. Etoposide-incorporated tripalmitin nanoparticles with different surface charge: Formulation, characterization, radiolabeling, and biodistribution studies. *The AAPS Journal* **6**, 55-64 (2004).
20. Harivardhan Reddy, L., Sharma, R.K., Chuttani, K., Mishra, A.K. & Murthy, R.S.R. Influence of administration route on tumor uptake and biodistribution of etoposide loaded solid lipid nanoparticles in Dalton's lymphoma tumor bearing mice. *J Control Release* **105**, 185-198 (2005).
21. Chen, L.C*., et al.* Pharmacokinetics, dosimetry and comparative efficacy of 188Re-liposome and 5-FU in a CT26-luc lung-metastatic mice model. *Nucl Med Biol* **39**, 35-43 (2012).
22. Li, S.-D. & Huang, L. Pharmacokinetics and Biodistribution of Nanoparticles. *Mol Pharm* **5**, 496-504 (2008).
23. Snehalatha, M., Venugopal, K., Saha, R.N., Babbar, A.K. & Sharma, R.K. Etoposide Loaded PLGA and PCL Nanoparticles II: Biodistribution and Pharmacokinetics after Radiolabeling with Tc-99m. *Drug Delivery* **15**, 277-287 (2008).
24. Garg, M*., et al.* Radiolabeling, pharmacoscintigraphic evaluation and antiretroviral efficacy of stavudine loaded 99mTc labeled galactosylated liposomes. *Eur J Pharm Sci* **33**, 271-281 (2008).
25. Semete, B*., et al.* In vivo evaluation of the biodistribution and safety of PLGA nanoparticles as drug delivery systems. *Nanomedicine* **6**, 662-671 (2010).

26. Yan, C., Gu, J., Guo, Y. & Chen, D. In vivo biodistribution for tumor targeting of 5-fluorouracil (5-FU) loaded N-succinyl-chitosan (Suc-Chi) nanoparticles. *Yakugaku Zasshi* **130**, 801-804 (2010).
27. Kaur, I.P., Bhandari, R., Bhandari, S. & Kakkar, V. Potential of solid lipid nanoparticles in brain targeting. *J Control Release* **127**, 97-109 (2008).
28. Xiao, K.*, et al.* The effect of surface charge on in vivo biodistribution of PEG-oligocholic acid based micellar nanoparticles. *Biomaterials* **32**, 3435-3446 (2011).
29. Hirn, S.*, et al.* Particle size-dependent and surface charge-dependent biodistribution of gold nanoparticles after intravenous administration. *European J Pharm Biopharm* **77**, 407-416 (2011).
30. Cole, A.J., David, A.E., Wang, J., Galbán, C.J. & Yang, V.C. Magnetic brain tumor targeting and biodistribution of long-circulating PEG-modified, cross-linked starch-coated iron oxide nanoparticles. *Biomaterials* **32**, 6291-6301 (2011).
31. Müller, R.H.*, et al.* Oral bioavailability of cyclosporine: Solid lipid nanoparticles (SLN®) versus drug nanocrystals. *Int J Pharm* **317**, 82-89 (2006).
32. O'Driscoll, C.M. & Griffin, B.T. Biopharmaceutical challenges associated with drugs with low aqueous solubility--The potential impact of lipid-based formulations. *Adv Drug Deliv Rev* **60**, 617-624 (2008).
33. Muchow, M., Maincent, P. & Muller, R. Lipid nanoparticles with a solid matrix (SLN, NLC, LDC) for oral drug delivery. *Drug Dev Ind Pharm* **34**, 1394-1405 (2008).
34. Kesisoglou, F., Panmai, S. & Wu, Y. Nanosizing — Oral formulation development and biopharmaceutical evaluation. *Adv Drug Deliv Rev* **59**, 631-644 (2007).
35. Florence, A.T. & Hussain, N. Transcytosis of nanoparticle and dendrimer delivery systems: evolving vistas. *Adv Drug Deliv Rev* **50**, S69-S89 (2001).
36. Charman, W.N. & Stella, V.J. *Lymphatic transport of drugs*, (CRC Press, 1992).
37. Zhang, X.*, et al.* Biodistribution and toxicity of nanodiamonds in mice after intratracheal instillation. *Toxicol Let* **198**, 237-243 (2010).
38. Szymendera, J. & Radwan, M. Letter: Intestinal absorption of pertechnetate: calculation by the oral-intravenous plasma activity quotients and inverse convolution method. *J Nucl Med* **15**, 314-316 (1974).
39. Saha, G.B. *Fundamentals of Nuclear Pharmacy*, (2010).

40. Chen, C.C., Tsai, T.H., Huang, Z.R. & Fang, J.Y. Effects of lipophilic emulsifiers on the oral administration of lovastatin from nanostructured lipid carriers: Physicochemical characterization and pharmacokinetics. *Eur J Pharm Biopharm* (2010).
41. Das, S. & Chaudhury, A. Recent Advances in Lipid Nanoparticle Formulations with Solid Matrix for Oral Drug Delivery. *AAPS PharmSciTech* (2010).
42. Tarr, B.D. & Yalkowsky, S.H. Enhanced Intestinal Absorption of Cyclosporine in Rats Through the Reduction of Emulsion Droplet Size. *Pharm Res* **6**, 40-43 (1989).
43. del Pozo-Rodríguez, A.*, et al.* Solid lipid nanoparticles as potential tools for gene therapy: In vivo protein expression after intravenous administration. *Intl J Pharm* **385**, 157-162 (2010).
44. Müller, R.H., Rühl, D., Lück, M. & Paulke, B.R. Influence of Fluorescent Labelling of Polystyrene Particles on Phagocytic Uptake, Surface Hydrophobicity, and Plasma Protein Adsorption. *Pharm Res* **14**, 18-24 (1997).
45. Weiss, J., Burhenne, J., Riedel, K.D. & Haefeli, W.E. Poor solubility limiting significance of in-vitro studies with HIV protease inhibitors. *AIDS* **16**, 674-676 (2002).
46. Föger, F., Kafedjiiski, K., Hoyer, H., Loretz, B. & Bernkop-Schnürch, A. Enhanced transport of P-glycoprotein substrate saquinavir in presence of thiolated chitosan. *J Drug Target* **15**, 132-139 (2007).
47. Pathak, S.M.*, et al.* Enhanced oral absorption of saquinavir with Methyl-Beta-Cyclodextrin—Preparation and in vitro and in vivo evaluation. *Eur J Pharm Sci* **41**, 440-451 (2010).
48. Ermak, T.H. & Giannasca, P.J. Microparticle targeting to M cells. *Adv Drug Deliv Rev* **34**, 261-283 (1998).
49. D'Souza, B.*, et al.* Oral microparticulate vaccine for melanoma using M-cell targeting. *J Drug Target* **20**, 166-173 (2011).
50. des Rieux, A.*, et al.* Helodermin-loaded nanoparticles: Characterization and transport across an in vitro model of the follicle-associated epithelium. *J Control Release* **118**, 294-302 (2007).
51. Ensign, L.M., Cone, R. & Hanes, J. Oral drug delivery with polymeric nanoparticles: the gastrointestinal mucus barriers. *Adv Drug Deliv Rev* **64**, 557-570 (2012).
52. Rejman, J., Oberle, V., Zuhorn, I.S. & Hoekstra, D. Size-dependent internalization of particles via the pathways of clathrin- and caveolae-mediated endocytosis. *Biochem J* **377**, 159-169 (2004).

53. Rieux, A.d*., et al.* Transport of nanoparticles across an in vitro model of the human intestinal follicle associated epithelium. *Eur J Pharml Sci***25**, 455-465 (2005).
54. Gaumet, M., Gurny, R. & Delie, F. Interaction of biodegradable nanoparticles with intestinal cells: the effect of surface hydrophilicity. *Int J Pharm* **390**, 45-52 (2010).
55. Liang, M*., et al.* Cellular Uptake of Densely Packed Polymer Coatings on Gold Nanoparticles. *ACS Nano* **4**, 403-413 (2009).
56. Roger, E., Lagarce, F., Garcion, E. & Benoit, J.P. Lipid nanocarriers improve paclitaxel transport throughout human intestinal epithelial cells by using vesicle-mediated transcytosis. *J Control Release* **140**, 174-181 (2009).
57. Tomoda, H., Kishimoto, Y. & Lee, Y.C. Temperature effect on endocytosis and exocytosis by rabbit alveolar macrophages. *J Biol Chem* **264**, 15445-15450 (1989).
58. Hillaireau, H. & Couvreur, P. Nanocarriers' entry into the cell: relevance to drug delivery. *Cell Mol Life Sci* **66**, 2873-2896 (2009).
59. Mathot, F*., et al.* Transport mechanisms of mmePEG750P(CL-co-TMC) polymeric micelles across the intestinal barrier. *J Control Release* **124**, 134-143 (2007).
60. Zhang, Z., Gao, F., Bu, H., Xiao, J. & Li, Y. Solid lipid nanoparticles loading candesartan cilexetil enhance oral bioavailability: in vitro characteristics and absorption mechanism in rats. *Nanomedicine* **8**, 740-747 (2012).
61. Matveev, S., Li, X., Everson, W. & Smart, E.J. The role of caveolae and caveolin in vesicle-dependent and vesicle-independent trafficking. *Adv Drug Deliv Rev* **49**, 237-250 (2001).
62. Rodal, S.K*., et al.* Extraction of cholesterol with methyl-beta-cyclodextrin perturbs formation of clathrin-coated endocytic vesicles. *Mol Biol Cell* **10**, 961-974 (1999).
63. Mayor, S. & Pagano, R.E. Pathways of clathrin-independent endocytosis. *Nat Rev Mol Cell Biol* **8**, 603-612 (2007).
64. Cheng, Z.-J*., et al.* Distinct Mechanisms of Clathrin-independent Endocytosis Have Unique Sphingolipid Requirements. *Mol Bio Cell* **17**, 3197-3210 (2006).
65. Sahay, G., Alakhova, D.Y. & Kabanov, A.V. Endocytosis of nanomedicines. *J Control Release* **145**, 182-195 (2010).
66. Nabi, I.R. & Le, P.U. Caveolae/raft-dependent endocytosis. *J Cell Biol* **161**, 673-677 (2003).

67. Kirkham, M. & Parton, R.G. Clathrin-independent endocytosis: New insights into caveolae and non-caveolar lipid raft carriers. *Biochim Biophys Acta* **1745**, 273-286 (2005).
68. Parton, R.G. & Richards, A.A. Lipid Rafts and Caveolae as Portals for Endocytosis: New Insights and Common Mechanisms. *Traffic* **4**, 724-738 (2003).
69. Paillard, A., Hindré, F., Vignes-Colombeix, C., Benoit, J.P. & Garcion, E. The importance of endo-lysosomal escape with lipid nanocapsules for drug subcellular bioavailability. *Biomaterials* **31**, 7542-7554 (2010).
70. del Pozo-Rodríguez, A.*, et al.* A proline-rich peptide improves cell transfection of solid lipid nanoparticle-based non-viral vectors. *J Control Release* **133**, 52-59 (2009).
71. Simionescu, M., Popov, D. & Sima, A. Endothelial transcytosis in health and disease. *Cell Tissue Res* **335**, 27-40 (2009).
72. Roger, E., Lagarce, F., Garcion, E. & Benoit, J.P. Lipid nanocarriers improve paclitaxel transport throughout human intestinal epithelial cells by using vesicle-mediated transcytosis. *J Control Release* **140**, 174-181 (2009).
73. Aungst, B.J. P-glycoprotein, secretory transport, and other barriers to the oral delivery of anti-HIV drugs. *Adv Drug Deliv Rev* **39**, 105-116 (1999).
74. Roger, E., Lagarce, F., Garcion, E. & Benoit, J.P. Reciprocal competition between lipid nanocapsules and P-gp for paclitaxel transport across Caco-2 cells. *Eur J Pharm Sci* **40**, 422-429 (2010).
75. Yunomae, K., Arima, H., Hirayama, F. & Uekama, K. Involvement of cholesterol in the inhibitory effect of dimethyl-β-cyclodextrin on P-glycoprotein and MRP2 function in Caco-2 cells. *FEBS Letters* **536**, 225-231 (2003).
76. Garrigues, A., Escargueil, A.E. & Orlowski, S. The multidrug transporter, P-glycoprotein, actively mediates cholesterol redistribution in the cell membrane. *Proc Natl Acad Sci U S A* **99**, 10347-10352 (2002).
77. Barakat, S.*, et al.* Modulation of p-glycoprotein function by caveolin-1 phosphorylation. *J Neurochem* **101**, 1-8 (2007).
78. Nieto Montesinos, R., Béduneau, A., Pellequer, Y. & Lamprecht, A. Delivery of P-glycoprotein substrates using chemosensitizers and nanotechnology for selective and efficient therapeutic outcomes. *J Control Release* **161**, 50-61 (2012).

CONCLUSIONS

Based on the results obtained from the experimental work, we can conclude with the following conclusions:

1. The application of the high pressure homogenization technique to prepare NLCs composed by Precirol ATO® 5, Poloxamer 188 and Tween 80 allowed us to obtain nanoparticles with a lower particle size and lower polidispersity index. The use of Tween 80 and Poloxamer 188 provided negatiely charged NLCs, whereas the combination of Tween 80 and CTAB provided positively charged nanoparticles.
2. After intravenous administration of NLCs with different particle size, surface charge and surfactant content to rats, a long permanence in blood and tissues was observed. The particle size, surface charge and surfactant content of the nanoparticles affected to their tissue biodistribution profile; however, no differences in the MRT values in blood were found. The highest accumulation of NLCs was observed in the kidneys, liver, bone marrow and spleen. Comparing the nanoparticles presenting similar particle size and different surface charge, we observed a difference on the biodistribution profile: in the kidneys there was a higher accumulation of the positive nanocarriers and, in the liver, negative nanoparticles were more uptaken than positive ones. The nanoparticles with the largest particle size showed a higher uptake in the lung and lower accumulation in liver and bone marrow, in comparison with the smaller ones.
3. A formulation based on NLCs composed by Precirol ATO® 5, Poloxamer 188 and Tween 80 was developed for spirinolactone (SPN). This nanocarrier presented a particle size of 150 nm and surface charge of -20 mV. The *in vitro* dissolution study carried out under sink conditions showed a very slow release of spironolactone from the nanocarriers and indicated a high stability of the SPN-NLCs in the dissolution media.
4. After the oral administration of SPN-NLCs to rabbits, the bioavailability of the drug was not enhanced; however, a shift in the metabolic profile was observed when compared to a reference formulation (a syrup). Radioactivity studies indicated that the SPN-NLCs were trapped in the intestinal mucosa.

5. In a Caco-2 model, NLCs of different particle size composed by Precirol ATO® 5, Poloxamer 188 and Tween 80 were able to increase the permeability of saquinavir, a BSC class IV drug and P-gp substrate, up to 3.5-fold. This increment was dependent on the size of the NLCS and the amount of surfactant used for their formulation. However, NLC transport was not increased in M cells.
6. NLCs composed by 1% Poloxamer 188 and 0.5% Tween 80, and prepared by high-pressure homogenization (particle size 247 nm) circumvented the P-gp efflux. Moreover, they used both a caveolae- and clathrin-mediated transcytosis, in contrast to the formulation composed by the same surfactants but in a higher proportion (particle size 165 nm) or prepared without high pressure homogenization (particle size 1,090 nm), which followed only caveolae-mediated transcytosis. Therefore, by modifying critical physicochemical parameters of the formulation we were able to overcome the P-gp drug efflux and alter the transcytosis mechanism of the nanoparticles. Our findings are encouraging for the delivery of class IV drugs and P-gp substrates by the oral route and support further nanotechnoloty approaches on this regard.

BIBLIOGRAPHY

Abdelwahed, W., Degobert, G., Stainmesse, S., Fessi, H., Freeze-drying of nanoparticles: Formulation, process and storage considerations. *Adv Drug Deliv Rev* 58 (2006) 1688-1713.

Acharya, S., Sahoo, S.K., PLGA nanoparticles containing various anticancer agents and tumour delivery by EPR effect, *Adv Drug Deliv Rev* 63 (2011) 170-183.

Aggarwal, P., Hall, J.B., McLeland, C.B., Dobrovolskaia, M.A., McNeil, S.E., Nanoparticle interaction with plasma proteins as it relates to particle biodistribution, biocompatibility and therapeutic efficacy. *Adv Drug Deliv Rev* 61 (2009) 428-437.

Alexis, F., Pridgen, E., Molnar, L.K., Farokhzad, O.C., Factors Affecting the Clearance and Biodistribution of Polymeric Nanoparticles, *Mol Pharm* 5 (2008) 505-515.

Allemann, E., Gurny, R., Doelker, E., Drug-loaded nanoparticles - preparation methods drug targeting issues. *Eur J Pharm Biopharm* 39 (1993) 173-191.

Allen, T.M, Cullis, P.R., Liposomal drug delivery systems: from concept to clinical applications. *Adv Drug Deliv Rev* (2012), In Press

A
midon, G., Lennernäs, H., Shah, V., Crison, J., A theoretical basis for a biopharmaceutic drug classification: the correlation of in vitro drug product dissolution and in vivo bioavailability. *Pharm Res* 12, (1995) 413-20.

Animals Guide for the Care and Use of Laboratory Animals, eigth ed., National Academies Press (US), Washington (DC), 2011.

Ballot, S., Noiret, N., Hindré, F., Denizot, B., Garin, E., Rajerison, H., Benoit, J.P. ^{99m}Tc/^{188}Re-labelled lipid nanocapsules as promising radiotracers for imaging and therapy: formulation and biodistribution, *Eur J Nucl Med Mol Imaging* 33 (2006) 602-607.

Banerjee, A., Önyüksel, H., Human pancreatic polypeptide in a phospholiipid-based micellar formulation, *Pharm Res* 29 (2012) 1698-1711.

Bates, T.R., Sequeria, J.A., Bioavailability of micronized griseofulvin from corn oil-in-water emulsion, aqueous suspension, and commercial tablet dosage forms in humans. *J Pharm Sci* 64 (1975) 793-7.

Brown, D.M., Dickson, C., Duncan, P., Al-Attili, F., Stone, V., Interaction between nanoparticles and cytokine proteins: impact on protein and particle functionality. *Nanotechnology* 21 (2010) 215104.

Bunjes, H., Lipid nanoparticles for the delivery of poorly water-soluble drugs. *J Pharm Pharmacol* 62 (2010) 1637-1645.

Caliph, S., Charman, W., Porter, C., Effect of short-, medium-, and long-chain fatty acid-based vehicles on the absolute oral bioavailability and intestinal lymphatic transport of halofantrine and assessment of mass balance in lymph-cannulated and non-cannulated rats. *J Pharm Sci* 89 (2000) 1073-84.

Chae, J.M., Mo, S.M., Oh, I.J., Effects of poloxamer 188 on the characteristics of poly(lactide-co-glycolide) nanoparticles, *J Nanosci Nanotechnol* 10 (2010) 3224-3227.

Chakraborty, S., Shukla, D., Mishra, B., Singh, S., Lipid - An emerging platform for oral delivery of drugs with poor bioavailability. *Eur J Pharm Biopharm* 73 (2009) 1-15.

Charman, W.N., Stella, V.J.,1992. *Lymphatic transport of drugs*, CRC Press.

Chen, C.C., Tsai, T.H., Huang, Z.R., Fang, J.Y., Effects of lipophilic emulsifiers on the oral administration of lovastatin from nanostructured lipid carriers: Physicochemical characterization and pharmacokinetics. *Eur J Pharm Biopharm* 74 (2010) 474-82

Chen, L.C., Chen, Y.H., Liu, I.H., Ho, C.L., Lee, W.C., Chang, C.H., Lang, K.L., Ting, G., Lee, T.W., Shien, J.H., Pharmacokinetics, dosimetry and comparative efficacy of ^{188}Re-liposome and 5-FU in a CT26-luc lung-metastatic mice model, *Nucl Med Biol* 39 (2012) 35-43.

Chen, M., Lipid excipients and delivery systems for pharmaceutical development: a regulatory perspective. *Adv Drug Deliv Rev* 60 (2008) 768-77.

Chung, N.S., Wasan, K.M., Potential role of the low-density lipoprotein receptor family as mediators of cellular drug uptake. *Adv Drug Deliv Rev* 56 (2004) 1315-1334.

Cole, A.J., David, A.E., Wang, J., Galbán, C.J., Yang, V.C., Magnetic brain tumor targeting and biodistribution of long-circulating PEG-modified, cross-linked starch-coated iron oxide nanoparticles, *Biomaterials* 32 (2011) 6291-6301.

Collins-Gold, L., Feichtinger, N., Wärnheim, T., Are lipid emulsions the drug delivery solution? *Modern Drug Discovery* 3 (2000) 44-48.

Constantinides, P.P., Chaubal, M.V., Shorr, R., Advances in lipid nanodispersions for parenteral drug delivery and targeting. *Adv Drug Deliv Rev* 60 (2008) 757-767.

Dahan, A., Hoffman, A. ,The effect of different lipid based formulations on the oral absorption of lipophilic drugs: the ability of in vitro lipolysis and consecutive ex vivo intestinal permeability data to predict in vivo bioavailability in rats. *Eur J Pharm Biopharm* 67 (2007) 96-105.

Dahan, A., Hoffman, A., Rationalizing the selection of oral lipid based drug delivery systems by an in vitro dynamic lipolysis model for improved oral bioavailability of poorly water soluble drugs. *J Control Release* 129 (2008) 1-10.

Dahan, A., Hoffman, A., Use of a dynamic in vitro lipolysis model to rationalize oral formulation development for poor water soluble drugs: correlation with in vivo data and the relationship to intra-enterocyte processes in rats. *Pharm Res* 23 (2006) 2165-74.

Daniel, M.C.*, et al.* Role of surface charge density in nanoparticle-templated assembly of bromovirus protein cages. *ACS Nano* 4 (2010) 3853-3860.

Das, S., Chaudhury, A., Recent Advances in Lipid Nanoparticle Formulations with Solid Matrix for Oral Drug Delivery. *AAPS PharmSciTech* 12 (2010) 62-76

Date, A.A., Joshi, M.D., Patravale, V.B., Parasitic diseases: Liposomes and polymeric nanoparticles versus lipid nanoparticles, *Adv Drug Deliv Rev* 59 (2007) 505-521.

Decuzzi, P., Godin, B., Tanaka, T., Lee, S.Y., Chiappini, C., Liu, X., Ferrari, M., Size and shape effects in the biodistribution of intravascularly injected particles, *J Control Release* 141 (2010) 320-327.

Dekanić, D., Bone marrow in male and female rats, *Experientia* 34 (1978) 1313-1314.

del Pozo-Rodríguez, A., Delgado, D., Solinís, M.A., Pedraz, J.L., Echevarría, E., Rodríguez, J.M., Gascón, A.R., Solid lipid nanoparticles as potential tools for gene therapy: In vivo protein expression after intravenous administration, *Int J Pharm* 385 (2010) 157-162.

del Pozo-Rodríguez, A., Solinís, M.A., Gascón, A.R., Pedraz, J.L., Short- and long-term stability study of lyophilized solid lipid nanoparticles for gene therapy. *Eur J Pharm Biopharm* 71 (2009) 181-189.

Delgado, D., Gascón, A.R., del Pozo-Rodríguez, A., Echevarria, E., Ruíz de Garibay, A.P., Rodríguez, J.M., Solinís, M.A., Dextran-protamine-solid lipid nanoparticles as a non-viral vector for gene therapy: in vitro characterization and in vivo transfection after intravenous administration to mice, *Int J Pharm* 425 (2012) 35-43.

Dobrovolskaia, M.A.*, et al.* Interaction of colloidal gold nanoparticles with human blood: effects on particle size and analysis of plasma protein binding profiles. *Nanomedicine* 5 (2009) 106-117.

Dufort, S., Sancey, L., Coll, J.L., Physico-chemical parameters that govern nanoparticles fate also dictate rules for their molecular evolution, *Adv Drug Deliv Rev* 64 (2012) 179-189.

Dutta, D.*, et al.* Adsorbed Proteins Influence the Biological Activity and Molecular Targeting of Nanomaterials. *Toxicol Sci*100 (2007) 303-315.

Esposito, E.*, et al.* Solid lipid nanoparticles as delivery systems for bromocriptine. *Pharm Res* 25 (2008) 1521-1530.

European Pharmacopeia. (2007). Dissolution test for solid dosage forms.

Fang, J.Y., Fang, C.L., Liu, C.H., Su, Y.H., Lipid nanoparticles as vehicles for topical psoralen delivery: solid lipid nanoparticles (SLN) versus nanostructured lipid carriers (NLC). *Eur J Pharm Biopharm* 70 (2008) 633-40.

Fatouros, D.G., Karpf, D.M., Nielsen, F.S., Müllertz, A., Clinical studies with oral lipid based formulations of poorly soluble compounds. *Ther Clin Risk Manag* 3 (2007) 591-604.

Florence, A.T., Hussain, N., Transcytosis of nanoparticle and dendrimer delivery systems: evolving vistas. *Adv Drug Deliv Rev* 50 (2001) S69-S89.

Florence, A.T., Nanoparticle uptake by the oral route: Fulfilling its potential? *Drug Discov Today: Technologies* 2 (2005) 75-81.

Gao, Y., Gu, W., Chen, L., Xu, Z., Li, Y., The role of daidzein-loaded sterically stabilized solid lipid nanoparticles in therapy for cardio-cerebrovascular diseases, *Biomaterials* 29 (2008) 4129-4136.

Gasco, M.R. Lipid nanoparticles: perspectives and challenges. *Adv Drug Deliv Rev* 59 (2007) 377-8.

Gaumet, M., Vargas, A., Gurny, R., Delie, F., Nanoparticles for drug delivery: The need for precision in reporting particle size parameters. *Eur J Pharm Biopharm* 69 (2008) 1-9.

Gelperina, S., Maksimenko, O., Khalansky, A., Vanchugova, L., Shipulo, E., Abbasova, K., Berdiev, R., Wohlfart, S., Chepurnova, N., Kreuter, J., Drug delivery to the brain using

surfactant-coated poly(lactide-co-glycolide) nanoparticles: Influence of the formulation parameters, *Eur J Pharm Biopharm* 74 (2010) 157-163.

Gershkovich, P., Hoffman, A., Uptake of lipophilic drugs by plasma derived isolated chylomicrons: Linear correlation with intestinal lymphatic bioavailability. *Eur J Pharm Sci* 26 (2005) 394-404.

Göppert, T.M., Müller, R.H., Plasma protein adsorption of Tween 80- and poloxamer 188-stabilized solid lipid nanoparticles, *J Drug Target* 11 (2003) 225-231.

Gref, R., *et al.* 'Stealth' corona-core nanoparticles surface modified by polyethylene glycol (PEG): influences of the corona (PEG chain length and surface density) and of the core composition on phagocytic uptake and plasma protein adsorption. *Colloids Surf B Biointerfaces* 18 (2000) 301-313.

Gref, R., *et al.* Biodegradable long-circulating polymeric nanospheres. *Science* 263 (1994) 1600-1603.

Gref, R., Lück, M., Quellec, P., Marchand, M., Dellacherie, E., Harnish, S., Blunk, T., Müller, R.H.,´Stealth´corona-core nanoparticles surface modified by polyethylene glycol (PEG): influences of the corona (PEG chain length and surface density) and of the core composition on phagocytic uptake and plasma protein adsorption. *Colloids Surf B Biointerfaces* 18 (2000) 301-313.

Guide for the Care and Use of Laboratory Animals. (2011). Washington (DC), National Academies Press (US).

Harivardhan Reddy, L., Sharma, R.K., Chuttani, K., Mishra, A.K., Murthy, R.S.R., Influence of administration route on tumor uptake and biodistribution of etoposide loaded solid lipid nanoparticles in Dalton's lymphoma tumor bearing mice, *J Control Release* 105 (2005) 185-198.

Hauss, D.J., Oral lipid-based formulations. *Adv Drug Deliv Rev* 59 (2007) 667-676.

He, C., Hu, Y., Yin, L., Tang, C., Yin, C., Effects of particle size and surface charge on cellular uptake and biodistribution of polymeric nanoparticles. *Biomaterials* 31, 3657-3666 (2010).

Hirn, S., Semmler-Behnke, M., Schleh, C., Wenk, A., Lipka, J., Schäffler, M., Takenaka, S., Möller, W., Schmid, G., Simon, U., Kreyling, W.G., Particle size-dependent and surface

charge-dependent biodistribution of gold nanoparticles after intravenous administration, *Eur J Pharm Biopharm* 77 (2011) 407-416.

Hoarau, D., Delmas, P., David, S., Roux, E., Leroux, J.C., Novel Long-Circulating Lipid Nanocapsules, *Pharm Res* 21 (2004) 1783-1789.

Jannin, V., Musakhanian, J., Marchaud, D., Approaches for the development of solid and semi-solid lipid-based formulations. *Adv Drug Deliv Rev* 60 (2008) 734-746.

Johnston, H., Brown, D., Kermanizadeh, A., Gubbins, E., Stone, V., Investigating the relationship between nanomaterial hazard and physicochemical properties: Informing the exploitation of nanomaterials within therapeutic and diagnostic applications. *J Control Release* 164 (2012) 307-313.

Joshi, M.D., Müller, R.H., Lipid nanoparticles for parenteral delivery of actives. *Eur J Pharm Biopharms* 71 (2009) 161-172.

Juliano, R.L., Stamp, D., The effect of particle size and charge on the clearance rates of liposomes and liposome encapsulated drugs. *Biochem Biophys Res Commun* 63 (1975) 651-658.

Kaukonen, A., Boyd, B., Charman, W., Porter, C., Drug solubilization behavior during in vitro digestion of suspension formulations of poorly water-soluble drugs in triglyceride lipids. *Pharm Res* 21 (2004) 254-60.

Kaur, I.P., Bhandari, R., Bhandari, S., Kakkar, V., Potential of solid lipid nanoparticles in brain targeting, *J Control Release* 127 (2008) 97-109.

Kesisoglou, F., Panmai, S., Wu, Y., Nanosizing - Oral formulation development and biopharmaceutical evaluation. *Adv Drug Deliv Rev* 59 (2007) 631-644.

Klyashchitsky, B.A., Owen, A.J., Drug Delivery Systems for Cyclosporine: Achievements and Complications. *J Drug Target* 5 (1998) 443-458.

Konan, Y.N., Gurny, R., Allémann, E., Preparation and characterization of sterile and freeze-dried sub-200 nm nanoparticles. *Int J Pharm* 233 (2002) 239-252.

Kossena, G., Charman, W., Boyd, B., Dunstan, D., Porter, C., Probing drug solubilization patterns in the gastrointestinal tract after administration of lipid-based delivery systems: a phase diagram approach. *J Pharm Sci* 93 (2004) 332-48.

Kossena, G., Low dose lipid formulations: effects on gastric emptying and biliary secretion. *Pharm Res* 24 (2007) 2084-96.

Krishnadas, A., Önyüksel, H., Rubinstein, I., Interactions of VIP, secretin and PACAP(1-38) with phospholipids: a biological paradox revisited, *Curr Pharm Des* 9 (2003) 1005-1012.
Krishnaiah, Y.S.R., Pharmaceutical Technologies for Enhancing Oral Bioavailability of Poorly Soluble Drugs. *J Bioequiv Availab* 2 (2010) 28-36.

Kuzmis, A., Lim, S.B., Desai, E., Jeon, E., Lee, B.S., Rubinstein, I., Önyüksel, H., Micellar nanomedicine of human neuropeptide Y, *Nanomedicine* 7 (2011) 464-471.

Lai, L.F., Guo, H.X., Preparation of new 5-fluorouracil-loaded zein nanoparticles for liver targeting, *Int J Pharm* 404 (2011) 317-323.

Langguth, P., Hanafy, A., Frenzel, D., Grenier, P., Nhamias, A., Ohlig, T., Vergnault, G., Spahn-Langguth, H., Nanosuspension formulations for low-soluble drugs: pharmacokinetic evaluation using spironolactone as model compound. *Drug Dev Ind Pharm* 31 (2005) 319-29.

Lepage, G. *et al*. Effect of an organized lipid matrix on lipid absorption and clinical outcomes in patients with cystic fibrosis. *J Pediatr* 141 (2002) 178-85.

Li, S.D., Huang,L., Pharmacokinetics and Biodistribution of Nanoparticles, *Mol Pharm* 5 (2008) 496-504.

Lim, S.B., Banerjee, A., Önyüksel, H., Improvement of drug safety by the use of lipid-based nanocarriers, *J Control Release* 163 (2012) 34-45.

Limayem Blouza, I., Charcosset, C., Sfar, S., Fessi, H., Preparation and characterization of spironolactone-loaded nanocapsules for paediatric use. *Int J Pharm* 325 (2006) 124-31.

Lipinski, C., Lombardo, F., Dominy, B., Feeney, P., Experimental and computational approaches to estimate solubility and permeability in drug discovery and development settings. *Adv Drug Deliv Rev* 46, (2001) 3-26.

Liu, D., Mori, A., Huang, L., Role of liposome size and RES blockade in controlling biodistribution and tumor uptake of GM1-containing liposomes. *Biochim Biophys Acta* 1104 (1992) 95-101.

Liu, W.*, et al.* Preparation and characterization of novel fluorescent nanocomposite particles: CdSe/ZnS core-shell quantum dots loaded solid lipid nanoparticles. *J Biomed Mater Res A* 84, (2008)1018-1025.

Manjunath, K.,Venkateswarlu, V., Pharmacokinetics, tissue distribution and bioavailability of nitrendipine solid lipid nanoparticles after intravenous and intraduodenal administration. *J Drug Target* 14 (2006) 632-645.

Mehnert, W., Mäder, K., Solid lipid nanoparticles: production, characterization and applications. *Adv Drug Deliv Rev* 47 (2001) 165-96.

Meng, H.*, et al.* Use of Size and a Copolymer Design Feature To Improve the Biodistribution and the Enhanced Permeability and Retention Effect of Doxorubicin-Loaded Mesoporous Silica Nanoparticles in a Murine Xenograft Tumor Model. *ACS Nano* 5 (2011) 4131-4144.

Merisko-Liversidge, E., Liversidge, G., Drug nanoparticles: formulating poorly water-soluble compounds. *Toxicol Pathol* 36 (2008) 43-8.

Merisko-Liversidge, E., Liversidge, G.G., Cooper, E.R., Nanosizing: a formulation approach for poorly-water-soluble compounds. *Eur J Pharm Sci* 18 (2003) 113-120.

Merisko-Liversidge, E., Liversidge, G.G., Nanosizing for oral and parenteral drug delivery: A perspective on formulating poorly-water soluble compounds using wet media milling technology. *Adv Drug Deliv Rev* 63 (2011) 427-440.

Merisko-Liversidge, E.M., Liversidge, G.G., Drug nanoparticles: formulating poorly water-soluble compounds, *Toxicol Pathol* 36 (2008) 43-48.

Muchow, M., Maincent, P., Müller, R.H., Lipid nanoparticles with a solid matrix (SLN, NLC, LDC) for oral drug delivery. *Drug Dev Ind Pharm* 34 (2008) 1394-405.

Mueller, E.A. *et al*. Improved dose linearity of cyclosporine pharmacokinetics from a microemulsion formulation. *Pharm Res* 11 (1994) 301-4.

Müller, R.H., Mäder, K., Gohla, S., Solid lipid nanoparticles (SLN) for controlled drug delivery - a review of the state of the art. *Eur J Pharm Biopharm* 50 (2000) 161-77.

Müller, R.H., Keck, C.M., Challenges and solutions for the delivery of biotech drugs--a review of drug nanocrystal technology and lipid nanoparticles. *J Biotechnol* 113 (2004) 151-170.

Müller, R.H., Radtke, M., Wissing, S.A., Nanostructured lipid matrices for improved microencapsulation of drugs. *Int J Pharm* 242 (2002)121-128.

Müller, R.H., Runge, S., Ravelli, V., Mehnert, W., Thünemann, A.F., Souto, E.B., Oral bioavailability of cyclosporine: Solid lipid nanoparticles (SLN®) versus drug nanocrystals. *Int J Pharm* 317 (2006) 82-89.

Müllertz, A., Ogbonna, A., Ren, S., Rades, T., New perspectives on lipid and surfactant based drug delivery systems for oral delivery of poorly soluble drugs. *J Pharm Pharmacol* 62 (2010)1622-36.

Mura, S., Couvreur, P., Nanotheranostics for personalized medicine. *Adv Drug Deliv Rev* 64 (2012) 1394-1416.

Nel, A.E.*, et al.* Understanding biophysicochemical interactions at the nano-bio interface. *Nat Mater* 8 (2009) 543-557.

Nyström, A.M., Fadeel, B., Safety assessment of nanomaterials: Implications for nanomedicine. *J Control Release* 161 (2012) 403-408.

O'Driscoll, C.M., Griffin, B.T., Biopharmaceutical challenges associated with drugs with low aqueous solubility--The potential impact of lipid-based formulations. *Adv Drug Deliv Rev,* 60, 617-624.

Odeberg, J.M., Kaufmann, P., Kroon, K.-G., Höglund, P., Lipid drug delivery and rational formulation design for lipophilic drugs with low oral bioavailability, applied to cyclosporine. *Eurn J Pharm Sci* 20 (2003) 375-382.

Olbrich, C., Gessner, A., Schröder, W., Kayser, O., Müller, R.H., Lipid-drug conjugate nanoparticles of the hydrophilic drug diminazene-cytotoxicity testing and mouse serum adsorption. *J Control Release* 96 (2004) 425-435.

Önyüksel, H., Séjourné, S., Suzuki, H., Rubinstein, I., Human VIP-alpha: a long-acting, biocompatible and biodegradable peptide nanomedicine for essential hypertension, *Peptides* 27 (2006) 2271-2275.

Overdiek HW, Merkus FW. 1987. The metabolism and biopharmaceutics of spironolactone in man. *Rev Drug Metab Drug Interact* 5 (2008) 273-302.

Owens, D.E., Peppas, N.A., Opsonization, biodistribution, and pharmacokinetics of polymeric nanoparticles, *Int J Pharm* 307 (2006) 93-102.

Ozcan, I., Segura-Sánchez, F., Bouchemal, K., Sezak, M., Ozer, O., Güneri, T., Ponchel, G., Pegylation of poly(γ-benzyl-L-glutamate) nanoparticles is efficient for avoiding mononuclear phagocyte system capture in rats, *Int J Nanomedicine* 5 (2010) 1103-1111.

Porter, C., Charman, W., Intestinal lymphatic drug transport: an update. *Adv Drug Deliv Rev* 50 (2001) 61-80.

Porter, C., Trevaskis, N., Charman, W., Lipids and lipid-based formulations: optimizing the oral delivery of lipophilic drugs. *Nat Rev Drug Discov* 6 (2007) 231-48.

Porter, C.J.H., Pouton, C.W., Cuine, J.F., Charman, W.N., Enhancing intestinal drug solubilisation using lipid-based delivery systems. *Adv Drug Deliv Rev* 60 (2008) 673-691.

Pouton, C.W., Formulation of poorly water-soluble drugs for oral administration: Physicochemical and physiological issues and the lipid formulation classification system. *Eur J Pharm Sci* 29 (2006) 278-287.

Pouton, C.W., Lipid formulations for oral administration of drugs: non-emulsifying, self-emulsifying and 'self-microemulsifying' drug delivery systems. *Eur J Pharm Sci* 11 Suppl 2 (2000) S93-8.

Pouton, C.W., Porter, C.J.H., Formulation of lipid-based delivery systems for oral administration: Materials, methods and strategies. *Adv Drug Deliv Rev* 60 (2008) 625-637.

Prashant, C., Dipak, M., Yang, C.T., Chuang, K.H., Jun, D., Feng, S.S., Superparamagnetic iron oxide – Loaded poly (lactic acid)-d-α-tocopherol polyethylene glycol 1000 succinate copolymer nanoparticles as MRI contrast agent, *Biomaterials* 31 (2010) 5588-5597.

Reddy, L., Sharma, R., Chuttani, K., Mishra, A., Murthy, R., Etoposide-incorporated tripalmitin nanoparticles with different surface charge: Formulation, characterization, radiolabeling, and biodistribution studies, *AAPS J* 6 (2004) 55-64.

Rubinstein, I., Ikezaki, H., Önyüksel, H., Intratracheal and subcutaneous liposomal VIP normalizes arterial pressure in spontaneously hypertensive hamsters, *Int J Pharm* 316 (2006) 144-147.

Sachs-Barrable, K., Lee, S.D., Wasan, E.K., Thornton, S.J., Wasan, K.M., Enhancing drug absorption using lipids: A case study presenting the development and pharmacological evaluation of a novel lipid-based oral amphotericin B formulation for the treatment of systemic fungal infections. *Adv Drug Deliv Rev* 60 (2008) 692-701.

Saha, G.B., 2010. Fundamentals of Nuclear Pharmacy. Sixth edition. New York, USA: Springer.

Small, D.M., A classification of biologic lipids based upon their interaction in aqeous systems. *J Am Oil Chem Soc* 45 (1968) 108-19.

Snehalatha, M., Venugopal, K., Saha, R.N., Babbar, A.K., Sharma, R.K., Etoposide Loaded PLGA and PCL Nanoparticles II: Biodistribution and Pharmacokinetics after Radiolabeling with ^{99m}Tc, *Drug Deliv* 15 (2008) 277-287.

Storm, G., Belliot, S.O., Daemen, T., Lasic, D.D., Surface modification of nanoparticles to oppose uptake by the mononuclear phagocyte system. *Adv Drug Deliv Rev* 17 (1995) 31-48.

Szymendera, J., Radwan, M., Intestinal pertechnetate: calculation by the oral-intravenous plasma activity quotients and inverse convolution method. *J Nucl Med* 15 (1974) 314-316.

Tarr, B.D., Yalkowsky, S.H.,1989. Enhanced Intestinal Absorption of Cyclosporine in Rats Through the Reduction of Emulsion Droplet Size. *Pharm Res* 6 (1989) 40-43.

Teeranachaideekul, V., Müller, R.H., Junyaprasert, V.B., Encapsulation of ascorbyl palmitate in nanostructured lipid carriers (NLC)--Effects of formulation parameters on physicochemical stability. *Int J Pharm* 340 (2007) 198-206.

Thorek, D.L., Tsourkas, A., Size, charge and concentration dependent uptake of iron oxide particles by non-phagocytic cells. *Biomaterials* 29 (2008) 3583-3590.

Trevaskis, N. Porter, C., Charman, W., The lymph lipid precursor pool is a key determinant of intestinal lymphatic drug transport. *J Pharmacol Exp Ther* 316, 881-891 (2006).

Trevaskis, N.L., Charman, W.N., Porter, C.J.H., Lipid-based delivery systems and intestinal lymphatic drug transport: A mechanistic update. *Adv Drug Deliv Rev* 60 (2008) 702-716.

Venishetty, V.K., Chede, R., Komuravelli, R., Adepu, L., Sistla, R., Diwan, P.V., Design and evaluation of polymer coated carvedilol loaded solid lipid nanoparticles to improve the oral bioavailability: A novel strategy to avoid intraduodenal administration. *Colloids Surf B Biointerfaces* 95 (2012) 1-9.

Wang, J., Byrne, J.D., Napier, M.E., DeSimone, J.M., More effective nanomedicines through particle design. *Small* 7 (2011) 1919-1931.

Wang, L.S., Chuang, M.C., Ho, J.A., Nanotheranostics - a review of recent publications. *Int J Nanomedicine* 7 (2012) 4679-4695.

Weis, M. *et al*. Bioavailability of four oral coenzyme Q10 formulations in healthy volunteers. *Mol Aspects Med* 15 Suppl (1994) s273-80.

Wissing, S.A., Kayser, O., Müller, R.H., Solid lipid nanoparticles for parenteral drug delivery. *Advanced Drug Delivery Reviews* 56 (2000) 1257-1272.

Xiao, K., Li, Y., Luo, J., Lee, J.S., Xiao, W., Gonik, A.M., Agarwal, R.G., Lam, K.S., The effect of surface charge on in vivo biodistribution of PEG-oligocholic acid based micellar nanoparticles, *Biomaterials* 32 (2011) 3435-3446.

Yamamoto, Y., Nagasaki, Y., Kato, Y., Sugiyama, Y., Kataoka, K., Long-circulating poly(ethylene glycol)-poly(D,L-lactide) block copolymer micelles with modulated surface charge. *J Control Release* 77 (2001) 27-38.

Yan, C., Gu, J., Guo, Y., Chen, D., In vivo biodistribution for tumor targeting of 5-fluorouracil (5-FU) loaded N-succinyl-chitosan (Suc-Chi) nanoparticles, *Yakugaku Zasshi* 130 (2010) 801-804.

Yang, S.C.*, et al.* Body distribution in mice of intravenously injected camptothecin solid lipid nanoparticles and targeting effect on brain. *J Control Release* 59 (1999) 299-307.

Ye, J., Wang, Q., Zhou, X., Zhang, N., Injectable actarit-loaded solid lipid nanoparticles as passive targeting therapeutic agents for rheumatoid arthritis. *Int J Pharm* 352 (2008) 273-279.

Zhang, X., Yin, J., Kang, C., Li, J., Zhu, Y., Li, W., Huang, Q., Zhu, Z., Biodistribution and toxicity of nanodiamonds in mice after intratracheal instillation. *Toxicol Lett* 198 (2010) 237-243.

Zhang,L., Gu, F.X, Chan, J.M., Wang, A.Z., Langer, R.S., Farokhzad, O.C., Nanoparticles in medicine: therapeutic applications and developments, *Clin Pharmacol Ther* 83 (2008) 761-769.

Vitoria-Gasteiz 2013

Universidad del País Vasco

Euskal Herriko Unibertsitatea